Scientific sector

Department of Agriculture, Forest, Food and Environmental Sciences (DAFE)

Ph.D. in

Agricultural, Forest and Food Sciences

Title of thesis

"*Old growth forests preservation, protection, and promotion: a framework for Pollino National Park monitoring*"

Scientific-Disciplinary Sector (SDS)

AGRI-03/B
(ex. AGR/05)

Ph.D. Coordinator

Prof.ssa Teresa ZOTTA

Ph.D. Student

Dott. Danilo TRAVASCIA

Supervisor

Prof. Francesco RIPULLONE

Co – Supervisor

Prof. Gianluca PIOVESAN

Prof.ssa Costanza FIORENTINO

Ciclo XXXVIII°

Abstract

Old-growth forests (OGFs) are natural ecosystems characterised by minimal human activity and exceptional structural and ecological complexity. Although rare, fragmented and often confined to remote areas, these forests play a crucial role in conserving biodiversity and maintaining ecosystem function. However, their structural complexity and long-term functional dynamics are not fully explored, particularly in Mediterranean regions, where climate change poses significant challenges. Forest structural complexity strongly influences biodiversity patterns, ecosystem functioning and resilience; however, quantitative analysis across spatial scales and over time still needs to be developed. This doctoral thesis aims to: (i) analyse forest structural heterogeneity in Mediterranean OGFs; (ii) upscale field-based structural indicators through advanced remote sensing modelling; and (iii) evaluate long-term canopy dynamics to test whether structurally complex forests exhibit enhanced functional stability. To achieve these aims, an integrated, scalable methodological framework combining field-based structural assessments, multi-source remote sensing, and long-term satellite time series was applied to old-growth forest (OGF) stands in Pollino National Park. In the first chapter, forest structural complexity was assessed at the plot level using the Structural Heterogeneity Index, which was derived from detailed field data. Multivariate ordination techniques were then employed to examine the relationships between structural attributes, environmental variables and plant species diversity. Results revealed the central role of structural heterogeneity in shaping plant community composition, interacting with topographic and site-related factors. In the second chapter, a multi-source remote sensing approach was implemented to spatially model forest structural complexity at a local scale. Random Forest model was applied to a range of predictors, including LiDAR metrics, multispectral indices, topographic variables and long-term vegetation trends, for classifying forest structural heterogeneity according to SHI classes. This approach enabled the production of high-resolution and spatially explicit maps of relative old-growthness, bridging ground-based ecological assessment and landscape-scale monitoring. In the third chapter, long-term forest canopy dynamics (1985-2024) were analysed using multi-decadal time series. Vegetation greenness trends, estimated at the pixel level, were assessed by combining Theil–Sen slope estimators and modified Mann–Kendall tests. Finally, block bootstrap resampling and effect-size metrics were implemented to compare trends across forest types and classes. The results revealed canopy greenness stability across the past four decades, while significant differences in trend magnitude were observed between old-growth stands and comparable managed areas.

By integrating field-derived structural indices, remote sensing-based spatial modelling and multi-decadal time series analysis, this thesis advances a novel technology-driven framework for assessing forest structural heterogeneity and functional dynamics. The proposed approach moves beyond binary OGF classification, characterising old-growthness as a continuous and spatially variable property, and provides a robust decision-support tool for adaptive forest monitoring and conservation strategies under climate change.

Acknowledgements

I would extend my sincere gratitude to Professor Francesco Ripullone, supervisor of this doctoral research, for the opportunity to embark on this Ph.D. program and for his steadfast scientific guidance. My thanks also go to Prof. Gianluca Piovesan and Dr. Costanza Fiorentino, whose expertise as co-supervisors was instrumental in shaping this thesis. I am grateful to the University of Basilicata, particularly the Department of Agriculture, Forest, Food and Environmental Sciences (DAFE), for providing the academic environment and institutional support necessary for this research. This work was further made possible by the Tech4You Project (Spoke 4 – PP 4.3.2), which facilitated the development of innovative methodologies and interdisciplinary approaches to forest ecosystem analysis. I sincerely thank GEOCART S.p.A. for their hospitality and technical guidance during a critical phase of this research, and Pollino National Park, particularly Dr. Aldo Schettino and Dr. Vittoria Marchianò, for their invaluable support during fieldwork. I also extend my gratitude to the University of Graz, represented by Prof. Manuela Hirschmugl and Harald Zandler, for scientific support and hospitality during my research abroad. My thanks also go to Professor Nicodemo Passalacqua for sharing essential knowledge and guidance.

I would acknowledge the research team, colleagues, and friends who contributed, directly or indirectly, to this work. Francesco T, Rossella C, Gabriele M, Michele C, Emanuele G, and Antonio L for their support and discussions, which significantly enhanced the outcomes of this research. I also appreciate all professors and colleagues who fostered a stimulating scientific and professional environment. Beyond the academic sphere, I owe a debt of gratitude to my parents, whose unwavering love, patience, and encouragement have sustained me throughout this journey. To my brother, my sister-in-law, and especially my niece Anita, thank you for the joy, warmth, and inspiration you bring into my life — your presence has been a constant source of light and motivation. I am especially grateful to Lucy, my partner, whose steadfast support, understanding, and presence have been my anchor and source of strength. I am also grateful to my friends, whose companionship and support have been invaluable: Chiara, Filippo, Luciano, Felicia, Francesco, Antonello, George, and Alberto, whose friendship and encouragement have enriched both my personal and professional path. Finally, I would like to reflect on all those I have encountered along this journey, whether they remained close or moved on. Every interaction has left a mark and contributed to my growth. And, at last, I wish to acknowledge myself for the perseverance, dedication, and courage that brought me to this achievement.

to Mom and Dad

General introduction

Old-growth forests (OGFs) represent distinct natural ecosystems characterised by high structural complexity, ecological stability, and long-term continuity, resulting from an extended period with minimal human interference. Compared to young or managed forests, OGFs exhibit unique features which define their ecological singularity (Wirth et al., 2009). Such ecosystems offer invaluable services such as biodiversity conservation, carbon storage, and microclimate regulation (de Assis Barros et al., 2022). Despite their crucial ecological role, OGFs currently face numerous threats, including illegal logging, habitat fragmentation, and land use changes. As a result, most OGFs are confined to remote, inaccessible, or strictly protected areas (Morales-Hidalgo et al., 2015). Therefore, enhancing our knowledge about their spatial distribution, long-term dynamics, and structure is crucial for developing effective conservation and management strategies — particularly in the context of ongoing climate change.

Progress in ecological research has led to considerable changes in the OGF concept. Initially, OGFs were defined based solely on stand age and specific structural attributes (Franklin et al., 2004). Several studies conducted during the 1980s and 1990s were focused on assessing diameter distribution, deadwood volumes, and canopy stratification (Spies and Franklin, 1991). However, this approach revealed significant limitations, especially when applied to diverse biogeographical regions (Bauhus et al., 2009). Later studies have therefore proposed a revised OGF definition, considering them as dynamic ecosystems naturally shaped by senescence processes resulting in a heterogeneous mosaic of canopy gaps and regeneration patches (Wirth et al., 2009). According to these revised concepts, OGFs should be defined by spatial and temporal complexity rather than fixed structural thresholds (Nagel et al., 2014).

Based on this foundation, Sabatini et al. (2018) and Barredo et al. (2021) recently expanded this perspective by adding criteria such as compositional stability, species-specific assemblages, and unique ecological functions. Considering these findings, OGFs have been broadly redefined to encompass multiple attributes representative of various development stages, reflecting site history and environmental context. Simultaneously, greater emphasis was placed on quantifying forest complexity and ecological continuity by using structure-based indicators. Since the pioneering work proposed by Spies and Franklin (1991), forest attributes such as tree diameter distribution, deadwood abundance, and canopy stratification have been widely acknowledged as reliable proxies for forest naturalness and ecosystem functioning.

Accordingly, several aggregated indices have been developed and applied globally, including the Late Succession Index (Whitman & Hagan, 2007), the Enhanced Structural Complexity Index (ESCI; Beckschäfer et al., 2013) and the Structural Heterogeneity Index (SHI; McElhinny et al., 2006; Sabatini et al., 2015). Such indices provided a comprehensive picture of forest structures, revealing significant variations in old-growth features according to site and environmental conditions. Considering this inherent complexity, moving towards more scalable monitoring techniques became essential.

At the same time, major advances were also made in the methodological approaches used to study OGFs. Although field-based inventories remain crucial for ensuring accurate forest characterisation, their application is restricted by high costs and limited spatial coverage (McElhinny et al., 2005). However, the advent of optical remote sensing technologies has gradually mitigated some of these limitations. Satellite images have played a crucial role in monitoring forest changes and vegetation dynamics over time (Masek et al., 2008). Various vegetation indices (VIs) such as the Normalised Difference Vegetation Index (NDVI) or the Enhanced Vegetation Index (EVI) can be derived using optical sensors. Such indices are commonly employed to analyse canopy vigour, leaf area, and photosynthetic activity. When analysed over an extended period, they could also offer valuable insights into forest productivity trends, disturbance history, and recovery processes. As demonstrated by several studies, these details are crucial to identifying trend trajectories, particularly when comparing OGFs and managed stands.

However, optical remote sensing technology imposes inherent limitations. According to Wulder et al. (2008), spectral imagery primarily captures canopy properties and surface reflectance, resulting in limited sensitivity to vertical forest structure. As a direct result, key features including multi-layered canopies, spatial heterogeneity and deadwood accumulation cannot be evaluated solely through optical data. Additionally, such limitations become particularly evident within the Mediterranean region, where topographic heterogeneity and mixed-species compositions further hinder spectral interpretation.

In this context, Light Detection and Ranging (LiDAR) technology represented a pioneering solution, providing three-dimensional point clouds and detailed canopy structural metrics (Dassot et al., 2011). Airborne LiDAR (ALS) has emerged as a crucial tool for assessing forest height distributions, vertical stratification, and gap dynamics (Matasci et al., 2018).

A large body of research highlighted the strong correlation between LiDAR-derived metrics and field-measured data (Martinuzzi et al., 2009). For instance, Teobaldelli et al. (2017) successfully employed LiDAR data to model forest structural attributes and diversity in the Mediterranean context. Furthermore, Lin et al. (2024) demonstrated how ALS data could be applied to predict fine dead fuel load.

Subsequently, these technologies were complemented by the introduction of Synthetic Aperture Radar (SAR) systems. Contrary to optical sensors, SAR technology can penetrate cloud cover, making it more sensitive to canopy moisture and structural properties (Dostálová et al., 2018). Santoro et al. (2022) further explored this hypothesis, revealing a strong correlation between SAR backscatter intensity and forest biomass, canopy structure, and moisture content. Nevertheless, a clear conclusion emerges when all these technologies are synthesised: OGFs' structural and functional complexity cannot be adequately assessed using a single technique. Consequently, a growing body of research has emphasised the importance of integrating data from multiple sensors to achieve a more comprehensive and reliable forest assessment.

To address these challenges, various multi-sensor approaches have been developed over the last decade (Dalponte et al., 2019). Machine learning (ML) algorithms have emerged as pivotal tools to support OGF mapping and detection (Maxwell et al., 2018). Among these, Random Forest classifiers (RF) have proven to be an effective technique by accommodating non-linear relationships, processing mixed data, and providing robust predictions even with limited training data (Belgiu & Drăguţ, 2016). Several studies conducted across various European regions, including boreal forests (Spracklen & Spracklen, 2019), temperate forests (Holaga et al., 2021), and the Carpathian Mountains (Munteanu et al., 2015), have further reinforced these assumptions, achieving classification accuracies of 80-85%. However, most of these studies treat OGF detection as a binary classification process, based on generalised thresholds rarely validated by field-based structural indices, which reduces their ability to capture gradual, site-specific variations in old-growthness in ecologically diverse regions. Such limitations are particularly consequential in the Mediterranean Basin, where significant knowledge gaps persist: OGFs are rarely mapped or documented, leading to substantial uncertainty about their full range of structural and compositional variability (Sabatini et al., 2018). Furthermore, a significant portion of potential OGFs remain undetected, particularly in remote, mountainous regions where systematic surveys combining field observations and remote sensing technologies remain scarce. Beyond data availability, key ecological uncertainties exist.

For instance, while numerous studies have shown a relationship between structural complexity and biodiversity, further studies are required to clarify how forest structure influences both biodiversity and plant species distribution (Mori et al., 2013; Chauvet et al., 2017). This topic holds major relevance within the Mediterranean ecosystems, where topography and climate play a pivotal role. Beyond data availability, key ecological uncertainties exist. For instance, while numerous studies have shown a relationship between structural complexity and biodiversity, further studies are required to clarify how forest structure influences both biodiversity and plant species distribution (Mori et al., 2013; Chauvet et al., 2017). Given the pivotal role of topography and climate, the relevance of this theme is particularly pronounced within Mediterranean ecosystems. Likewise, further challenges are posed by methodological limitations. Indeed, multi-sensor approaches remain largely unexplored in the Mediterranean region. Additionally, comparative analyses aimed at examining long-term dynamics in old-growth and managed forests are rarely conducted. The lack of supporting evidence limits our current understanding - particularly about how these forest ecosystems should respond to ongoing climate change (Seidl et al., 2014; Gazol et al., 2018) - and how increased structural complexity might enhance their resilience to external stressors.

To address knowledge gaps, this thesis proposes three interconnected studies focused on Mediterranean OGFs:

i. Forest structural heterogeneity was quantitatively characterised using the Structural Heterogeneity Index (SHI) and analysed by multivariate approaches to investigate relationships between structural attributes, topographic factors, and vascular plant species distributions. Here, two objectives were pursued: first, to identify the key environmental drivers of structural complexity; and second, to evaluate their influence on plant diversity along ecological gradients.
ii. Building on the previous field-based characterisation, a predictive modelling framework was implemented to assess the spatial variability of relative old-growthness within three mixed old-growth forest sites. For this purpose, multi-source remote sensing data was utilised. Reference conditions were established using SHI-derived classes, while RF was trained integrating airborne LiDAR structural metrics, multispectral vegetation indices, long-term canopy dynamics, topographic variables, and a proxy to represent cumulative human pressure.

As part of this study, our primary objective was to generate a quantitative, spatially explicit map to identify forest patches with higher levels of relative old-growthness, thereby supporting conservation and monitoring strategies.

iii. Long-term forest dynamics within OGFs and paired managed stands were examined by conducting a comparative analysis on 40 years of temporal trends. Canopy greenness dynamics were quantified using the Enhanced Vegetation Index (EVI), derived from Landsat time series, and analysed by combining robust non-parametric trend estimators with block-level bootstrap inference. In this context, our key aim was to identify contrasting dynamic trajectories between old-growth and managed forests, assessing whether increased structural complexity could confer enhanced resilience to climate-related stressors.

Overall, these studies enhance our theoretical and practical knowledge concerning the assessment of OGF within the Mediterranean Basin. By integrating structural indicators, multiple remote sensing technologies, and long-term temporal analysis within a single, scalable workflow, this thesis moves beyond the binary OGF classification by characterising old-growthness as a continuous, spatially variable property — thereby establishing a coherent framework to support conservation efforts within a biodiversity hotspot increasingly threatened by climate change and land use fragmentation.

References

- Barredo JI, Brailescu C, Teller A, Sabatini FM, Mauri A, Janouskova K (2021). Mapping and assessment of primary and old-growth forests in Europe. EUR 30661 EN, Publications Office of the European Union, Luxembourg, ISBN 978-92-76-34230-4, JRC124671. DOI: 10.2760/13239
- Bauhus J (2009). *Rooting patterns of old-growth forests: is aboveground structural and functional diversity mirrored belowground?. In Old-growth forests: Function, fate and value* (pp. 211-229). Berlin, Heidelberg: Springer Berlin Heidelberg. DOI: https://doi.org/10.1007/978-3-540-92706-8_10
- Beckschäfer P, Mundhenk P, Kleinn C, Ji Y, Yu D, Harrison R (2013). Enhanced Structural Complexity Index: An Improved Index for Describing Forest Structural Complexity. Open Journal of Forestry, 3, 23-29. DOI: 10.4236/ojf.2013.31005
- Belgiu M, Drăguţ L (2016). *Random forest in remote sensing: A review of applications and future directions*. ISPRS journal of photogrammetry and remote sensing, 114, 24-31. DOI: https://doi.org/10.1016/j.isprsjprs.2016.01.011
- Chauvet M, Kunstler G, Roy J, Morin X (2017). *Using a forest dynamics model to link community assembly processes and traits structure*. Functional Ecology, 31(7), 1452-1461. DOI: https://doi.org/10.1111/1365-2435.12847
- Dalponte M, Frizzera L, Gianelle D (2019). *Individual tree crown delineation and tree species classification with hyperspectral and LiDAR data*. PeerJ, 6, e6227. DOI: https://doi.org/10.7717/peerj.6227
- Dassot M, Constant T, Fournier M (2011). *The use of terrestrial LiDAR technology in forest science: application fields, benefits and challenges*. Annals of forest science, 68(5), 959-974. DOI: https://doi.org/10.1007/s13595-011-0102-2
- de Assis Barros L, Venter M, Elkin C, Venter O (2022). *Managing forests for old-growth attributes better promotes the provision of ecosystem services than current age-based old-growth management. Forest Ecology and Management*, *511*, 120130. DOI: https://doi.org/10.1016/j.foreco.2022.120130
- Dostálová A, Wagner W, Milenković M, Hollaus M (2018). *Annual seasonality in Sentinel-1 signal for forest mapping and forest type classification*. International Journal of Remote Sensing, 39(21), 7738-7760. DOI: https://doi.org/10.1080/01431161.2018.1479788
- Franklin JF, Van Pelt R (2004). *Spatial aspects of structural complexity in old-growth forests*. Journal of Forestry, 102(3), 22-28. DOI: https://doi.org/10.1093/jof/102.3.22

- Gazol A, Camarero JJ, Vicente-Serrano SM, Sánchez-Salguero R, Gutiérrez E, de Luis M, Galván JD (2018). *Forest resilience to drought varies across biomes*. Global change biology, 24(5), 2143-2158. DOI: https://doi.org/10.1111/gcb.14082
- Hologa R, Scheffczyk K, Dreiser C, Gärtner S (2021). *Tree species classification in a temperate mixed mountain forest landscape using random forest and multiple datasets*. Remote Sensing, 13(22), 4657. DOI: https://doi.org/10.3390/rs13224657
- Lin D, Giannico V, Lafortezza R, Sanesi G, Elia M (2024). *Use of airborne LiDAR to predict fine dead fuel load in Mediterranean forest stands of Southern Europe*. Fire Ecology, 20(1), 58. DOI: https://doi.org/10.1186/s42408-024-00287-7
- Martinuzzi S, Vierling LA, Gould WA, Falkowski MJ, Evans JS, Hudak AT, Vierling KT (2009). *Mapping snags and understory shrubs for a LiDAR-based assessment of wildlife habitat suitability*. Remote Sensing of Environment, 113(12), 2533-2546. DOI: https://doi.org/10.1016/j.rse.2009.07.002
- Masek JG, Huang C, Wolfe R, Cohen W, Hall F, Kutler J, Nelson P (2008). *North American forest disturbance mapped from a decadal Landsat record*. Remote Sensing of Environment, 112(6), 2914-2926. DOI: https://doi.org/10.1016/j.rse.2008.02.010
- Matasci G, Hermosilla T, Wulder MA, White JC, Coops NC, Hobart GW, Zald HS (2018). *Large-area mapping of Canadian boreal forest cover, height, biomass and other structural attributes using Landsat composites and lidar plots*. Remote sensing of environment, 209, 90-106. DOI: https://doi.org/10.1016/j.rse.2017.12.020
- Maxwell AE, Warner TA, Fang F (2018). I*mplementation of machine-learning classification in remote sensing: An applied review*. International journal of remote sensing, 39(9), 2784-2817. DOI: https://doi.org/10.1080/01431161.2018.1433343
- McElhinny C, Gibbons P, Brack C (2006). *An objective and quantitative methodology for constructing an index of stand structural complexity*. Forest Ecology and management, 235(1-3), 54-71. DOI: https://doi.org/10.1016/j.foreco.2006.07.024
- McElhinny C, Gibbons P, Brack C, Bauhus J (2005). *Forest and woodland stand structural complexity: its definition and measurement*. Forest Ecology and Management, 218(1-3), 1-24. DOI: https://doi.org/10.1016/j.foreco.2005.08.034
- Morales-Hidalgo D, Oswalt SN, Somanathan E (2015). *Status and trends in global primary forest, protected areas, and areas designated for conservation of biodiversity from the Global Forest Resources Assessment 2015*. Forest Ecology and Management, 352, 68-77. DOI: https://doi.org/10.1016/j.foreco.2015.06.011

- Mori AS, Shiono T, Koide D, Kitagawa R, Ota AT, Mizumachi E (2013). *Community assembly processes shape an altitudinal gradient of forest biodiversity*. Global Ecology and Biogeography, 22(7), 878-888. DOI: https://doi.org/10.1111/geb.12058
- Munteanu C, Kuemmerle T, Keuler NS, Müller D, Balázs P, Dobosz M, Radeloff VC (2015). *Legacies of 19th century land use shape contemporary forest cover*. Global Environmental Change, 34, 83-94. DOI: https://doi.org/10.1016/j.gloenvcha.2015.06.015
- Nagel TA, Svoboda M, Kobal M (2014). *Disturbance, life history traits, and dynamics in an old‐growth forest landscape of southeastern Europe*. Ecological Applications, 24(4), 663-679. DOI: https://doi.org/10.1890/13-0632.1
- Sabatini FM, Burrascano S, Keeton WS, Levers C, Lindner M, Pötzschner F, Kuemmerle T (2018). *Where are Europe's last primary forests?*. Diversity and distributions, 24(10), 1426-1439. DOI: https://doi.org/10.1111/ddi.12778
- Sabatini FM, Burrascano S, Lombardi F, Chirici G, Blasi C (2015). *An index of structural complexity for Apennine beech forests*. IForest, 8, 314-323. DOI: https://doi.org/10.3832/ifor1160-008
- Santoro M, Cartus O, Fransson JE (2022). *Dynamics of the Swedish forest carbon pool between 2010 and 2015 estimated from satellite L-band SAR observations*. Remote Sensing of Environment, 270, 112846. DOI: https://doi.org/10.1016/j.rse.2021.112846
- Seidl R, Rammer W, Spies TA (2014). *Disturbance legacies increase the resilience of forest ecosystem structure, composition, and functioning*. Ecological Applications, 24(8), 2063-2077. DOI: https://doi.org/10.1890/14-0255.1
- Spies TA, Franklin JF (1991). *The structure of natural young, mature, and old-growth Douglas-fir forests in Oregon and Washington*. Wildlife and vegetation of unmanaged Douglas-fir forests, 1, 91-109. [online] Available at: https://andrewsforest.oregonstate.edu/sites/default/files/lter/pubs/pdf/pub1244.pdf
- Spracklen BD, Spracklen DV (2019). *Identifying European old-growth forests using remote sensing: A study in the Ukrainian Carpathians*. Forests, 10(2), 127. DOI: https://doi.org/10.3390/f10020127
- Teobaldelli M, Cona F, Saulino L, Migliozzi A, D'Urso G, Langella G, Saracino A (2017). *Detection of diversity and stand parameters in Mediterranean forests using leaf-off discrete return LiDAR data*. Remote Sensing of Environment, 192, 126-138. DOI: https://doi.org/10.1016/j.rse.2017.02.008

- Whitman AA, Hagan JM (2007). *An index to identify late-successional forest in temperate and boreal zones*. Forest Ecology and Management, 246(2-3), 144-154. DOI: https://doi.org/10.1016/j.foreco.2007.03.004
- Wirth C, Gleixner G, Heimann M (2009). *Old-growth forests: function, fate and value–an overview*. Old-growth forests: Function, fate and value, 3-10. DOI: https://doi.org/10.1007/978-3-540-92706-8_1
- Wulder MA, Bater CW, Coops NC, Hilker T, White JC (2008). *The role of LiDAR in sustainable forest management*. The forestry chronicle, 84(6), 807-826. DOI: https://doi.org/10.5558/tfc84807-6

Table of Contents

List of tables

Table 3.1. An overview concerning the investigated OGF sites, including site identification, forest name, forest type, dominant tree species, elevation, and the corresponding Site of Community Importance (SCI) code.

Table 3.2. Managed stand details. Summary of the environmental and geographical properties of managed forest stands, including the distance to their respective old-growth reference stands.

Table 3.3. Temporal distribution of satellite data sources. Summary of the Landsat satellite collections and their respective time windows utilised to reconstruct vegetational index trajectories from 1985 to 2024.

Table 3.4. Descriptive statistics of Sen's slope values (1985–2024) at the pixel level (n) for mixed and pure beech forests. Data are grouped by forest class (managed vs. OGF) and show the mean, median, standard deviation (SD), and interquartile range (Q25 and Q75) of long-term canopy trajectories.

Table 3.5. Proportion of the positive and negative EVI Sen Slope values in old-growth and managed forests, stratified by forest type. Values represent the percentage of pixels exhibiting greening (positive) or browning(negative), derived from annual maximum EVI time series (1985–2024).

Table 3.1. Summary statistics of pixel-wise trend significance derived from the m-MK test applied to annual maximum EVI time series, stratified by forest type, management class, and site. For each stand, the table includes: total area, number of analysed pixels, proportion of pixels exhibiting statistically significant monotonic trends, as well as the median values of both Kendall's τ and corresponding Z statistics to characterise the central tendency of trend direction and strength.

Table 3.7. EVI Sen's slope: block-level descriptive statistics. Block-level descriptive statistics of the median EVI Sen's slope for OGFs and NOGFs, grouped by forest type.

Table 3.8. Results from block bootstrap analyses based on 100 × 100 m grid cells. Reported values represent the difference in mean block-level median EVI Sen's slope (OGF-NOGF), with 95% bootstrap confidence intervals. Effect size is expressed as Cliff's δ.

Table 3.9. Results from global block bootstrap analyses conducted within each forest type. Results are based on block-level median EVI Sen's slope values aggregated across all study sites within each forest type. Reported values represent the difference in mean block medians (OGF-NOGF), with 95% bootstrap confidence intervals and associated effect sizes (Cliff's δ).

List of Figures

Figure 2.2. Conceptual scheme describing field sampling design adopted according to the 'Building an Old-Growth Forest Network for Southern Apennine Parks' project. Macro-plots (100 × 100 m; outlined in red) were subdivided into a standard grid of 20 × 20 m. Within each grid cell, forest structural attributes were recorded, and alphanumeric labels (A1–E5) were used to identify microplots within the core area.

Figure 2.3. Structural heterogeneity index distribution across the three investigated forest stands: Bosco Magnano (BM), Vaccarizzo (CA) and Cugno dell'Acero (TP). The boxplots show SHI values derived from field microplots, highlighting their variability. Numeric labels indicate median SHI values at the stand level.

Figure 2.4. Stand-level Sen's slope estimates (yr^{-1}) derived from annual maximum NDVI and EVI Landsat time series for the three investigated forest stands. Points represent Sen's slope values for each index, indicating the magnitude and direction of long-term vegetation trends.

Figure 2.5. Spatial distribution of high Structural Heterogeneity Index (SHI). Red areas denote pixels classified as High SHI. White lines represent the officially established OGF's boundaries. Reported percentages indicate the proportion of each study area classified as high SHI.

Figure 2.6. Relative importance of predictor variables derived from the random forest classifier model. Importance scores were standardised to a relative scale of 0-100. Variables were then ranked in ascending order, based on their importance, thereby highlighting their respective contributions to model performance.

Figure 3.1. Study area and surveyed forest sites. Park boundaries are plotted on a digital elevation model (DEM), highlighting the spatial distribution of the six stands designated as old-growth forests (OGFs). Red dots represent mixed forest sites — Bosco Vaccarizzo, Bosco Magnano and Cugno dell'Acero — while green dots correspond to pure beech forest sites — Pollinello, Grattaculo and Cozzo Ferriero.

Figure 3.2. Block spatial aggregation applied to EVI Theil-Sen slope values within the 'Bosco Magnano' site. Here, the basemap shows EVI TS values derived from the Landsat time series (1985–2024). Black polygons denote the forest boundaries. The regular grid shows the spatial blocks of 100 × 100 m used for aggregation. Black dots represent individual pixels included in the analysis, while red squares show how median EVI-TS values were computed for each grid cell.

Figure 3.3. Spatial distribution of long-term EVI trends within the Pollino National Park. The background map shows Sen's slope values derived from the Enhanced Vegetation Index (EVI). Positive values (green and yellow) represent increasing vegetation greenness over time, while negative values (blue and purple) represent decreasing trends. Red and black points represent mixed and beech forests, respectively.

Figure 3.4. Kernel density distributions of block-level median EVI Sen's slope for mixed forests and pure beech forests. Density curves compare OGF and managed stands, highlighting differences in the magnitude and distribution of long-term forest trends.

Figure 3.5. Bootstrap distributions of differences in mean EVI TS values between OGF and NOGF, for mixed forests and pure beech forests. The distributions were based on 1,000 bootstrap iterations using block medians EVI TS. The dashed lines mark the observed difference between the OGF and NOGF, while the shaded areas represent the 95% confidence interval.

Abbreviations and acronyms

AC	Monte Sparviere
ALS	Airborne Laser Scanning
BI	Brightness Index
bi_aut	Brightness Index autumn
bi_sum	Brightness Index summer
Block	Aggregated spatial unit (100 × 100 m grid cell)
BM	Bosco Magnano
BV	Buonvicino
CA	Bosco Vaccarizzo
CCA	Canonical Correspondence Analysis
CHM	Canopy Height Model
CI	Confidence interval
CWD	Coarse Woody Debris
DBH	Diameter at Breast Height
DDT	Downed Dead Trees
DL	Deep Learning
DTM	Digital Terrain Model
EU	European Union
ETM+	Enhanced Thematic Mapper Plus (Landsat 7)
EVI	Enhanced Vegetation Index
EVI TS	Theil–Sen slope of annual maximum EVI
evi_aut	EVI autumn
EVI_sen	Theil–Sen slope of EVI
evi_sum	EVI summer
GEE	Google Earth Engine
GHM	Global Human Modification Index
GNSS	Global Navigation Satellite System
KA	Cohen's Kappa
KMO	Kaiser–Meyer–Olkin test

Landsat	Land Remote-Sensing Satellite program
LiDAR	Light Detection and Ranging
LTV	Living Tree Volume
MAD	Median absolute deviation
ML	Machine Learning
m-MK	Modified Mann-Kendall test
MK	Mann-Kendall test
NDVI	Normalised Difference Vegetation Index
ndvi_aut	NDVI autumn (seasonal composite)
NDVI_sen	Theil–Sen slope of NDVI (trend)
ndvi_sum	NDVI annual summer (seasonal composite)
NOGF / NOGFs	Non–old-growth forest(s) (managed reference stands)
OA	Overall Accuracy
OGF / OGFs	Old-growth forest(s)
OLI	Operational Land Imager (Landsat 8)
PA	Producer's Accuracy
PCA	Principal Component Analysis
PCoA	Principal Coordinate Analysis
Pixel	The smallest spatial unit of raster data
PO	Pollinello
Pollino NP	Pollino National Park
QA_PIXEL	Quality Assessment pixel band used for cloud and shadow masking
QMD	Quadratic Mean Diameter
RDA	Redundancy Analysis
RO	Cozzo Ferriero
RS	Remote Sensing
S2 / Sentinel-2	Sentinel-2 satellite mission
SAR	Synthetic Aperture Radar
SC	Serra di Crispo
SCI	Site of Community Importance

SD	Standard deviation
SDT	Standing Dead Trees
SHI	Structural Heterogeneity Index
Slope	Slope
TLS	Terrestrial Laser Scanning
TM	Thematic Mapper (Landsat 5)
TP	Cugno dell'Acero
TS	Theil–Sen slope estimator
UA	User's Accuracy
UTM	Universal Transverse Mercator
VI / VIs	Vegetation Index / Indices
VIG	Grattaculo
VP	Variation Partitioning
WGS 84	World Geodetic System 1984
Zkurt	Kurtosis of canopy height distribution
Zmax	Maximum canopy height
Zmean	Mean canopy height
Zmin	Minimum canopy height
Zsd	Standard deviation of canopy height
Zskew	Skewness of canopy height distribution
Δ	Difference between OGF and NOGF (mean EVI Theil–Sen slope values)

Chapter 1: Forest structural diversity in Mediterranean old-growth stands

Summary: *A quantitative ecological framework was established to characterise structural heterogeneity within Mediterranean old-growth forests. Using field-based data, several structural attributes were combined to calculate the Structural Heterogeneity Index (SHI). Structural patterns were then analysed in relation to topographic variables and vascular plant species composition, using multivariate analyses. As a result, it was shown that structural heterogeneity varied significantly across forest stands and that observed differences were closely linked to plant species diversity and site-specific conditions. Overall, this chapter established that old-growthness cannot be inferred solely from structural metrics but must be assessed using a multidimensional approach. These findings established a novel, comprehensive, and multidimensional ecological reference framework for future research, as well as the theoretical foundation for the subsequent research phase, where field-derived structural heterogeneity was assessed in terms of its spatial distribution using multi-source remote sensing approaches.*

Multiple dimensions of old-growth forest complexity: the role of structure, topography, and vascular plant diversity

Travascia D.[1], Piovesan G.[2], Passalacqua N.[3], Borghetti M.[1], Bernardo L.[3], Burrascano S.[4], Colangelo M.[1], Fiorentino C.[1], Gargano D.[3], Lapolla A.[1], Marchianò V.[5], Rivelli A. R.[1], Schettino A.[5], Ripullone F.[1]

[1] *Department of Agricultural, Forest, Food and Environmental Sciences, University of Basilicata, Via dell'Ateneo Lucano 10, 85100 Potenza, Italy*

[2] *Department of Ecological and Biological Sciences (DEB), University of Tuscia, Largo dell'Università, 01100 Viterbo, Italy*

[3] *Department of Biology, Ecology, and Earth Science, University of Calabria, Via Pietro Bucci, 87036 Arcavacata, Italy*

[4] *Department of Plant Biology, University of Rome "Sapienza", Via Eudossiana, 00184 Rome, Italy*

[5] *Pollino National Park, Complesso monumentale Santa Maria della Consolazione, 85048 Rotonda, Italy*

Abstract

Old-growth forests (OGFs) are rare ecosystems of high conservation value, providing critical benchmarks for biodiversity and ecosystem functioning. Yet, their complexity is difficult to assess because structural indicators alone often fail to capture the influence of site conditions and floristic composition. This study aimed to (i) quantify structural heterogeneity in OGFs, (ii) explore relationships between site conditions, vascular plant diversity, and structural patterns, and (iii) assess their combined influence on forest ecosystem complexity. Structural attributes, topographic variables, and floristic composition were recorded in 1-hectare plots across nine OGF sites in Pollino National Park (southern Italy). A Structural Heterogeneity Index (SHI) was computed, and relationships between structure, topography, and plant diversity were analysed using Canonical Correspondence Analysis (CCA), Principal Coordinate Analysis (PCoA), and Variation Partitioning (VP). The SHI revealed strong variation among forest types, with beech and mixed stands showing the highest heterogeneity. Elevation and slope explained 18.8% of structural variation, while plant diversity was primarily driven by forest type. VP demonstrated that structural attributes—particularly large trees, canopy cover, and deadwood decay classes—accounted for 23.5% of floristic variation, exceeding the role of topography (12.8%). Stand structure and topography effectively explain the compositional patterns of distinct, naturally clustered forest types. These findings demonstrate that OGF complexity cannot be reduced to structure alone, but emerges from the integration of structural, topographic, and floristic dimensions. This multidimensional perspective provides a stronger foundation for identifying and conserving Europe's last OGFs.

1. Introduction

Forest ecosystems are facing unprecedented challenges worldwide, which stem from anthropogenic pressures and climate change, and result in losses of biodiversity and ecosystem services (Pörtner et al., 2021; Pereira et al., 2020). In this context, the scientific understanding and conservation of old-growth forests (OGFs) have gained increasing international relevance, given their irreplaceable ecological functions as biodiversity reservoirs, and their capacity to sustain essential ecological processes (O'Brien et al., 2021; Pasques & Munné-Bosch, 2024).

OGFs represent the culmination of long-term, undisturbed ecological dynamics and are characterised by distinctive structural and compositional features, such as the presence of large and ancient trees, multilayered canopies, abundant coarse wood debris, and species-rich understories (Balloffet & Dumroese 2022).

These ecosystems play a crucial role in a multitude of ecological processes (Keenan et al., 2012), including carbon sequestration and storage, water regulation, and nutrient cycling, thus contributing significantly to climate change mitigation efforts, while providing essential habitats for numerous endangered species (Gilhen-Baker et al., 2022).

Despite their undeniable ecological and conservation importance, OGFs are extremely rare in Europe, currently covering only about 3% of the continent's forest area, equating to approximately 158 million hectares, due to centuries of intensive land use and logging (Forest Europe 2020; Sabatini et al., 2020; O'Brien et al., 2021). Their limited representation underscores the urgent need to advance strategies for identifying, protecting, and monitoring OGFs, as highlighted by the EU Biodiversity Strategy for 2030 (Brumelis et al., 2011; Barredo et al., 2021).

In recent decades, efforts to define and assess OGFs have increasingly relied on the use of structural indicators that reflect forest complexity and ecological integrity. Since the pioneering work of Spies & Franklin (1991), structural attributes such as tree diameter distributions, deadwood abundance, and canopy stratification have been recognised as reliable proxies for assessing forest naturalness and ecosystem functions. The structure-based approach is still the most commonly used (Storch et al., 2023; Concha et al., 2023; Borghi et al., 2024), often through the use of aggregated indices, e.g., 'late succession index' (Whitman & Hagan, 2007), 'Enhanced Structural Complexity Index' (ESCI) (Beckschäfer et al., 2013), and the 'Structural Heterogeneity Index' (SHI) (McElhinny et al., 2006; Sabatini et al., 2015).

Still, the identification of OGFs remains a significant challenge due to the natural variability in structural and age attributes even within similar forest types, which likely derives from site-specific environmental features such as soil fertility and biogeoclimate (Ziaco et al., 2012; Burrascano et al., 2013; Gray et al., 2023; Barnett et al., 2023; Bruening et al., 2024). In this view, recent research has emphasised the integration of floristic and environmental variables - particularly topographic and edaphic factors - into OGF assessments to better capture the ecological gradients underpinning structural variation (van Galen et al., 2018). Topographic attributes such as elevation, slope and aspect are key determinants of microclimatic conditions and resource distribution, directly influencing tree growth, mortality, and regeneration dynamics (Jucker et al., 2018). Concurrently, vascular plant species composition has been recognised as a sensitive indicator of environmental conditions and ecological continuity, by reflecting both long-term successional processes and present-day ecological conditions (Slezák & Axmanová 2016). The structural complexity of OGFs, in fact, could generate pronounced spatial variability of key ecological parameters, such as light penetration, soil moisture and nutrient availability (Lindenmayer & Bowd 2022).

In this context, understory vascular flora can provide fine-scale insights into the environmental gradients and the structural heterogeneity of forest stands (Giorgini et al., 2015; Filibeck et al., 2015).

In light of these considerations, this study aims to investigate the interrelationships among forest structural complexity, site environmental conditions, and vascular plant diversity within 9 distinct OGFs sites located in the Pollino National Park (Southern Italy). We hypothesize that: (1) forest structural heterogeneity differs significantly across forest types, reflecting variations in disturbance regimes, and site's environment and history; (2) topographic variables drive forest structure development affecting key attributes such as tree size distribution, deadwood accumulation, and canopy complexity; and (3) vascular plant diversity patterns are closely linked to forest structure and site-specific environmental features, highlighting the central role of structural attributes in shaping ecological processes within OGFs. To test these hypotheses, we pursue the following objectives: (1) to compare the structural complexity and plant species distribution across nine OGF sites representing different forest types along a 1100 elevational gradient; (2) to explore how topographic gradients influence structural attributes; (3) to examine how stand structure and site topography interact in defining OGFs' plant community.

Ultimately, this research aims to contribute to a comprehensive understanding of OGFs' complexity, offering valuable insights to improve conservation strategies in line with European biodiversity objectives.

2. Materials and methods

2.1 Study area

The Pollino National Park (Pollino NP) is the largest protected area in Italy, covering about 190,000 hectares in southern Italy (Compagnucci et al., 2002). Topography is complex, with altitudes ranging from 52 to 2,267 m a.s.l. The Park lies in a transitional zone between temperate and Mediterranean climate (Blasi & Michetti 2005), with hot and dry summers at lower altitudes, and cold and snowy winters at the highest. Rainfall ranges from 300 mm/year on the Ionian side to 2,000 mm/year on the Tyrrhenian side (Todaro et al., 2007). In the inner area, at 2000 m a.s.l., the average winter temperature is -3.2°C, while the average summer temperature is 13.5°C (Colangelo et al., 2021). Such topographical and climate variability supports a widely diverse vegetation. Below 800 m a.s.l., Mediterranean scrub dominates, with species such as holm oak (*Quercus ilex* L.) and downy oak (*Quercus pubescens* Willd.). From 800 to 1400 m a.s.l., forests include turkey oak (*Quercus cerris* L.), Oriental hornbeam (*Carpinus orientalis* Mill.) and various maple species. Above 1,400 m a.s.l., beech forests (*Fagus sylvatica* L.) are prevalent, sometimes combined with silver fir (*Abies alba*). Close to the tree line, Bosnian pine (*Pinus heldreichii* Christ var. *leucodermis*) thrives in extreme conditions with scattered individuals or groups of trees, hosting some of the oldest trees in Europe (Piovesan et al., 2018; 2019a; 2020). Despite climate changes, these forests sustained stable growth rates (Colangelo et al., 2021), showing their resilience and conservation value (Baliva et al., 2024).

2.2 Old-growth forests' sites

Nine old-growth forest (OGF) stands within the Pollino NP were selected to capture the park's ecological and structural diversity (Fig. 1.1). Site selection was based on (i) confirmed evidence of minimal anthropogenic disturbance, (ii) presence of structural indicators of maturity (e.g., large trees, multilayered canopies, and abundant deadwood), and (iii) representation of distinct forest types along altitudinal and bioclimatic gradients. The sites encompass a gradient from Mediterranean to montane conditions, including mixed deciduous forests with *Quercus cerris*, *Carpinus orientalis*, and *Abies alba*, as well as high-elevation stands of *Fagus sylvatica* and

Pinus heldreichii. This range allows testing how structural heterogeneity and vascular plant diversity respond to topography and forest type.

Key attributes—such as elevation, stand composition, living tree volume, and maximum age—are summarised in Table 1.1. Together, these sites provide a representative framework for assessing the links among structure, environmental conditions, and floristic diversity in highly natural forest ecosystems of southern Italy.

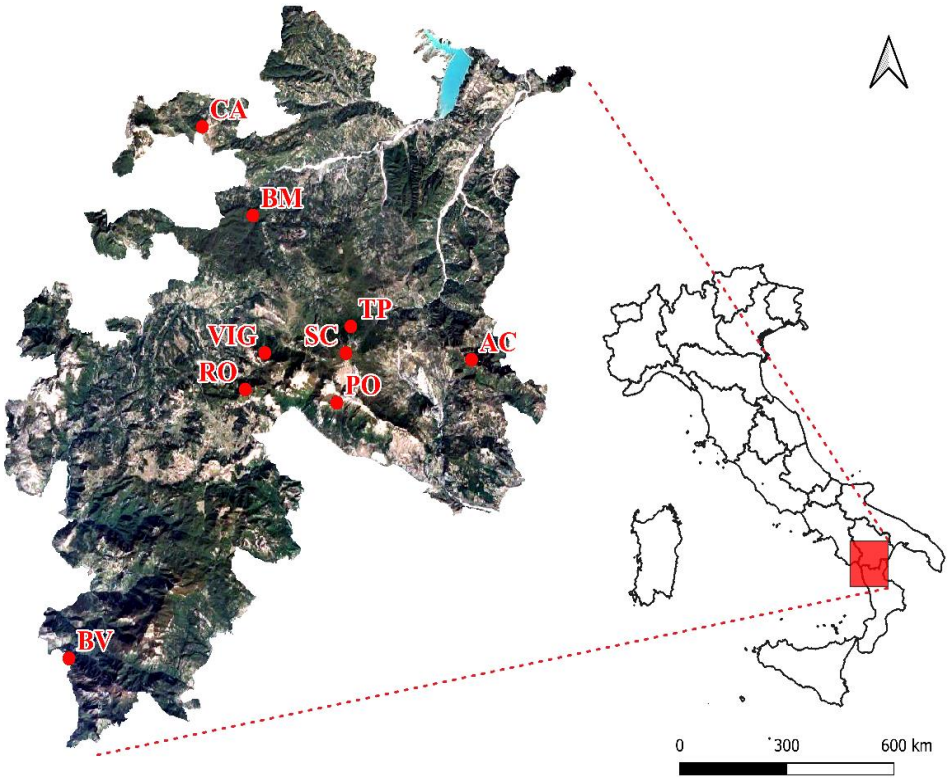

Figure 1.1. Study areas within the Pollino National Park, Italy. Right: the location of the Pollino National Park in Italy. Left: the spatial distribution of the 9 OGFs within the area of the Pollino National Park. BV (Buonvicino), BM (Bosco Magnano), CA (Vaccarizzo), AC (Monte Sparviere), TP (Cugno dell'Acero), RO (Cozzo Ferriero), VIG (Grattaculo), PO (Pollinello) and SC (Serra di Crispo).

1) **Buonvicino (BV)** – Holm oak (*Quercus ilex*) forest at ~850 m a.s.l., representing Mediterranean old-growth conditions on lower slopes and forming the xeric limit of the studied gradient. 2) **Bosco Magnano (BM)** – Mixed *Fagus sylvatica–Quercus cerris* forest (~850 m a.s.l.), along the Peschiera River, representative of structurally diverse low- to mid-elevation stands. 3) **Bosco Vaccarizzo (CA)** – Beech–silver fir forest (~950 m a.s.l.), transitional between

temperate deciduous and montane conifer zones, allowing comparison of mixed-species structural patterns.

4) **Monte Sparviere (AC)** – Maple-dominated forest (1200–1500 m a.s.l.) with multiple *Acer* species on nutrient-rich soils, characterised by multilayered canopies and high compositional heterogeneity, including all the main Mediterranean species, such as Lobel's maple (*Acer cappadocicum* Gled. subsp. *lobelii*) and Montpellier maple (*Acer monspessulanum* L.). 5) **Cugno dell'Acero (TP)** – Mixed *Abies alba–Fagus sylvatica* stand (~1400 m a.s.l.) with very tall fir trees, representing advanced structural development under minimal disturbance, which contributes to its ecological value (Ripullone et al., 2016). 6) **Cozzo Ferriero (RO)** – Pure beech forest (~1750 m a.s.l.), UNESCO World Heritage site, with numerous monumental individuals, some of which exceed 500 years old, representing reference conditions for high structural maturity and long-term ecological continuity. 7) **Grattaculo (VIG)** – High-altitude beech forest (~1750 m a.s.l.) with a distinctive understory of endemic and microthermic species (*Asyneuma trichocalycinum*, *Ranunculus brutius* and *Lamium galeobdolon*), highlighting floristic responses to montane microclimates. 8) **Pollinello (PO)** – High-elevation beech stand (~1950 m a.s.l., UNESCO site in 2021) hosting some of the oldest beech trees in Europe and remarkable vascular plant species such as the holly fern (*Polystichum lonchitis* L.), exemplifying structural and floristic adaptation near the tree line. 9) **Serra di Crispo (SC)** – Bosnian pine (*Pinus heldreichii*) stand (1850–2130 m a.s.l.), included as an extreme case of structural longevity and low disturbance, vegetating very close to other stands that contain *Italus*, Europe's oldest dated trees (1,236 years) (Piovesan et al., 2019b).

Table 1.1. Information about the 9 examined OGFs: site abbreviation, forest type, site of community importance (SCI code), geographical coordinates (latitude and longitude), area (in hectares), elevation range (in metres), living tree volume (LTV), maximum stand age, maximum tree height (Max height), and maximum diameter at breast height (Max diameter).

Abb.	Forest type	SCI code	Coordinates		Area (ha)	Elevation (m)	LTV (m^3)	Max Age	Max height	Max diameter	Main and sporadic tree species
			Lat	*Long*							
BV	Holm oak forest	IT9310032	39.685	15.889	20	850	551	140	20	150	Holm oak forest. Dominant: *Quercus ilex* L. Sporadic: *Acer campestre* L; *Fraxinus ornus* L.; *Crataegus monogyna* Jacq.; *Alnus cordata* L.; and *Quercus pubescens* Willd.
BM	Mixed forest	IT9210040	40.05	16.105	18	850	516	261	50	150	Mixed forest Codominant: *Fagus sylvatica* L. and *Quercus cerris* L., Sporadic: *Abies alba* Mill.; *Carpinus betulus* L.; *Alnus glutinosa* L.; and *Ilex aquifolium* L.
CA	Mixed forest	IT9210070	40.124	16.048	21	950	349	231	30	160	Mixed forest Codominant: *Fagus sylvatica* L., and *Abies alba* Mill. Sporadic: *Alnus cordata* Loisel.; *Acer campestre* L.; *Quercus cerris* L.; *Quercus pubescens* Willd.; and *Ilex aquifolium* L.
AC	Maple forest	IT9310019	39.928	16.354	72	1300	478	187	29	110	Maple forest. Codominant: *Acer campestre* L.*; Acer opalus* Mill.*; Acer pseudoplatanus* L. Sporadic: *Fagus sylvatica* L.; *Abies alba* Mill.; and *Alnus cordata* Loisel.
TP	Mixed forest	IT9210075	39.957	16.216	83	1400	635	329	36	110	Codominant: *Abies alba* Mill.; and *Fagus sylvatica* L. Sporadic: *Pyrus communis* L.; and *Quercus cerris*
RO	Beech forest	1133ter-045	39.906	16.094	70	1750	582	398	28	125	Pure beech: *Fagus sylvatica* L
VIG	Beech forest	IT9210125	39.936	16.117	54	1750	388	428	26	85	Pure: *Fagus sylvatica* L.; Sporadic: *Acer cappadocicum* Gled. subsp. *lobelii*
PO	Beech forest	1133qui-082	39.896	16.167	20	1950	450	400	21	68	Pure: *Fagus sylvatica* L
SC	Bosnian Pine	IT9210245	39.935	16.21	100	2050	53	305	14	160	Pure: *Pinus heldreichii* Christ. subsp. *leucodermis*

2.3 Field sampling

Within the core area of each site, a 1-hectare plot was established and subdivided into 25 subplots of 400 m² each (Fig. 1.2). Due to topographical constraints (aspect, slope etc.) the sample area in certain forest stands was reduced (CA = 0.36 ha, RO = 0.68 ha, PO = 0.64 ha, BV = 0.40 ha, and VIG = 0.64 ha).

Figure 1.2. **Sampling scheme.** The 1-hectare plot was divided into 25 subplots measuring 20 x 20 m (400 m²), which were catalogued following an alphanumeric code and oriented according to site slope.

Subsequently, vascular plant species' composition and abundance were recorded in each subplot. Likewise, geographical coordinates and topographical data, i.e., elevation, slope and aspect, were recorded and reported in the UTM 32N WGS 84 system.

Deadwood components, including standing dead trees (SDT), snags, downed dead trees (DDT), coarse woody debris (CWD) and stumps, were measured using different protocols. For SDT, DDT and snags, we measured the tree diameter at breast height (DBH) when greater than 5 cm and height (h) when greater than 130 cm. CWD was recorded for fragments with a diameter greater than 5 cm and a length of over 100 cm. Each fragment was classified according to the decay classes proposed by Hunter (1990). For stumps, we measured upper diameter (when greater than 5 cm) and height. Finally, a complete inventory of living trees, shrubs and the regeneration layer was performed using a 5 cm DBH and a 130 cm height threshold.

We also recorded tree species, crown features, tree inclination angles, and spatial arrangement. By considering all investigated OGFs, a total of 168 subplots were surveyed.

3. Data Analysis

We calculated 24 structural variables easily obtainable from routinely collected data in forest monitoring programmes (Chirici et al., 2011), including living tree basal area, canopy cover, coarse woody debris volume, number of living trees, number of trees with diameters over 40 cm, number of diameter classes, number of decay classes, necromass' volume, height standard deviation and maximum diameter at breast height (Tab. 1.2). In particular, the living tree, DST and DDT volume was obtained through double-entry volume equations from the Italian National Forest Inventory. While for deadwood components such as snags, stumps and CWD, the following equation was used (Eq. 1.1):

$$\text{(Equation 1.1)} \quad V = (\pi * h/3) * (R^2 + r^2 + (R * r)$$

Where *V* is the volume, *h* the height, *R* the major radius, and *r* the minor radius.
Before performing any analysis, a preliminary statistical test was conducted to identify potential outliers. As a result, the SC site, significantly different from the other stands, was excluded to prevent bias in results, reducing the sample size from 168 to 143.

Table 1.2. List of structural attributes used in this study at the subplot scale.

Abbreviation	Variable	Unit of measure
BA_living_tree	Basal area living tree	m^2
BASnagST	Basal area of Snag and Dead standing tree	m^2
Canopy_cover	Canopy cover	%
Vol_CWD	Volume Coarse Woody Debris	m^3
Density_living_tree	No. Living trees	No. trees
DensSnagST	No. Snag & Dead standing trees	No. trees
Vol_necromass	Volume necromass	m^3
Vol_living_tree	Volume of living trees	m^3
N_dbh	No. Diameter class	No. classes
N_decay_classes	No. Decay classes	No. classes
Vol_SnagST	Volume Snag and Dead standing tree	m^3
n_dbh_40	No. Tree with DBH > 40	No. trees
n_dbh_50	No. Tree with DBH > 50	No. trees
n_dbh_70	No. Tree with DBH > 70	No. trees
Tree_rich	No. Tree species	No. tree species
Vol_stump	Volume stump	m^3
Vol_ddt	Volume of downed dead tree	m^3
Dom_height	Average of the 5 highest trees	m

QMD	Quadratic mean diameter	cm
H_sd	Height Standard deviation	m
Gini	Gini index (basal area)	m^2
dlR	Dead-to-live ratio	m^3
dbh_max	Max diameter	cm
dbh_min	Min diameter	cm

3.1 Forest structure assessment

The SHI was calculated for each subplot, following the methodology suggested by Sabatini et al. (2015). SHI is a simple aggregated index that includes several pieces of information developed to estimate the forest's structural complexity. To compute the SHI values, a systematic multi-step process was adopted: 1**)** *Data cleaning*: outliers were removed based on their interquartile range. A preliminary selection was made by excluding all variables with a kurtosis > |2|. All eligible variables were then reduced by pairwise correlation using Pearson's coefficient $r > 0.55$. Note that, before their exclusion, all unsuitable variables were statistically transformed to normalise their distribution and make them appropriate for analysis.

Among these variables, Density_living_tree (DLT.log), n_dbh_40 (n_dbh_40.log) and QMD (qmd.log) were treated by applying a logarithmic transformation, while N_dbh (ndbh.sq), n_dbh_50 (n_dbh_50.sq) and Dom_height (Dom_height.sq) were processed by a square root transformation. Finally, Vol_necromass (nec.tuk) and dlR (DLR.tu) were adjusted via Tukey's transformation. 2) *Statistical tests for PCA*: selected variables were tested for Principal Component Analysis (PCA) through the Kaiser-Meyer-Olkin and Bartlett tests. 3) *PCA implementation*: PCA was then performed using the functions provided by the 'FactoMineR' and 'factoextra' packages (Kassambara et al., 2017) available in R Studio (ver. R-4.3.1). Based on the contribution from the first 3 axes, a subset of 9 attributes was selected, including BA_living_tree, dbh_max, H_sd, N_decay_classes, DLT.log, Dom_height.sq, dbh_40.log, dbh_50.sq and DLR.tu. 4) *Quartile classification*: the 9 variables were then classified into quartiles (corresponding to the 12th, 37.5th, 62.5th, and 87.5th percentiles). A score from 0 to 10 was assigned to each quartile.

Lastly, to ensure a uniform score distribution, the linear regression model was applied. 5) *SHI derivation*: for each microplot, we summed the individual structural attribute scores to calculate SHI values, then transformed them into percentage values. To investigate the relationship between forest structure heterogeneity and topography, each topographical variable was divided into three

quantile-based groups. Finally, SHI distribution was tested using the Kruskal-Wallis's test to assess potential differences within the identified topographic groups.

3.2 Canonical Correspondence Analysis

CCA is a multivariate technique renowned for its effectiveness in revealing complex relationships (Chahouki et al., 2011), and was employed here to further study how topographical factors affect forest complexity. This model is reliable even when some unimodal species-environment interactions are not satisfied (Ramette, 2017), and in the case of community records with a high proportion of zero values. Before analysis, the aspect data were transformed by applying the cosine function to derive a 'northness' variable, ranging from +1 (north) to -1 (south), and the sine function for the 'eastness' variable, also ranging between +1 (east) and -1 (west).

All variables were standardised using the '*decostand*' function and 'range' method, available in the vegan R package (Oksanen et al., 2024). A correlation matrix was computed to detect and exclude all variables with a Pearson's coefficient greater than 0.60. Excluding highly correlated variables prevents data redundancy, improving the CCA clustering and model (Tanioka & Yadohisa, 2012). The CCA was performed by using the '*cca*' function of the vegan package. A Monte Carlo permutation test was performed using 999 random iterations. The model significance was assessed using the '*anova.cca'* function, and the topographical variables' contribution was estimated by applying the '*anova.term*' function.

3.3 Vascular plant species composition

To investigate patterns of plant species diversity, we run a PCoA on presence/absence data of vascular plant species, which is particularly effective for data unsuitable for Euclidean distance measures. Before running the PCoA, species occurring in less than 3 subplots were excluded (McCune and Grace, 2002).

As a result, the original dataset decreased from about 300 species to 151 species. We adopted the Jaccard similarity index to derive the distance matrix for the PCoA, for which we used the '*pcoa*' function from the bee package (Paradis et al., 2019). The first two PCoA components were then used to perform a correlation analysis with the original species abundances, employing the '*cor2m*' function in the ecodist package (Goslee & Urban, 2007) to identify the most relevant taxa. The

vascular plant species with a correlation greater than 0.6 were selected and discussed (Chytrý et al., 2024). Subsequently, Spearman's Rank Correlation was applied utilising the '*cor.test*' function to examine the relationship between SHI values and the first three PCoA axes.

3.4 Variation Partitioning Analysis

Variation Partitioning (VP) was conducted to assess the shared and distinct contributions of structural forest attributes and topographic variables in explaining vascular plant species composition and distribution. We focused especially on the links between forest structural attributes and vascular plant composition, using topographical variables as covariates.

Our original datasets were standardised by removing all highly correlated variables (Pearson's $r > 0.60$). The first three PCoA axes, representing the main gradients in vascular plant species composition and distribution, were employed as response variables for the VP model. Model accuracy was estimated by performing a Redundancy Analysis (RDA), first on the complete model, including both structural and topographic variables, and then considering each set of variables to evaluate their relative contribution. Subsequently, the statistical significance of the models was tested using the '*anova*' function available in the vegan package. Finally, the statistical significance of each attribute was examined for "*terms*" by employing the '*anova*' function, while the variance inflation factor (VIF) was assessed to ensure the absence of multicollinearity.

4. Results

4.1 Key forest attributes and structure complexity

The PCA, performed as part of the SHI, proved essential for identifying key structural attributes, with 62.9% of the total variance accounted for by the first three PCA dimensions. Dimension 1 (23.2%) was linked to tree size and basal area, i.e., BA_living_tree and dbh40.log. Conversely, Dimension 2 (21.0%) was associated with tree height heterogeneity and greater diameter classes (dbh50.sq). However, additional structural attributes, such as Dom_height.sq and H_sd, increased the relevance of height-related metrics in explaining vertical complexity (Appendix S2, Fig. S1.1). Finally, Dimension 3 (18.7%) highlighted metrics associated with deadwood volume and decay classes (DLR.tu and N_decay_classes) (Appendix S2, Fig. S1.2).

These variables fulfilled a large part of the 8 sources of heterogeneity proposed by Sabatini et al. (2015), providing a detailed representation of the forest structure diversity at the considered sites (Appendix S1, Tab. S1.1). The SHI distribution (Fig. 1.3) shows a considerable variation among the sites. The highest SHI values were found in beech and mixed forests, i.e., RO (73.65%), TP (72.84%), and VIG (65.52%). Conversely, the lowest value was found in a pure holm oak forest, i.e., BV (55.60%), BM (58.41%).

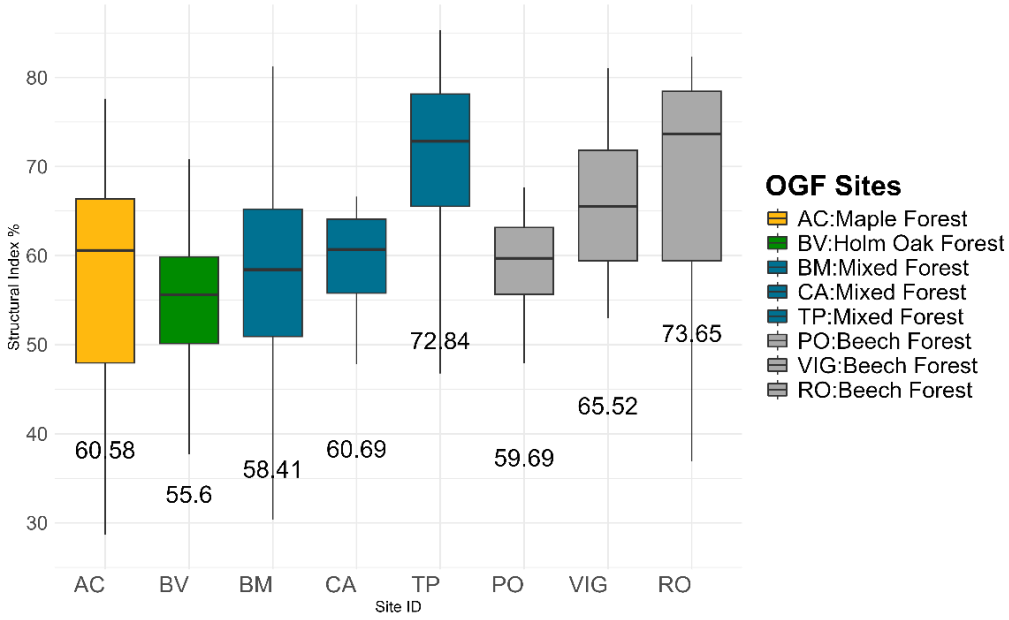

Figure 1.3. SHI values distribution across sites. Whiskers indicate the minimum and maximum within 1.5 × IQR, boxes show the 25th–75th percentile, and horizontal lines represent medians. Site-specific means are reported below each box, with colours denoting forest types: AC = Maple (orange), BM/CA/TP = Mixed (blue/light blue), BV = Holm Oak (green), PO/RO/VIG = beech (grey).

In addition, Kruskal-Wallis tests (Fig. 1.4) provided valuable insights about the role of topography in shaping forest structure complexity. Elevation emerged as a key factor significantly affecting SHI values, as evidenced by findings across all three defined groups (Chi-square = 12.686, *p*-value = 0.001759). Similarly, Slope was found to have a statistically significant effect on SHI values (Chi-square = 8.094, *p*-value = 0.017), indicating that changes in terrain steepness might be associated with considerable variability in forest structure.

Conversely, groups related to the aspect_cos and aspect_sin did not show any significant variations in SHI values (p-value = 0.38 and 0.30, respectively), suggesting that terrain orientation had less relevance.

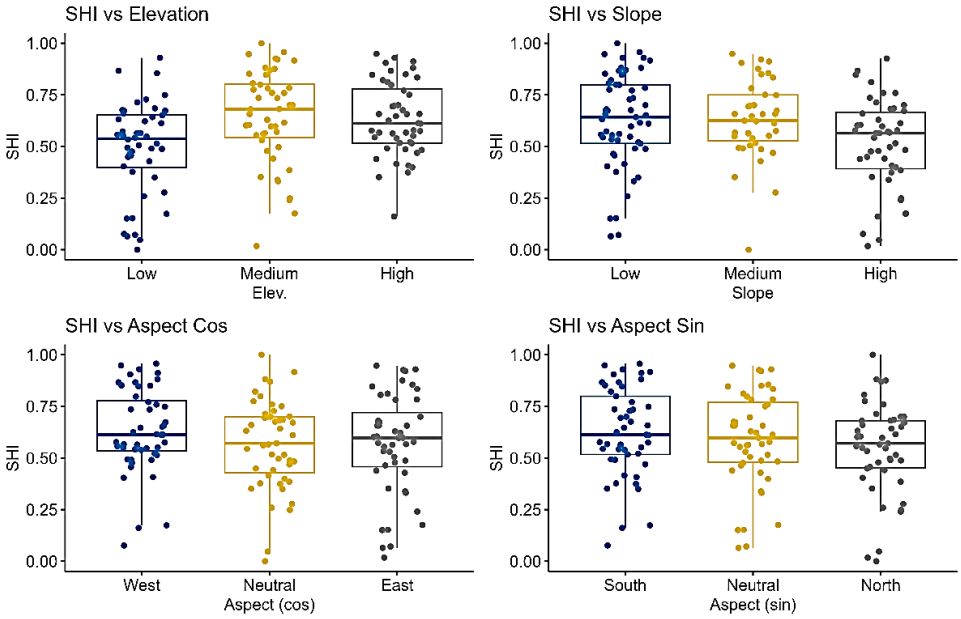

Figure 1.4. SHI distribution across topographical variable classes. Each box plot represents the distribution of SHI values within the respective categories, highlighting the variability of forest structure in response to these environmental factors. In the top row, SHI values are compared across the identified Elevation and Slope classes, while in the bottom row, the SHI variations are shown with respect to aspect_cos and aspect_sin.

4.2 Topography partially drives forest structure complexity

In the CCA, topographic variables contributed to 18.79% of the total variance of structural attributes (Tab. 1.3).

Table 1.3. Partitioning of the scaled Chi-square showed database variability explained by the constrained and unconstrained components. Here, the total inertia (0.52116) is referred to the overall model variability. Of this, the constrained inertia (0.09791, 18.79%) represented the variance expressed by the topographic variables. Conversely, the unconstrained inertia (0.42325, 81.21%) represented the unexplained model variance, which could be attributed to other factors not included in this analysis.

Partitioning of scaled Chi-square		
	Inertia	***Proportion***
Total	0.52116	1.0000
Constrained	0.09791	0.1879
Unconstrained	0.42325	0.8121

However, most of the variance (81.21%) was not explained by topography, suggesting an effect from other factors, including past disturbance events (human and natural), soil type, or climatic context. Especially elevation, slope and aspect (sin and cos) played a key role in modelling forest structure variations (Fig. 1.5). Relevant attributes, such as coarse woody debris volume (Vol_CWD), number of decay classes (N_decay_classes), necromass volume (Vol_necromass), and basal area of living trees (BA_living_trees), frequently employed in the OGF's definition, were mainly located along the negative section of the CCA1 axis. Such attributes, representative of mature and undisturbed forest ecosystems, were oriented towards PO, RO and VIG sites, characterised by greater elevation and slope.

Whereas attributes such as tree richness (Tree_rich), maximum diameter at breast height (dbh_max), canopy cover (Canopy_cover), height standard deviation (H_sd), and Gini coefficient (based on basal area of diameter classes; Gini) were positively correlated with the CCA1 axis and related to sites at lower altitude and slope, such as CA, BV and BM. Additional attributes, such as Vol_stump, BA_snagST and N_dbh, located in the upper quadrant, appeared instead to be related to the TP site.

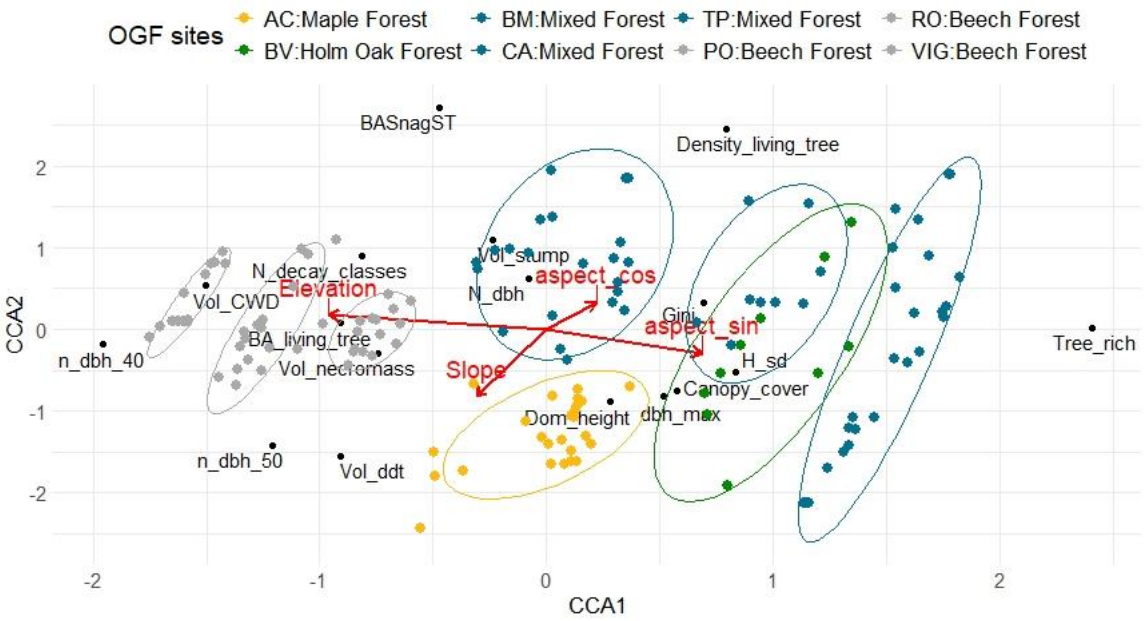

Figure 1.5. Ecological gradients and OGFs structure. The CCA biplot shows the main relationships between structural attributes (in black) and topographic variables (in red) within the studied sites (points and ellipses). Elevation and slope were found to be the main variables affecting OGFs' variability, clustering sites in different areas. Structural attributes such as N_decay_classes and BA_living_tree were prominent in sites such as RO, PO, and VIG. Other attributes, including Density_living_tree, H_sd, Canopy_cover, and dbh_max, in contrast, clustered sites as CA, BV and BM.

Finally, the permutation test confirmed the CCA model accuracy (Appendix S1, Tab. S1.2). In the CCA, Elevation was the most significant variable, with the highest Chi-square value (0.05719) and F-ratio (18.6466); while Slope showed a Chi-square = 0.02150, F = 7.0087.

Both these variables, however, were highly significant (Tab. 1.4). Also, aspect_cos and aspect_sin contributed significantly, even if aspect_cos had lower significance (F = 2.1302). Conversely, the remaining variance (Chi-square = 0.42325) accounted for the unexplained proportion.

Table 1.4. Topographic variable's contribution.

Permutation test for CCA under reduced model (Terms)				
Number of permutations: 999				
	Df	**ChiSquare**	**F**	**Pr(>F)**
Elevation	1	0.05719	18.6466	0.001 ***
Slope	1	0.02150	7.0087	0.001 ***
aspect_cos	1	0.00653	2.1302	0.028 *
aspect_sin	1	0.01269	4.1384	0.001 ***
Residual	138	0.42325		

4.3 Vascular plants cluster across OGFs

The first three PCoA components explained 36.84% of the total variance, capturing the main variation affecting the vascular plant species' composition and distribution within the examined OGFs. The PCoA biplot (Fig. 1.6) showed three distinct clusters: pure beech forests (PO, RO, and VIG) in the middle right side; mixed temperate forests (CA, TP, BM, and BV) in the upper left quadrant; and the AC site in the lower left quadrant.

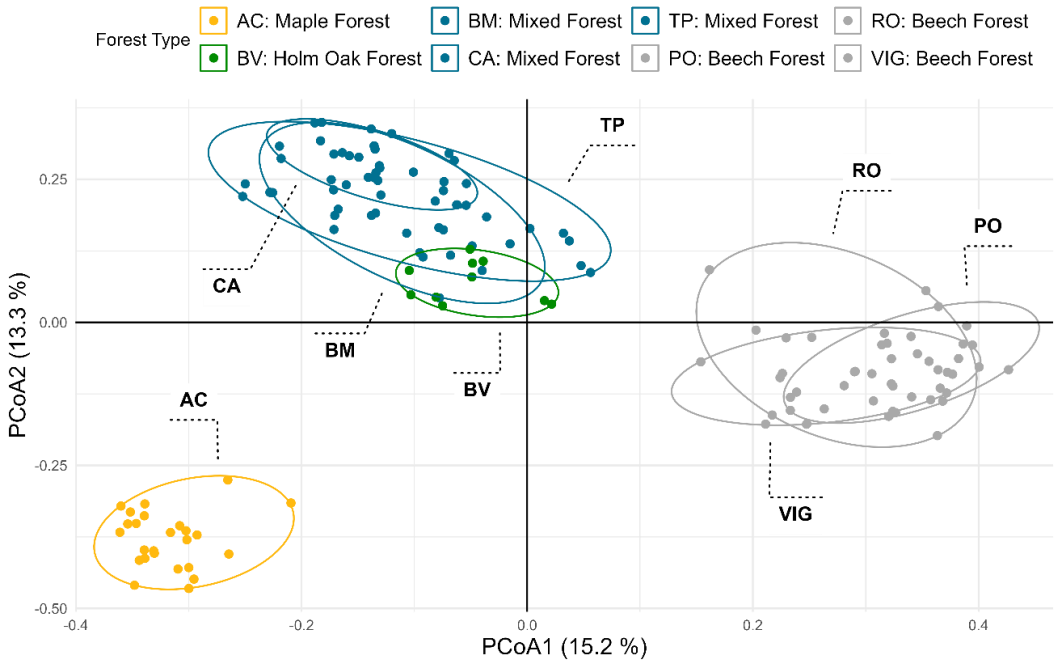

Figure 1.6. **PCoA ordination based on vascular plant species dissimilarities across OGF sites**. Together, the first two axes explained 28.5% of the total variance. In this graph, each point represented a subplot, marked and grouped by ellipses according to their site.

Species typical of temperate European deciduous forests were commonly found across the examined sites. Nine species, including *Polystichum setiferum*, *Lactuca muralis*, *Aremonia agrimonioides*, and *Daphne laureola*, were common to all three groups, while 18 species, including *Sanicula europaea*, *Galium odoratum*, *Viola riviniana*, *Cardamine chelidonia*, and *Clinopodium grandiflorum*, were found exclusively in mixed forests and beech forests, highlighting the floristic affinity of the two forest groups dominated by *Fagus sylvatica*.

In contrast, the differentiation between beech forests and mixed forests was determined by the presence of microthermic species in the former (e.g., *Adenostyles australis*, *Asyneuma trichocalycinum*, *Senecio squalidus*, and *Carduus affinis*) and mesophilous macrothermic species in the latter (e.g. *Ilex aquifolium*, *Ruscus aculeatus*, *Hedera helix*, and *Cyclamen hederifolium*).

Notably, the species characterising beech forests were biogeographically relevant, being endemic and/or South-European *orophilous* species (Di Pietro, 2009; Dillenberger & Kadereit, 2013; Peruzzi et al., 2015). AC was distinguished by the presence of eutrophic/nitrophilous species, such as *Alliaria petiolata, Arctium lappa,* and *Urtica dioica*. Its floristic affinities with mixed or beech forests were partly mediated by eutrophic taxa, such as *Geum urbanum, Rumex sanguineum,* and *Arum cylindraceum,* with the former, and *Hordelymus europaeus, Elymus caninus, Galium aparine, Anthriscus nemorosa, Epilobium montanum,* and *Ranunculus brutius* with the latter.

Species mostly found in high altitude beech forests, such as *Adenostyles australis*, *Asyneuma trichocalycinum,* and *Senecio squalidus*, or also in mixed forests, such as *Galium odoratum*, and *Clinopodium grandiflorum*, were positively correlated with PCoA1, whereas a negative correlation was observed in species found in maple forests, such as *Arum cylindraceum, Fraxinus excelsior,* and *Urtica dioica*. PCoA2 showed a positive correlation to species such as *Abies alba*, *Quercus cerris, Ilex aquifolium,* and *Ruscus aculeatus*, typically observed in the studied mixed forests.

In contrast, species with a negative correlation, such as *Doronicum orientale*, *Elymus caninus*, *Fraxinus excelsior*, *Galium aparine*, *Hordelymus europaeus*, *Poa nemoralis*, and *Ranunculus brutius*, emphasised areas with nutrient-rich soil, providing a valuable insight to distinguish forest stands according to their climatic and soil properties.

Finally, a negative correlation was observed between PCoA3 and a few species, including *Abies alba*, *Cardamine chelidonia* and *Viola riviniana*, reflecting an ecological gradient consisting of wet, shaded, undisturbed forests with complex vertical structures (Appendix S2, Fig. S1.3). Spearman's correlation analysis between the PCoA axes and SHI values provided additional insights. Specifically, PCoA1 showed a non-significant correlation with SHI (p-value = 0.55), while elevation was the primary factor influencing this component (Appendix S2, Fig. S1.4). In contrast, PCoA2 was strongly and positively correlated with SHI values (p-*value* = 0.00005), underscoring the key role of forest structure in shaping plant species distribution, particularly in

mixed temperate multilayered forests, with an understory composed mainly of species such as *Ilex aquifolium* and *Ruscus aculeatus* (Appendix S2, Fig. S1.5). Likewise, PCoA3 showed a positive correlation with SHI (p-value = 0.0099), suggesting that greater structural complexity is associated with a decreased presence of shade-tolerant species such as *Abies alba*, *Cardamine chelidonia*, and *Viola riviniana* (Appendix S2, Fig. S1.6). All these outcomes suggest that forest structure is a significant factor in plant species distribution, requiring a more detailed investigation.

4.4 The role of forest structure and topography in shaping the vascular plant species distribution

Based on the previous analyses, a VP was conducted to deepen our understanding of the main topographical and structural factors influencing the composition of flora within the study areas. In particular, VP analysis allowed us to isolate forest structure and topography influence, revealing their shared and distinct contribution to the variability observed in the vascular plant composition (Appendix S2, Fig. S1.7). According to the VP results (Tab. 1.5), 31.2% of the total variance in vascular plant species composition was explained by the combined effect of forest structural attributes and topographical variables. More specifically, structural attributes accounted for 23.5% of the variance, whereas topographical variables contributed only 12.8%. Nevertheless, a substantial proportion of the variance (32.4%) remained unexplained, reflecting the inherent complexity of old-growth floristic assemblages — where stochastic processes, fine-scale disturbances and non-linear successional dynamics collectively shape vascular plant species composition, resulting in non-linear relationships that cannot be fully accounted for by a single set of forest structure or topography predictors.

Table 1.5. Partitioning of variance in vascular plant composition explained by (X1) forest structure and (X2) topography (full RDA model). Reported values include adjusted R^2, individual fractions, and the percentage of variance explained by pure effects, shared effects, and residuals.

Partition of variance in RDA				
Fraction	**Description**	**Adj.R^2**	**Individua fraction**	**Explained variance (%)**
X1	Forest structure effect	0.54834	0.23538	23.5
X2	Topography effect	0.44102	0.12806	12.8
X1 + X2	Shared effect	0.67640	0.31296	31.2
Residuals			0.32360	32.3

The statistical significance of the model was also confirmed by a permutation test (Tab. 1.6), thereby further supporting the strong relationship between structural attributes and topography in explaining the distribution and composition of vascular plant species.

The RDA ordination plot (Fig. 1.7) provides a visual representation of the obtained results, highlighting clearly how plant species distribution is affected by forest structure and topographical variables.

Table 1.6. Permutation test for the RDA model, including forest structural attributes and topographical variables.

Permutation test for RDA under reduced model				
Number of permutations: 999				
	Df	**Variance**	**F**	**Pr (>F)**
Model	19	0.155842	16.512	0.001 ***
Residual	122	0.060603		

Axis 1 (RDA1 = 32.9%) primarily reflected topographic gradients, being positively associated with elevation, slope, and the abundance of medium diameter trees (n_dbh_40). Conversely, it showed negative relationships with tree species richness, dominant height (Dom_height), and aspect (aspect_sin).

Axis 2 (RDA2 = 26.4%), on the other hand, captured variation in different stand structural attributes. Indeed, this axis was positively associated with tree density (Density_living_tree), canopy cover (Canopy_cover), and number of decay classes (N_decay_classes), while showing a negative association with tree species richness (Tree_rich).

The key role of forest structure and topographical variables also emerged through the second permutation test (Tab. 1.7). Basal area of stumps and standing dead trees (BASnagST), canopy cover (Canopy_cover), number and volume of living trees (Density_living_tree; Vol_living_tree), volume of coarse woody debris (Vol_CWD), number of decay classes (N_decay_classes), number of trees with dbh > 40, 50 and 70 cm (n_dbh_40; n_dbh_50; n_dbh_70), tree species richness (Tree_rich) and height heterogeneity (H_sd) all showed a highly significant effect on the vascular plant species composition (p = 0.001).

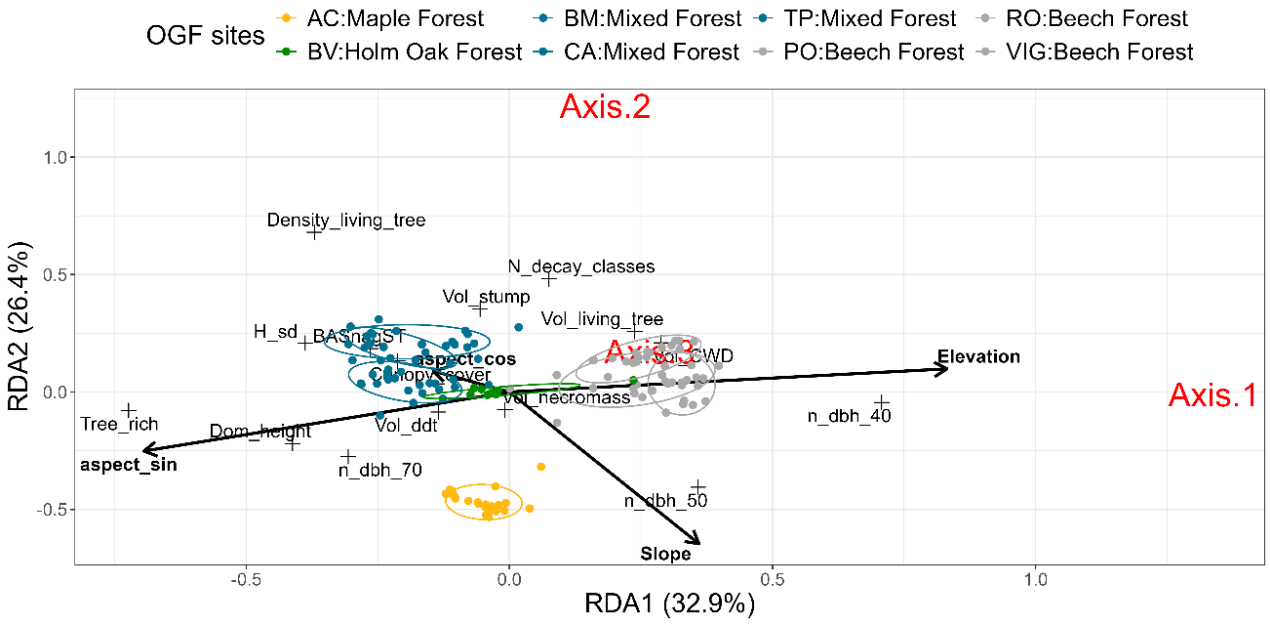

Figure 1.7. RDA biplot (including structural, floristic, and topographical data). RDA biplot shows the relationships between vascular plant species assemblage (response variable), explanatory variables (structural and topographical variables), and OGF sites (colored according to forest type).

Furthermore, topographical attributes such as elevation (Elevation) and slope (Slope), as well as, with minor relevance, aspect in its sine and cosine transformations (aspect_cos; aspect_sin), also revealed considerable influences ($p = 0.02$). Conversely, no significant findings were observed for necromass volume (Vol_necromass) or some of its components, such as stump (Vol_stumps) and downed dead trees volume (Vol_ddt). These variables were consistent not only with the findings of previous studies but also with the commonly accepted criteria used to define OGF worldwide.

In conclusion, the Redundancy Analysis (RDA) revealed that the clustered plant distribution of the four old-growth forest compositional types is driven by a complex interaction between site topography and structural tree traits. Surprisingly, stand structure proved to be more influential on these interrelationships, with attributes like dominant height, canopy cover, density of large trees and living trees, and the basal area of snags playing a major role in driving the clustering of forest communities.

Table 1.7. Permutation test results for individual forest structural and topographical variables in the RDA model.

Permutation test for RDA under reduced model (by Term)					
Number of permutations: 999					
Variable	**Abbrevation**	**Df**	**Variance**	**F**	**Pr(>F)**
Basal area of Snags and standing dead trees	BASnagST	1	0.019282	38.82	0.001 ***
Canopy cover	Canopy_cover	1	0.007775	15.65	0.001 ***
Volume of coarse woody debris	Vol_CWD	1	0.010552	21.24	0.001 ***
No. Living tree /ha	Density_living_tree	1	0.028985	58.35	0.001 ***
Volume of necromass	Vol. necromass	1	0.000936	1.88	0.129
Volume of living trees	Vol_living_trees	1	0.007322	14.74	0.001 ***
No. Decay classes	N_decay_classes	1	0.008133	16.37	0.001 ***
No. Tree with DBH > 40	n_dbh_40	1	0.018069	36.37	0.001 ***
No. Tree with DBH > 50	n_dbh_50	1	0.008576	17.26	0.001 ***
No. Tree with DBH > 70	n_dbh_70	1	0.003503	7.05	0.001 ***
No. Tree species	Tree_rich	1	0.008032	16.17	0.001 ***
Volume of stump	Vol_stump	1	0.000856	1.72	0.144
Volume of downed dead trees	Vol_ddt	1	0.000620	1.25	0.282
Dominant height	Dom_height	1	0.001329	2.68	0.061
Height Standard deviation	H_sd	1	0.005115	10.30	0.001 ***
Elevation	Elevation	1	0.019233	38.72	0.001 ***
Slope	Slope	1	0.004636	9.33	0.001 ***
Aspect (North - South)	aspect_cos	1	0.001195	2.40	0.066
Aspect (East - West)	aspect_sin	1	0.001692	3.41	0.019 *
Residual		122	0.060603		

5. Discussion

The present study investigated the environmental factors affecting forest structural and compositional complexity of nine old-growth forests (OGFs) within Pollino NP. The findings provide valuable insights into how topographic, structural, and floristic factors interact to shape spatial heterogeneity and ecological attributes that characterise these forest ecosystems.

5.1 Topographic gradient significantly drives forest structural heterogeneity

Our results provide support for demonstrating that topography exerts a significant influence on forest structural heterogeneity. Elevation and slope together explained nearly one-fifth of the total variance in structural attributes, confirming that physical gradients shape key dimensions of forest architecture even in highly mature stands.

Structural diversity was largely governed by tree size distribution, basal area, and vertical stratification, complemented by variation in deadwood abundance and decay stages. According to Fantini et al. (2020), lower SHI values are often linked to a decrease in the abundance of large trees, as in the case of PO, and to the removal of dead wood by the local population, as in the case of BV and BM. In contrast, remote stands at higher elevation and on steep slopes—such as RO and VIG—displayed high SHI scores, abundant coarse woody debris, and diverse decay classes, suggesting that reduced accessibility protects structural integrity from anthropogenic disturbance. These findings align with the defining traits of old-growth ecosystems and emphasise how elevation and slope interact to modulate structural maturity.

Indeed, as demonstrated by Badalamenti et al. (2017), certain structural thresholds – such as deadwood volumes exceeding 30 m^3/ha, high basal area, and multilayered canopy – can serve as benchmarks for identifying and prioritising conservation areas in similar ecological contexts.

Local topographic gradients also generate mesoclimatic and microclimatic variation influencing soil moisture, radiation, and temperature regimes (De Frenne et al., 2021; McNichol et al., 2024). Such conditions govern tree growth and mortality, gap dynamics, and regeneration, ultimately affecting the spatial distribution of vertical layers. Although elevation can limit tree growth and canopy height (Ziaco et al., 2012; Sabatini et al., 2015), the large residual variance observed (81%) indicates that additional local drivers — including soil fertility, disturbance history, and climatic context — contribute to structural differentiation, and should therefore be regarded as an ecologically relevant signal rather than a modelling limitation.

Old-growth systems are inherently characterised by non-linear developmental dynamics, including gap-phase cycles, multi-cohort regeneration, and stochastic processes, which do not follow predictable topographic gradients (Nagel et al., 2014). In addition, historical management practices — including selective logging, grazing pressure, and past silvicultural activities — may have resulted in structural changes that persist over decades and cannot be fully captured by topographic variables alone.

In contrast, parameters such as variation in height and diameter distribution and maximum diameter at breast height pointed to greater vertical and horizontal structural heterogeneity, which may potentially support higher biodiversity (Pickering et al., 2024).

The high values of standing dead tree volume and canopy height in site AC may reflect the legacy of recurrent natural disturbances that have a greater impact on taller trees (Jackson et al., 2024), in line with successional trajectories proposed by Oliver & Larson (1996) and Franklin et al. (2002).

5.2 Stand structure and topography as dominants of vascular plant composition

Vascular plant species composition was strongly associated with forest structure and topography. Ordination methods identified three main floristic assemblages - pure beech stands, mixed temperate and maple forests - reflecting differences in structural and topographic variables.
For instance, Adenostyles australis, Asyneuma trichocalycinum, Senecio squalidus, and Carduus affinis, typically occurring in cold, mountain environments, suggest the ecological distinctiveness of high-altitude beech forests. Additionally, the occurrence of certain species, some of which are endemic to Southern European mountains, highlights the biogeographical significance of these communities.

Conversely, species such as Alliaria petiolata, Arctium lappa, and Urtica dioica are characteristic of eutrophic and nitrophilous environments, often associated with recurring disturbance processes (Matuszkiewicz et al., 2024). In fact, their occurrence highlights the understory vegetation's sensitivity to local nutrient enrichment and anthropogenic pressures. In this context, BV and AC sites also showed interesting floristic patterns. BV, a pure low-mountain holm oak forest, exhibited an unexpected similarity in vascular plant composition to mixed forests dominated by beech, silver fir, or turkey oak. This similarity could be related to its location on the slopes facing the Tyrrhenian Sea, where diverse climate conditions may allow holm oak to spread up to higher elevations, promoting its contact with mountainous forests.

In contrast, AC, a stand dominated by maple, exhibited a distinct vascular plant assemblage, thereby emphasising its uniqueness in terms of forest composition, topography, and structure within the studied areas. Specifically, AC was distinguished by the presence of Alliaria petiolata, Arctium lappa, and Urtica dioica, which might be indicative of local disturbances due to grazing.

Moreover, the co-occurrence of such contrasting indicator species demonstrates how forest structure and topographic features could interact with both climatic and disturbance-related factors, ultimately shaping plant species composition and ecological functioning within OGF ecosystems.

Structural attributes showed a leading role in shaping flora diversity, since they were responsible for 23.5% of the total variance, with variation associated with the stand's old-growthness and microclimatic stability. Indeed, the abundance of old or large trees could be essential in stabilising site microclimate, providing a suitable environment for specialised vascular plant species (Lindenmayer 2017).

5.3 Structure and topography integration to explain old-growth dynamics and compositional clustering

Canopy complexity emerged as a critical determinant of understory plant composition, influencing light penetration and microclimatic stability. The number of decay classes further emphasised the ecological significance of deadwood decomposition phases, which enhance soil fertility and provide crucial habitats for saproxylic organisms and herbaceous species (Graf et al., 2022). Together, these features contribute to higher biodiversity and ecosystem multifunctionality. Similarly, tree species richness and deadwood volume were closely associated with vascular plant composition, indicating that complex forest structures promote richer and more stable plant communities.

These attributes delineate a compositional gradient primarily driven by tree species diversity and resource availability: greater canopy and species diversity expand ecological niches, while necromass accumulation supports decomposer communities including fungi, invertebrates, mosses, lichens, and vascular plants (Chećko et al., 2015).

The structural complexity of OGFs functions as both a buffer and a stabilising mechanism. It mitigates the effects of climate extremes and maintains high biodiversity through an intricate network of microhabitats and ecological niches. This complexity enhances resilience by distributing ecological risk among multiple species and functional roles (Ontl et al., 2020).

Site-specific patterns provide further evidence of the structural–floristic linkage. Attributes such as the basal area of snags and standing dead trees, and the number of diameter classes—particularly evident in the TP site—suggest natural regeneration following disturbance events. These features are often associated with structurally heterogeneous stands that exhibit late-successional dynamics and ecological continuity typical of mature, undisturbed forests.

Such traits can serve as valuable indicators of natural forest development and may be used in future research to assess the degree of structural maturity across different forest types and biogeographic regions. The combination of structural and floristic attributes observed in this study could thus guide the identification of ecologically significant stands for conservation and restoration programs. However, their interpretation should always consider local ecological context, forest type, and dominant tree species.

Our findings align with previous studies (Bauhus et al., 2009; Müller & Bütler, 2010) that emphasise the ecological importance of large trees, necromass, and vertical heterogeneity as essential components for maintaining biodiversity. These structural attributes are not merely local characteristics but represent globally transferable principles.

Integrating them into conservation and management frameworks could enhance forest resilience to climate change and sustain biodiversity over the long term—especially considering that just 1% of the largest trees can store up to 50% of a forest's total carbon (Lutz et al., 2018). Forest stands characterised by elevated levels of structural complexity therefore emerge as biodiversity hotspots, underscoring the ecological value of mature and old-growth forests. These insights align with broader conservation frameworks (e.g., Chazdon, 2008; Gauthier et al., 2015) advocating integrative approaches that merge structural, ecological, and socio-economic perspectives. Adopting such multidimensional strategies is essential to safeguard the integrity and functionality of forest ecosystems in the face of accelerating global change.

5.4 Study limitations and opportunities

The present analysis focused on nine OGF sites within Pollino NP. These stands were selected to capture the park's ecological and structural diversity. The selection was based on (i) confirmed evidence of minimal anthropogenic disturbance, (ii) presence of structural indicators of maturity (e.g., large trees, multilayered canopies, and abundant deadwood), and (iii) representation of distinct forest types along altitudinal and bioclimatic gradients. While the sample size may appear limited, it reflects the rarity and spatial restriction of Mediterranean old-growth ecosystems, where undisturbed forest patches are exceptionally scarce and typically confined to remote, topographically complex areas. Accordingly, each site represents an ecologically distinct and irreplaceable reference area, characterised by significant scientific and ecological value.

Based on our results, further validation of SHI across different ecological contexts is necessary to assess its robustness as a synthetic indicator of forest naturalness. The application of the SHI revealed marked differences among the examined OGFs: sites such as RO, TP, and VIG displayed higher structural complexity, whereas BV, BM, and PO showed comparatively lower levels.

For example, the high level of naturalness in PO (Piovesan et al., 2020) was likely not captured by the SHI because topographic factors, particularly elevation and slope, were found to strongly influence structural attributes such as the abundance of large trees and tree height, determining a limit to the bio-space occupied by the canopy.

While structural metrics are essential for characterising forest ecosystems (LaRue et al., 2023), a more holistic assessment would also integrate vascular plant composition, soil properties, and climatic conditions. Since these factors are not included in the SHI assessment, it is possible to assume that SHI provides an overview of forest structures rather than a comprehensive view of their functions. Despite the insights gained when considering topography, unexplained variances point to the need for further research incorporating variables such as disturbance history, soil properties, and stand climate not considered within our surveys (Thom & Seidl, 2016).

Indeed, tools like dendrochronology, soil analysis, canopy temperature by means of satellite data, and microclimate loggers alongside LiDAR/TLS could help to capture key ecological processes that explain variance beyond structural metrics.

Combining these variables with mixed-effects modelling and long-term monitoring will clarify causal pathways, improve predictive power, and make conservation strategies more robust under changing climatic conditions. Overall, long-term ecological monitoring would be particularly valuable for a better comprehension of forest structural dynamics and understanding how forest structure influences floristic responses over time in a changing climate. Integrating these attributes could enhance our capacity to refine conservation strategies and implement adaptive management practices aimed at sustaining the ecological integrity of OGFs in the face of environmental change.

6. Conclusion

This study demonstrates that the ecological complexity of old-growth forests (OGFs) results from the synergistic interaction of structural, topographic, and floristic factors. Topographic gradients shape the physical framework for structural development; structural attributes then govern microclimate, habitat diversity, and species composition; and their interaction defines the spatial clustering of forest communities.

The findings emphasise that effective conservation must move beyond single-metric structural indicators. The Structural Heterogeneity Index (SHI) provides a summary of complexity but should always be interpreted alongside topographic and floristic data.

Although this research focused on Mediterranean mountain OGFs, these mechanisms appear consistent across forest biomes. In temperate and boreal forests alike, topographic variation influences resource distribution and disturbance exposure, while structural heterogeneity mediates ecological processes that sustain biodiversity. Thus, the structural–topographic–floristic framework applied here offers a transferable approach for evaluating forest naturalness, resilience, and ecological integrity across environmental contexts. Mediterranean OGFs, such as those in the Pollino NP, exemplify global processes of self-organisation in long-undisturbed ecosystems, where vertical stratification, large trees, and persistent deadwood maintain functional stability over centuries. These insights reinforce the need to preserve mature and old-growth stands to ensure biodiversity and ecosystem resilience.

Conservation priorities should favour stands with abundant large trees, high deadwood diversity, and multilayered canopies—features that enhance biodiversity, carbon storage, and ecosystem resilience. Where strict protection is not feasible, adaptive management should aim to emulate natural disturbance regimes and promote structural diversification to recover functions typical of old-growth conditions. Further, integrating structural metrics with remote-sensing, dendrochronological, and microclimatic data within long-term monitoring networks can improve our capacity to anticipate forest responses to environmental change. Two crucial implications emerge from these findings. First, conservation strategies must balance socio-economic factors with natural forest dynamics. Socio-economic drivers—such as deadwood timber demand and rural dependency—can disrupt natural processes, reducing structural complexity and long-term resilience.

To address these challenges, strategies should include community-focused management, alternative livelihoods, and financial support that promote local development while ensuring the effective conservation of these unique forests and their ecosystem services (Liu et al., 2022). By adopting this multidimensional perspective, forest conservation can move toward a more holistic understanding of naturalness and resilience. Old-growth forests worldwide—whether Mediterranean, temperate, or boreal—represent irreplaceable benchmarks of ecological continuity and should be managed as living archives of biodiversity and as models for sustainable forest futures.

References

- Badalamenti E, La Mantia T, La Mantia G, Cairone A, La Mela Veca DS (2017). *Living and dead aboveground biomass in Mediterranean forests: Evidence of old-growth traits in a Quercus pubescens Willd. sl stand*. Forests, 8(6), 187. DOI: https://doi.org/10.3390/f8060187
- Baliva M, Palli J, Perri F, Iovino F, Luzzi G, Piovesan G (2024). *The return of tall forests: Reconstructing the canopy resilience of an extensively harvested primary forest in Mediterranean mountains*. Science of The Total Environment, 953, 175806. DOI: https://doi.org/10.1016/j.scitotenv.2024.175806
- Balloffet N, Dumroese RK (2022). *The national reforestation strategy and the REPLANT Act: Growing and nurturing resilient forests*. In Jain, Theresa B, Schuler TM. comp. Foundational concepts in silviculture with emphasis on reforestation and early stand improvement - 2022 National Silviculture Workshop. Proc. RMRS-P-80. Fort Collins, CO: U.S. Department of Agriculture, Forest Service, Rocky Mountain Research Station. 3 p. [online] Available at: https://www.usda.gov/sites/default/files/documents/reforestation-strategy.pdf
- Barnett K, Aplet GH, Belote RT (2023). Classifying, inventorying, and mapping mature and old-growth forests in the United States. Frontiers in Forests and Global Change, 5, 1070372. DOI: https://doi.org/10.3389/ffgc.2022.1070372
- Barredo JI, Brailescu C, Teller A, Sabatini FM, Mauri A, Janouskova K (2021). *Mapping and assessment of primary and old-growth forests in Europe*. EUR 30661 EN, Publications Office of the European Union, Luxembourg, ISBN 978-92-76-34230-4, JRC124671. DOI: 10.2760/13239
- Bauhus J, Puettmann K, Messier C (2009). *Silviculture for old-growth attributes*. Forest Ecology and Management, 258(4), 525-537. DOI: https://doi.org/10.1016/j.foreco.2009.01.053
- Beckschäfer P, Mundhenk P, Kleinn C, Ji Y, Yu D, Harrison R (2013). *Enhanced Structural Complexity Index: An Improved Index for Describing Forest Structural Complexity*. Open Journal of Forestry, 3, 23-29. DOI: 10.4236/ojf.2013.31005
- Blasi C, Michetti L (2005). *Biodiversity and climate*. Biodiversity in Italy contribution to the national biodiversity strategy (pp. 57–66). Rome, Italy: Palombi Editori. [online] Available at: chrome-

extension://efaidnbmnnnibpcajpcglclefindmkaj/https://www.mase.gov.it/sites/default/files/archivio/biblioteca/protezione_natura/ecoregioni_italia_eng.pdf

- Borghi C, Francini S, McRoberts RE, Parisi F, Lombardi F, Nocentini S, Chirici G (2024). *Country-wide assessment of biodiversity, naturalness and old-growth status using national forest inventory data*. European Journal of Forest Research, 143(1), 271-303. DOI: https://doi.org/10.1007/s10342-023-01620-6
- Bruening JM, Dubayah RO, Pederson N, Poulter B, Calle L (2024). *Definition criteria determine the success of old-growth mapping*. Ecol. Indic. 159, 111709. DOI: https://doi.org/10.1016/j.ecolind.2024.111709
- Brumelis G, Jonsson BG, Kouki J, Kuuluvainen T, Shorohova E (2011). *Forest naturalness in northern Europe: perspectives on processes, structures and species diversity*. Silva Fennica vol. 45 no. 5 article id 446. DOI: https://doi.org/10.14214/sf.446
- Burrascano S, Keeton WS, Sabatini FM, Blasi C (2013). *Commonality and variability in the structural attributes of moist temperate old-growth forests: A global review*. Forest Ecology and Management, 291, 458-479. DOI: https://doi.org/10.1016/j.foreco.2012.11.020
- Castellaneta M, Schettino A, Travascia D, Lapolla A, Colangelo M, Marchianò V, Bernardo L, Gargano D, Passalacqua N, Rivelli AR, Misano G, Regina L, Maradei V, Digilio S, Viggiano P, Ripullone F (2023). *I boschi vetusti nel Parco del Pollino: situazione attuale e prospettive future*. Forest@ 20: 22-29. DOI: https://doi.org/10.3832/efor4303-020
- Chahouki M (2011). *Multivariate Analysis Techniques in Environmental Science*. DOI: 10.5772/26516.
- Chazdon RL (2008). *Beyond deforestation: restoring forests and ecosystem services on degraded lands*. science, 320(5882), 1458-1460. DOI: 10.1126/science.1155365
- Chećko E, Jaroszewicz B, Olejniczak K, Kwiatkowska-Falińska AJ (2015). *The importance of coarse woody debris for vascular plants in temperate mixed deciduous forests*. Canadian Journal of Forest Research, 45(9), 1154-1163. DOI: https://doi.org/10.1139/cjfr-2014-0473
- Chirici G, Winter S, McRoberts RE (2011). *National forest inventories: contributions to forest biodiversity assessments*. Springer, Berlin and Heidelberg, Germany, pp. 206. DOI: https://doi.org/10.1007/978-94-007-0482-4

- Chytrý M, Řezníčková M, Novotný P, Holubová D, Preislerová Z, Attorre F, Biurrun I, Blažek P, Bonari G, Borovyk D, Čeplová N, Danihelka J, Davydov D, Dřevojan P, Fahs N, Guarino R, Güler B, Hennekens SM, Hrivnák R, Kalníková V, Kalusová V, Kebert T, Knollová I, Knotková K, Koljanin D, Kuzemko A, Loidi J, Lososová Z, Marcenò C, Midolo G, Milanović D, Mucina L, Novák P, von Raab-Straube E, Reczyńska K, Schaminée JHJ, Štěpánková P, Świerkosz K, Těšitel J, Těšitelová T, Tichý L, Vynokurov D, Willner S, Axmanová I (2024) *FloraVeg.EU – an online database of European vegetation, habitats and flora*. Applied Vegetation Science 27: e12798. DOI: https://doi.org/10.1111/avsc.12798
- Colangelo M, Camarero JJ, Gazol A, Piovesan G, Borghetti M, Baliva M, Ripullone F (2021). *Mediterranean old-growth forests exhibit resistance to climate warming*. Science of the total environment, 801, 149684. DOI: https://doi.org/10.1016/j.scitotenv.2021.149684
- Compagnucci F, Mazzoni F (2002). *Il Territorio dei Parchi Nazionali Italiani*. Quaderni di Ricerca, No. 172, Università degli Studi di Ancona Dipartimento di Economia, Ancona. [online] Available at: https://ideas.repec.org/p/anc/wpaper/172.html
- Concha VC, Caviedes J, Novoa FJ, Altamirano TA, Ibarra JT (2023). *Structural complexity is a better predictor than single habitat attributes of understory bird densities in Andean temperate forests*. Ornithological Applications, Volume 125, Issue 4, 6 November 2023, duad035. DOI: https://doi.org/10.1093/ornithapp/duad035
- De Frenne P, Lenoir J, Luoto M, Scheffers BR, Zellweger F, Aalto J, Hylander K (2021). *Forest microclimates and climate change: Importance, drivers and future research agenda*. Global change biology, 27(11), 2279-2297. DOI: https://doi.org/10.1111/gcb.15569
- Di Pietro R (2009). *Observations on the beech woodlands of the Apennines (peninsular Italy): an intricate biogeographical and syntaxonomical issue*. Mediterranean Botany, 30, 89. [online] Available at: https://www.researchgate.net/profile/Romeo-Di-Pietro-2/publication/272805949_Observations_on_the_beech_woodlands_of_the_Apennines_peninsular_Italy_An_intricate_biogeographical_and_syntaxonomical_issue/links/54ef1ed90cf25238f93bba98/Observations-on-the-beech-woodlands-of-the-Apennines-peninsular-Italy-An-intricate-biogeographical-and-syntaxonomical-issue.pdf
- Dillenberger MS, Kadereit JW (2013). *The phylogeny of the European high mountain genus Adenostyles (Asteraceae-Senecioneae) reveals that edaphic shifts coincide with dispersal*

events. American Journal of Botany, 100(6), 1171-1183. DOI: https://doi.org/10.3732/ajb.1300060

- Fantini S, Fois M, Casula P, Fenu G, Calvia G, Bacchetta G (2020). *Structural heterogeneity and old-growthness: A first regional-scale assessment of Sardinian forests*. Annals of Forest Research, 63(2), 103-120. DOI: https://doi.org/10.15287/afr.2020.1968
- Filibeck G, Adams J, Brunetti M, Di Filippo A, Rosati L, Scoppola A, Piovesan G (2015). *Tree ring ecological signal is consistent with floristic composition and plant indicator values in Mediterranean Fagus sylvatica forests*. Journal of Ecology, 103(6), 1580-1593. DOI: https://doi.org/10.1111/1365-2745.12478
- FOREST EUROPE (2020). *State of Europe's Forests 2020*. p. 392. [online 2025] Available at: https://foresteurope.org/wp-content/uploads/2016/08/SoEF_2020.pdf
- Franklin JF, Spies TA, Van Pelt R, Carey AB, Thornburgh DA, Berg DR, Lindenmayer DB, Harmon ME, Keeton WS, Shaw DC, Bible K, Chen J (2002). *Disturbances and structural development of natural forest ecosystems with silvicultural implications, using Douglas-fir forests as an example*. Forest Ecology and Management, 155: 399-423. DOI: https://doi.org/10.1016/S0378-1127(01)00575-8
- Gauthier S, Bernier P, Kuuluvainen T, Shvidenko AZ, Schepaschenko DG (2015). *Boreal forest health and global change*. Science, 349(6250), 819-822. DOI: 10.1126/science.aaa9092
- Gilhen-Baker M, Roviello V, Beresford-Kroeger D, Roviello GN (2022). *Old growth forests and large old trees as critical organisms connecting ecosystems and human health*. A review. Environmental Chemistry Letters, 20(2), 1529-1538. DOI: https://doi.org/10.1007/s10311-021-01372-y
- Giorgini D, Giordani P, Casazza G, Amici V, Mariotti MG, Chiarucci A (2015). *Woody species diversity as predictor of vascular plant species diversity in forest ecosystems*. Forest Ecology and Management, 345, 50-55. DOI: https://doi.org/10.1016/j.foreco.2015.02.016
- Goslee SC, Urban DL (2007). *The ecodist package for dissimilarity-based analysis of ecological data*. Journal of Statistical Software, *22*, 1-19. DOI: http://hdl.handle.net/10.18637/jss.v022.i07
- Graf M, Seibold S, Gossner MM, Hagge J, Weiß I, Bässler C, Müller J (2022). *Coverage based diversity estimates of facultative saproxylic species highlight the importance of deadwood for*

biodiversity. Forest Ecology and Management, 517, 120275. DOI: https://doi.org/10.1016/j.foreco.2022.120275

- Gray AN, Pelz K, Hayward GD, Schuler T, Salverson W, Palmer M, Woodall CW (2023). Perspectives: *The wicked problem of defining and inventorying mature and old-growth forests*. *Forest* Ecology and Management, 546, 121350. DOI: https://doi.org/10.1016/j.foreco.2023.121350
- HUNTER ML (1990). *Wildlife, forests and forestry: principles for managing forests for biological diversity*. Englewood Cliffs, NJ: Prentice Hall, Englewood Cliffs, New Jersey, USA, 370 pp. [online 2025] Available at: https://nnrg.org/wp content/uploads/2015/03/seymourchapter.pdf
- Jackson TD, Fischer FJ, Vincent G, Gorgens EB, Keller M, Chave J, Coomes DA (2024). *Tall Bornean forests experience higher canopy disturbance rates than those in the eastern Amazon or Guiana shield*. Global Change Biology, 30(9), e17493. DOI: https://doi.org/10.1111/gcb.17493
- Jucker T, Bongalov B, Burslem DF, Nilus R, Dalponte M, Lewis SL, Coomes DA (2018). *Topography shapes the structure, composition and function of tropical forest landscapes*. Ecology letters, 21(7), 989-1000. DOI: https://doi.org/10.1111/ele.12964
- Kassambara A, Mundt F (2017). *Package 'factoextra'. Extract and visualize the results of multivariate data analyses*, 76. [online] Available at: https://rpkgs.datanovia.com/factoextra/
- Keenan RJ, Read SM (2012). *Assessment and management of old-growth forests in south eastern Australia*. Plant Biosystems-An International Journal Dealing with all Aspects of Plant Biology, 146(1), 214-222. DOI: https://doi.org/10.1080/11263504.2011.650726
- LaRue EA, Knott JA, Domke GM, Chen HY, Guo Q, Hisano M, Fei S (2023). S*tructural diversity as a reliable and novel predictor for ecosystem productivity*. Frontiers in Ecology and the Environment, 21(1), 33-39. DOI: https://doi.org/10.1002/fee.2586
- Lindenmayer D, Bowd E (2022). *Critical ecological roles, structural attributes and conservation of old growth forest: lessons from a case study of Australian mountain ash forests*. Frontiers in Forests and Global Change, 5, 878570. DOI: https://doi.org/10.3389/ffgc.2022.878570
- Lindenmayer DB (2017). *Conserving large old trees as small natural features*. Biological Conservation, 211, 51-59. DOI: https://doi.org/10.1016/j.biocon.2016.11.012

- Liu J, Jiang B, Yuan W, Jin C, Jiao J, Wang Z, Wu C (2022). *Socioeconomic and environmental factors jointly shape beta diversity of woody species in eastern China*. Applied Vegetation Science, 25(1), e12641. DOI: https://doi.org/10.1111%2Favsc.12641
- Lutz JA, Furniss TJ, Johnson DJ, Davies SJ, Allen D, Alonso A, Zimmerman JK (2018). *Global importance of large-diameter trees*. Global Ecology and Biogeography, 27(7), 849-864. DOI: https://doi.org/10.1111/geb.12747
- Matuszkiewicz JM, Affek AN, Zaniewski P, Kołaczkowska E (2024). *Early response of understory vegetation to the mass dieback of Norway spruce in the European lowland temperate forest*. Forest Ecosystems, 11, 100177. DOI: https://doi.org/10.1016/j.fecs.2024.100177
- McCune B, Grace JB (2002). *Analysis of ecological communities*. MjM Software Design: Gleneden Beach. ISBN 0-9721290-0-6. 300 pp. DOI: https://doi.org/10.1016/S0022-0981(03)00091-1
- McElhinny C, Gibbons P, Brack C (2006). *An objective and quantitative methodology for constructing an index of stand structural complexity*. Forest Ecology and management, 235(1-3), 54-71. DOI: https://doi.org/10.1016/j.foreco.2006.07.024
- McNichol BH, Wang R, Hefner A, Helzer C, McMahon SM, Russo SE (2024). *Topography-driven microclimate gradients shape forest structure, diversity, and composition in a temperate refugial forest*. Plant-Environment Interactions, 5(3), e10153. DOI: https://doi.org/10.1002/pei3.10153
- Müller J, & Bütler R (2010). *A review of habitat thresholds for dead wood: a baseline for management recommendations in European forests*. European Journal of Forest Research, 129(6), 981-992. DOI: https://doi.org/10.1007/s10342-010-0400-5
- Nagel TA, Svoboda M, Kobal M (2014). *Disturbance, life history traits, and dynamics in an old‐growth forest landscape of southeastern Europe*. Ecological Applications, 24(4), 663-679. DOI: https://doi.org/10.1890/13-0632.1
- O'Brien L, Schuck A, Fraccaroli C, Pötzelsberger E, Winkel G, Lindner M. (2021). *Protecting old-growth forests in Europe - a review of scientific evidence to inform policy implementation*. Final report. European Forest Institute. DOI: https://doi.org/10.36333/rs1
- Oksanen J, Simpson G, Blanchet F, Kindt R, Legendre P, Minchin P, O'Hara R, Solymos P, Stevens M, Szoecs E, Wagner H, Barbour M, Bedward M, Bolker B, Borcard D, Borman T,

Carvalho G, Chirico M, De Caceres M, Durand S, Evangelista H, FitzJohn R, Friendly M, Furneaux B, Hannigan G, Hill M, Lahti L, McGlinn D, Ouellette M, Ribeiro Cunha E, Smith T, Stier A, Ter Braak C, Weedon J (2024). *vegan: Community Ecology Package*. R package version 2.7-0. [online] Available at: https://github.com/vegandevs/vegan

- Oliver CD, Larson BC (1996). *Forest Stand Dynamics, Update Edition*. Yale School of the Environment Other Publications. 1. [online 2025] Available at: https://elischolar.library.yale.edu/fes_pubs/1
- Ontl, T. A., Janowiak, M. K., Swanston, C. W., Daley, J., Handler, S., Cornett, M., Hagenbuch, S., Handrick, C., McCarthy, L., & Patch, N. (2020). *Forest Management for Carbon Sequestration and Climate Adaptation*. *Journal of Forestry*, 118(1), 86–101. DOI: https://doi.org/10.1093/jofore/fvz062
- Paradis E, Schliep K (2019). "ape 5.0: an environment for modern phylogenetics and evolutionary analyses in R." *Bioinformatics*, 35, 526-528. DOI: https://doi.org/10.1093/bioinformatics/bty633
- Pasques O, Munné-Bosch S (2024). *Ancient trees are essential elements for high-mountain forest conservation: Linking the longevity of trees to their ecological function*. Proceedings of the National Academy of Sciences, 121(7), e2317866121. DOI: https://doi.org/10.1073/pnas.2317866121
- Pereira HM, Rosa IM, Martins IS, Kim H, Leadley P, Popp A, Alkemade R (2020). *Global trends in biodiversity and ecosystem services from 1900 to 2050*. BioRxiv, 2020-04. DOI: 10.1126/science.adn3441
- Peruzzi L, Domina G, Bartolucci F, Galasso G, Peccenini S, Raimondo FM, Albano A, Alessandrini A, Banfi E, Barberis G, Bernardo L, Bovio M, Brullo S, Brundu G, Brunu A, Camarda I, Carta L, Conti F, Croce A, Iamonico D, Iberite M, Iiriti G, Longo D, Marsili S, Medagli P, Pistarino A, Salmeri C, Santangelo A, Scassellati E, Selvi F, Soldano A, Stinca A, Villani M, Wagensommer RP, Passalacqua NG (2015). *An inventory of the names of vascular plants endemic to Italy, their loci classici and types*. Phytotaxa 196 (1): 1–217. DOI:10.11646/phytotaxa.196.1.1
- Pickering MA, Elia A, Girardello M, Otón G, Capobianco S, Piccardo M, Ceccherini G, Forzieri G, Migliavacca M, Cescatti A (2024). *Assessing the relationship between forest*

structural diversity and resilience in a warming climate (No. EGU24-16017). Copernicus Meetings. DOI: 10.5194/egusphere-egu24-16017

- Piovesan G, Baliva M, Calcagnile L, D'Elia M, Dorado-Liñán I, Palli J, Quarta G (2020). *Radiocarbon dating of Aspromonte sessile oaks reveals the oldest dated temperate flowering tree in the world*. Ecology, 101(12), 1-4. DOI: https://doi.org/10.1002/ecy.3179
- Piovesan G, Biondi F, Baliva M, De Vivo G, Marchianò V, Schettino A, Di Filippo A (2019b). Lessons from the wild. Ecology, 100(9), 1-4. DOI: https://doi.org/10.1002/ecy.2737
- Piovesan G, Biondi F, Baliva M, Dinella A, Di Fiore L, Marchiano V, Di Filippo A (2019a). *Tree growth patterns associated with extreme longevity: Implications for the ecology and conservation of primeval trees in Mediterranean mountains*. Anthropocene, 26, 100199. DOI: https://doi.org/10.1016/j.ancene.2019.100199
- Piovesan G, Biondi F, Baliva M, Saba EP, Calcagnile L, Quarta G, Di Filippo A (2018). *The oldest dated tree of Europe lives in the wild Pollino massif*. Ecology, 99(7), 1682-1684. DOI: https://doi.org/10.1002/ecy.2231
- Pörtner HO, Scholes RJ, Agard J, Leemans R, Archer E, Bai X,Ngo H (2021). *IPBES-IPCC co-sponsored workshop report on biodiversity and climate change*. [online 2025] Available at: https://library.wur.nl/WebQuery/wurpubs/592922
- R Core Team (2023) *R (4.3.1): A Language and Environment for Statistical Computing*. R Foundation for Statistical Computing, Vienna. [online] Available at: https://www.R-project.org/
- Ramette A (2007). *Multivariate analyses in microbial ecology*. *FEMS microbiology ecology*, *62*(2), 142-160. DOI: https://doi.org/10.1111/j.1574-6941.2007.00375.x
- Ripullone F, Gentilesca T, Lauteri M, Rita A, Rivelli AR, Schettino A, Borghetti M (2016). *Apical dominance ratio as an indicator of the growth conditions favouring Abies alba natural regeneration under Mediterranean environment*. European journal of forest research, 135, 377-387. DOI: https://doi.org/10.1007/s10342-016-0941-3
- Sabatini FM, Bluhm H, Kun Z, Aksenov D, Atauri JA, Buchwald E, Burrascano S, Cateau E, Diku A, Duarte IM, López ÁBF, Garbarino M, Grigoriadis N, Horváth F, Keren S, Kitenberga M, Kiš A, Kraut A, Ibisch PL, Larrieu L, Lombardi F, Matovic B, Melu RN, Meyer P, Midteng R, Mikac S, Mikoláš M, Mozgeris G, Panayotov M, Pisek R, Nunes L, Ruete A, Schickhofer M, Simovski B, Stillhard J, Stojanovic D, Szwagrzyk J, Tikkanen OP, Toromani E,

Volosyanchuk R, Vrška T, Waldherr M, Yermokhin M, Zlatanov T, Zagidullina A, Kuemmerle T (2020). *European Primary Forest Database (EPFD) v2.0*. bioRxiv, 2020.2010.2030.362434. DOI: https://doi.org/10.1101/2020.10.30.362434

- Sabatini FM, Burrascano S, Lombardi F, Chirici G, Blasi C (2015). *An index of structural complexity for Apennine beech forests*. IForest, 8, 314-323. DOI: https://doi.org/10.3832/ifor1160-008
- Slezák M, Axmanová I (2016). *Patterns of plant species richness and composition in deciduous oak forests in relation to environmental drivers*. Community Ecology, 17(1), 61-70. DOI: https://doi.org/10.1556/168.2016.17.1.8
- Spies TA, Franklin JF (1991). The structure of natural young, mature, and old-growth Douglas-fir forests in Oregon and Washington. Wildlife and vegetation of unmanaged Douglas-fir forests, 1, 91-109. [online] Available at: https://andrewsforest.oregonstate.edu/publications/1244
- Storch F, Boch S, Gossner MM, Feldhaar H, Ammer C, Schall P, Bauhus J (2023). *Linking structure and species richness to support forest biodiversity monitoring at large scales*. Annals of Forest Science, 80(1), 3. DOI: https://doi.org/10.1186/s13595-022-01169-1
- Tanioka K, Yadohisa H (2012). *Effect of Data Standardization on the Result of k-Means Clustering*. 59-67. DOI: https://doi.org/10.1007/978-3-642-24466-7_7
- Thom D, Seidl R (2016). *Natural disturbance impacts on ecosystem services and biodiversity in temperate and boreal forests*. Biological Reviews, 91(3), 760-781. DOI: https://doi.org/10.1111/brv.12193
- Todaro L, Andreu L, D'Alessandro CM, Gutiérrez E, Cherubini P, Saracino A (2007). *Response of Pinus leucodermis to climate and anthropogenic activity in the National Park of Pollino (Basilicata, Southern Italy)*. Biological conservation, 137(4), 507-519. DOI: https://doi.org/10.1016/j.biocon.2007.03.010
- van Galen LG, Jordan GJ, Musk RA, Beeton NJ, Wardlaw TJ, Baker SC (2018). *Quantifying floristic and structural forest maturity: An attribute-based method for wet eucalypt forests*. Journal of Applied Ecology, 55(4), 1668-1681. DOI: https://doi.org/10.1111/1365-2664.13133
- Whitman A, Hagan JM (2007). *An index to identify late-successional forest in temperate and boreal zones*. Forest Ecology and Management, 246(2-3), 144-154. DOI: https://doi.org/10.1016/j.foreco.2007.03.004

- Ziaco, E., Di Filippo, A., Alessandrini, A., Baliva, M., D'Andrea, E., & Piovesan, G. (2012). *Old-growth attributes in a network of Apennines (Italy) beech forests: disentangling the role of past human interferences and biogeoclimate*. Plant Biosystems-An International Journal Dealing with all Aspects of Plant Biology, 146(1), 153-166. DOI: https://doi.org/10.1080/11263504.2011.650729

Appendices – Chapter 1

Appendix S1. Supplementary Tables

Table S1.1. Heterogeneity classes proposed by Sabatini et al., (2015). These classes capture the key structural attributes affecting forest biodiversity and ecosystem functions. Each class represents a distinct source of heterogeneity, such as vertical stratification, tree species composition, deadwood abundance, and tree size distributions, features which contribute to complex and resilient forest ecosystems.

Source of Heterogeneity	Description	Selected Variable
Vertical Heterogeneity	Stands with a variety of tree heights likely have a mix of ages, leading to high vertical and horizontal variation. This variation influences demographics, resource distribution (light), and understory development.	H_sd, Dom_height
Tree Compositional Diversity	A mix of shade-tolerant and shade-intolerant species can create a multi-layered canopy. This diversity can promote herb-layer variety due to differences in light transmission and litter quality between tree species.	
Uneven-agedness	In landscapes with frequent small-scale disturbances, an uneven-aged structure might be natural or due to close-to-nature forestry practices. The variation in tree sizes indicates a diversity of niches for various plants and animals.	DLT.log
Density of Large Living Trees	Large trees store significant carbon and provide habitat for threatened or ecologically important species, by offering a variety of niches, i.e., rough bark, hollows, exposed deadwood, sap flows, and dead branches/tops.	dbh40.log, dbh50.sq,
Growing Stock	Living above-ground biomass indicates a stand's carbon storage. Older-growth stands, with a higher biomass, more effectively moderate the surface temperature and support a higher percentage of forest specialist herbaceous species.	dbh_max, BA_living_tree
Total Deadwood Volume	Deadwood is crucial for biodiversity by providing niches for specialized organisms. These organisms often have limited dispersal abilities and rely on the long-term availability of deadwood for survival. Their absence in managed stands can lead to local extinctions.	
Deadwood Decay Classes	The lack of deadwood in specific decay stages indicates a disruption in its supply, usually due to recent harvesting or removal. This can affect nutrient cycling and the diversity/abundance of saproxylic organisms.	N_dacay_classes
Standing Deadwood, Dead Trees, and Snags	Standing dead trees and snags offer niches like hollows, cracks, and cavity strings, which are vital for various species of breeding birds, mammals, invertebrates, lichens, and bryophytes.	DLR.tu

Table S1.2. Results from the CCA permutation test. The model comprised 4 degrees of freedom (Df = 4) and showed a Chi-square value of 0.09791 and a high F-ratio (F = 7.9809), both of which indicated a significant contribution of the constrained variables. Furthermore, its highly significant *p*-value (Pr(>F) = 0.001*) highlighted the relevance of topographic variables (altitude, slope, aspect_sin, and aspect_cos) in capturing the heterogeneity of forest structure.

Permutation test for CCA under reduced model				
Number of permutations: 999				
	Df	**ChiSquare**	**F**	**Pr(>F)**
Model	4	0.09791	7.9809	0.001 ***
Residual	138	0.42325		

Appendix S2. Supplementary Figures

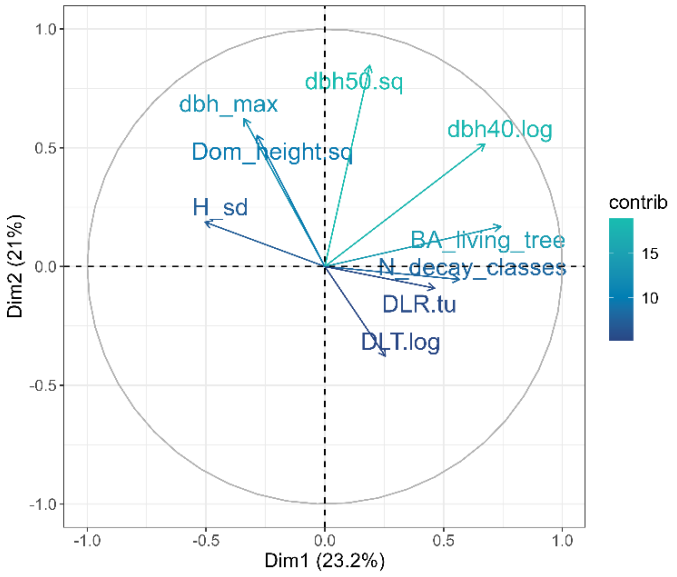

Figure S1.1. Principal component analysis of forest structural attributes (Dim 1 vs. Dim 2). PCA biplot shows the relationships between forest structural attributes, with the first two dimensions, Dim 1 and Dim 2, explaining 44.2% of the total variance. The arrows represent the contribution and direction of each variable to the ordering, with colour intensity showing the relative contribution to the principal components.

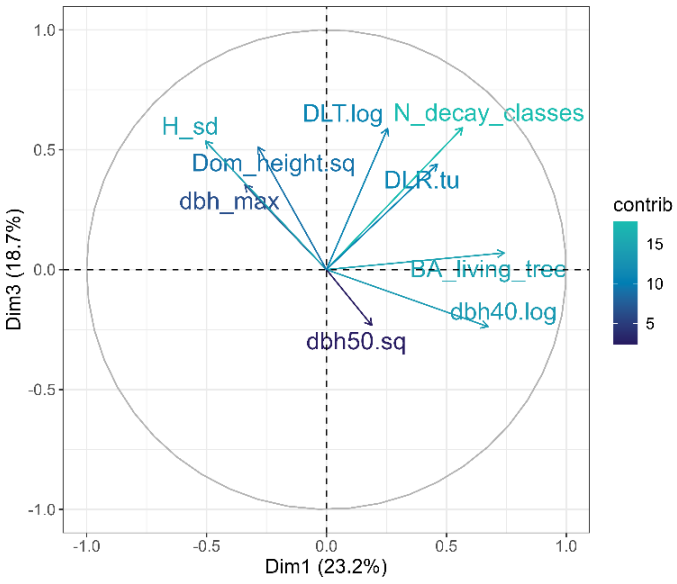

Figure S1.2. Principal component analysis of forest structural attributes (Dim 1 vs. Dim 3). The biplot shows interrelationships among forest structural variables, where Dimension 1 (23.2%) and Dimension 3 (18.7%) together explain 41.9% of the total variance. The arrow direction denotes the orientation of each variable in the multivariate space, while its length represents the relative contribution to sorting. Colour intensity represents the relative contribution of each variable to the principal components.

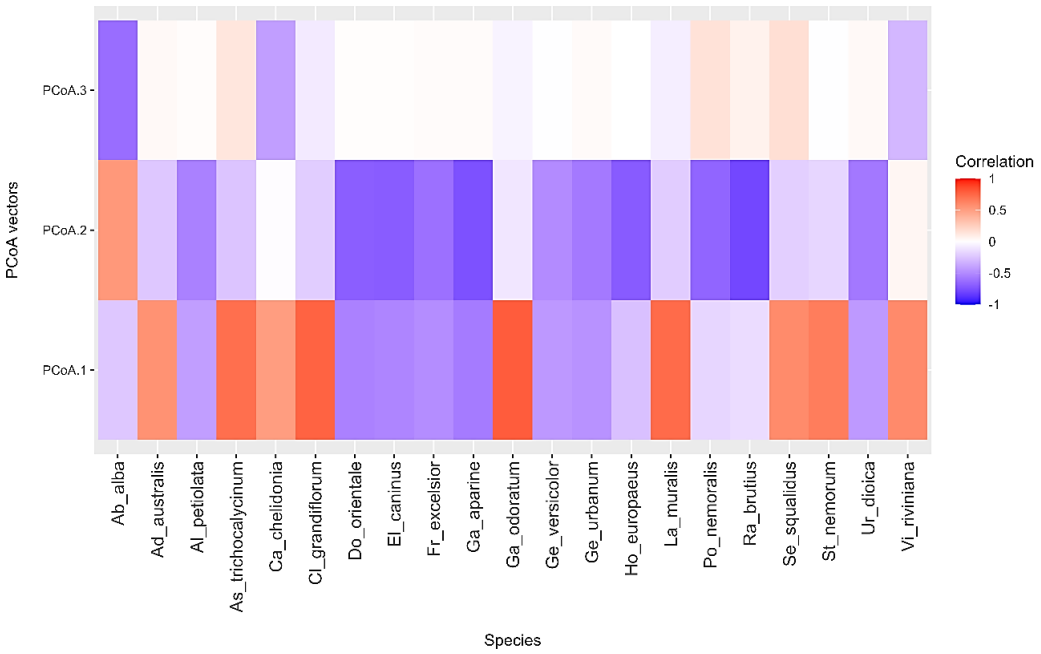

Figure S1.3. **Correlation matrix between PCoA axes and vascular plant species composition in old-growth forests.** The heat map shows the correlation between individual species and the sorting axes, ranging from blue (negative correlations) to red (positive correlations).

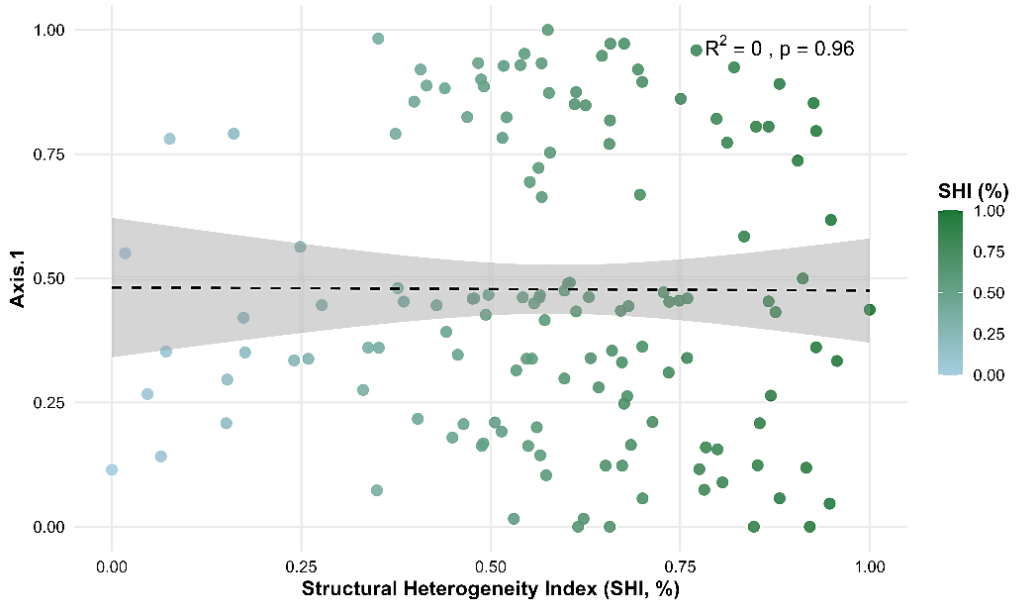

Figure S1.4. Relationship between the structural heterogeneity Index (SHI) and PCoA Axis 1. The scatterplot illustrates the linear relationship between SHI and PCoA Axis 1 scores across old-growth forest sites. Each point represents a site, with colour intensity indicating SHI values. The dashed line represents the fitted linear regression model, and the shaded area shows the 95% confidence interval. The *p*-value (> 0.9568) indicates that variation in SHI is not significantly explained by PCoA Axis 1, suggesting a limited association between overall forest structural heterogeneity and the main compositional gradient of vascular plant communities.

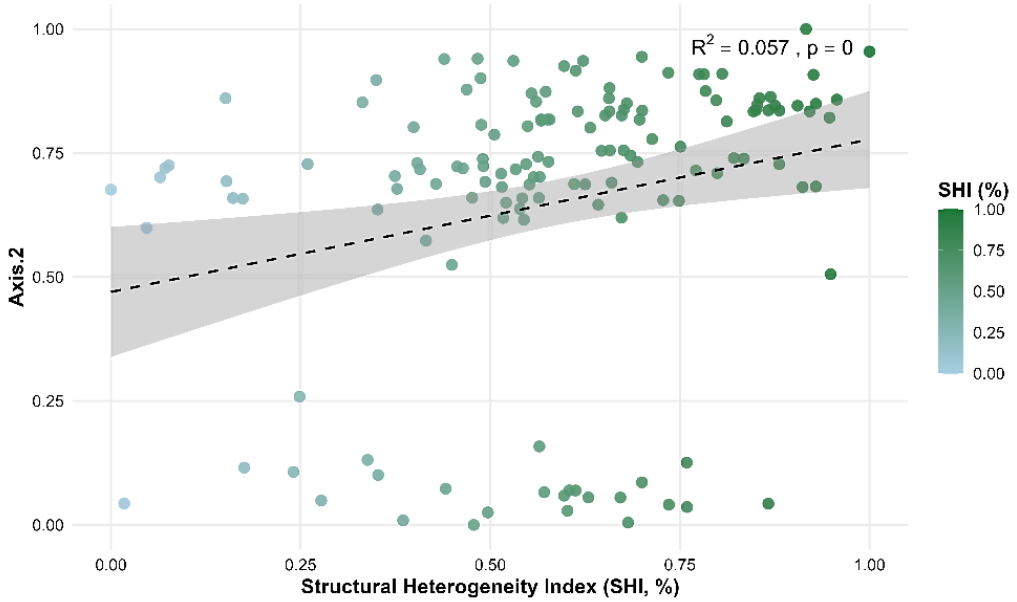

Figure S1.5. Relationship between structural heterogeneity (SHI) and PCoA Axis 2. The scatterplot shows a significant linear relationship between SHI and PCoA Axis 2 scores ($p < 0.0042$). Higher SHI values were associated with shifts in vascular plant community composition along this axis, suggesting that increasing forest structural heterogeneity is linked to compositional differentiation in the understorey flora.

Figure S1.6. Relationship between structural heterogeneity (SHI) and PCoA Axis 3. The scatterplot shows a significant positive linear relationship between SHI and PCoA Axis 3 scores ($p < 0.0099$), suggesting that finer-scale variation in vascular plant community composition, represented by Axis 3, is influenced by differences in forest structural heterogeneity.

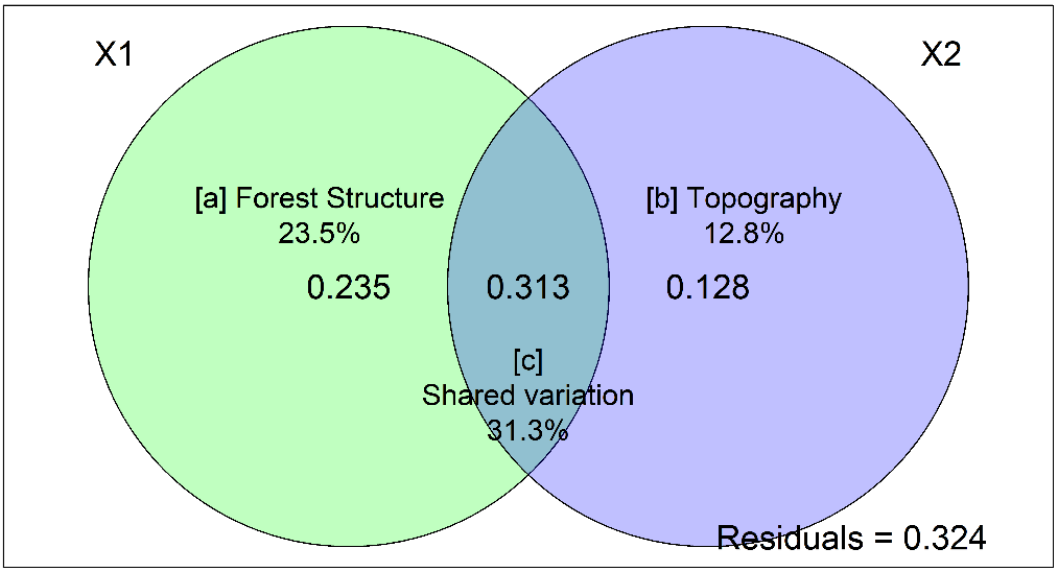

Figure S1.7. Partitioning of vascular plant community variation explained by forest structure and topography in old-growth forests. The diagram shows the proportion of explained variation in species composition attributed uniquely to forest structural attributes (component [a]; 23.5%), uniquely to topographic variables (component [b]; 12.8%), and to their shared contribution (component [c]; 31.3%). Residual unexplained variation accounts for 32.4% of the total variance. Forest structure explained a larger portion of community variation than topography, indicating that structural heterogeneity is a stronger driver of plant compositional differences among OGF sites.

Chapter 2: Spatial modelling of structural complexity using multi-source remote sensing

Summary: *Building on previous findings, this chapter aims to examine and map the structural heterogeneity within three designated Mediterranean old-growth forests using a multi-source remote sensing approach. Specifically, structural classes, as defined by the Structural Heterogeneity Index (SHI), were used to train Random Forest (RF) classifiers, integrating airborne LiDAR metrics, multispectral Sentinel-2 vegetation indices, multi-decadal vegetation trends, topographic variables, and a proxy to measure cumulative human pressure. Results demonstrated that forest structural heterogeneity could be successfully predicted at a fine spatial resolution. LiDAR-derived metrics proved to be essential predictors, followed by seasonal spectral data and long-term canopy trends. By establishing a quantitative, scalable approach, this study provides a replicable model to identify and prioritise forest patches with the highest conservation value, thereby supporting informed decision-making processes.*

Mapping forest structure complexity within protected old-growth forest sites: an example from Pollino National Park

Travascia D.[1], Alvites Diaz C. I.[2], Lacovara B.[3], Fiorentino C.[1], Piovesan G.[4], Ripullone F.[1]

[1] *Department of Agricultural, Forest, Food and Environmental Sciences, University of Basilicata, Via dell'Ateneo Lucano 10, 85100 Potenza, Italy*

[2] *School of Forest, Fisheries, and Geomatics Sciences, University of Florida, Gainesville, FL 32611, United States*

[3] *GEOCART S.p.A., Viale del Basento, 120, 85100 Potenza, Italy*

[4] *Department of Ecological and Biological Sciences (DEB), University of Tuscia, Largo dell'Università, 01100 Viterbo, Italy*

Abstract

Old-growth forests (OGFs) are recognised as vital ecosystems for biodiversity and carbon storage. Nevertheless, the management of these forests is frequently hindered by imprecise, non-quantitative boundary definitions. Currently, several officially designated OGFs encompass forest patches with highly variable structural integrity. This study presents a diagnostic approach to quantify and rank "old-growthness" within designated boundaries – assessing structural heterogeneity as a primary ecological indicator. This research was conducted across three Mediterranean mixed-forest stands located in the Pollino National Park. To characterise forest architecture, a ground-based Structural Heterogeneity Index (SHI) was derived using inventory data from 59 sample plots. SHI-derived classes were then modelled using a Random Forest (RF) classifier combined with multi-source remote sensing data. Predictors included LiDAR-derived canopy metrics, Sentinel-2 vegetation indices, multi-decadal spectral trends, topographic variables, and a proxy to estimate cumulative human pressure. The RF model successfully distinguished between high and low structural heterogeneity, achieving an overall accuracy of 0.84 (Cohen's Kappa = 0.68). LiDAR-derived metrics were identified as the most important predictors in our analysis, supplemented by long-term spectral trajectories and human-pressure proxies, which provided valuable diagnostic details. Results showed that only a specific subset of the current OGF area is characterised by significant structural complexity, which typically occurs in late-successional conditions — highlighting considerable variability within designated protected areas. These findings established a replicable and scalable framework to guide conservation efforts, allowing for effective spatial prioritisation. By employing a binary model to estimate the potential old-growthness within forest sites, the park's authorities would move beyond conventional boundaries and identify highly ecologically intact patches. Furthermore, our approach also aligns directly with the EU Biodiversity Strategy for 2030, providing a robust framework for targeted monitoring and protection of forest ecosystems with the highest structural and ecological integrity.

1. Introduction

Old-growth forests (OGFs), also known as primary, virgin or ancient forests, represent ecosystems developed over centuries without significant human impact (Merce et al., 2014). These forests can be defined by the significant abundance of large, aged trees, multi-layered canopies, and substantial amounts of dead wood (Christensen et al., 2005; Burrascano et al., 2013). Such features are essential to provide a wide range of ecosystem services, including biodiversity conservation (Paillet et al., 2010), climate regulation, carbon storage (Luyssaert et al., 2008; Frey et al., 2016), soil and water protection (Brockerhoff et al., 2017), as well as cultural and recreational value (Gunes & Hens, 2007). Despite their significant role, such forests are increasingly threatened by land-use practices, ecosystem fragmentation, and climate change.

Currently, less than three per cent of total forest area in Europe is classified as OGF (Hirschmugl et al., 2023). Consequently, the European Union (EU) has called for their systematic detection, mapping, and protection under the Biodiversity Strategy for 2030 (Kirchmeir et al., 2023). According to Hirschmugl et al. (2023), a wide range of approaches for mapping OGFs has been developed over the last decade. More specifically, these methods can be categorised into three main groups: (i) Metric-based approaches: focused on deriving forest structural attributes from remote sensing (RS) sources, including LiDAR, GEDI, Sentinel and Landsat; (ii) Direct approaches: based on machine learning techniques applied on RS data for large-scale mapping; and (iii) Indirect approaches: based on pre-existing data, such as geospatial datasets, supplemented by literature reviews and questionnaires. However, progress towards a fully integrated monitoring tool remains constrained due to both technical and ecological challenges. Among these, data resolution and modelling uncertainties pose significant challenges, further compounded by the intricate characteristics of natural ecosystems, where inherent biological complexity and non-linear dynamics often elude standardised sampling and predictive frameworks.

In this context, multi-source RS data has emerged as a promising strategy to overcome some of these limitations. For instance, optical sensors, such as Sentinel-2 and Landsat, can provide multispectral data to derive vegetation indices (VIs) and monitor phenological trends (Banskota et al., 2014). This, in turn, enables forest ecosystem assessments. Synthetic aperture radars (SAR), including Sentinel-1, enhance optical data by virtue of their sensitivity to canopy structure and moisture content (Spracklen et al., 2021; Le Toan et al., 2011).

Furthermore, LiDAR technology, embracing both airborne (ALS) and terrestrial (TLS) systems, facilitates highly precise detection of forest structure, offering valuable insights concerning canopy height, forest strata, and understorey density (Thomas et al., 2008; Maltamo et al., 2014). Numerous studies have recently demonstrated how crucial remote sensing and advanced modelling techniques, including machine learning (ML) and deep learning (DL), are in enhancing our ability to monitor natural forest ecosystems. According to Spracklen & Spracklen (2019), the combination of Sentinel-2 images using machine learning (ML) techniques proved advantageous in mapping tree species and OGFs in Ukraine. Similarly, Lalèchère et al. (2024) conducted a study to determine the effectiveness of various RS sources in identifying overmature forests. Nevertheless, some challenges remain, including the lack of a standardised OGF definition (Bruening et al., 2024) as well as the limited availability of field-collected data.

In addition, such approaches are rarely employed, particularly in the Mediterranean basin, where climate change effects are most evident. Moreover, a further critical issue concerns the limited integration of long-term data in identifying potential OGFs. According to Burrascano et al. (2013), OGFs should not be defined exclusively by current structure, but also by their ecological continuity. In this context, the Landsat satellite series offers a critical opportunity to reconstruct multi-decadal vegetation trends, providing sufficient historical data to identify stands characterised by functional stability and ecological resilience (Banskota et al., 2014; Colangelo et al., 2021). However, this need for time-based evidence is frequently undermined by a lack of detail in designated OGF boundaries. Although numerous areas are formally protected, their administrative boundaries are frequently established without quantitative or structural assessments. Consequently, these areas contain a variety of forest patches, some of which differ considerably in their old-growth status.

In this context, our study aims to quantify and rank the relative old-growthness degree within officially designated OGF patches. To this end, a novel integrated approach — combining field-validated structural indices with multi-source remote sensing data and machine learning — was adopted to generate spatially explicit maps of structural heterogeneity at a fine scale. Unlike existing mapping methodologies, which rely on indirect remote sensing proxies without field validation, this approach uses SHI-derived classes as ecologically grounded reference conditions, directly linking ground-based measurements to landscape-scale predictions.

The SHI was derived through detailed field measurements collected across 59 sample plots and categorised into high and low structural complexity classes, which served as reference variables for the predictive modelling framework. This approach was founded on the established ecological principle that high structural heterogeneity constitutes a distinctive hallmark of old-growth ecosystems (Ducey et al., 2013). Furthermore, according to Uhl et al. (2025), forest structural heterogeneity could also be considered an indicator of ecological continuity, limited human disturbance, and late successional stages, which in turn are strongly linked to increased biodiversity (Paillet et al., 2010; Burrascano et al., 2013; Di Filippo et al., 2017; Sabatini et al., 2018; Concha et al., 2023).

Predictor variables were selected to encompass a range of ecological dimensions, including three-dimensional structure metrics obtained from LiDAR, seasonal vegetation indices derived from Sentinel-2, and long-term trends from Landsat. Topographic factors — including elevation and slope — as well as a cumulative human pressure index, were also considered. Based on this framework, three main hypotheses were tested: (1) integrating structural, spectral, temporal, and socio-ecological predictors would reliably discriminate high versus low SHI classes; (2) LiDAR-derived structural metrics would be the most significant predictors; and (3) long-term vegetation index trends could reveal evidence of ecological continuity extending beyond single-season spectral analysis.

2. Materials and Methods

2.1 Study Area

The Pollino National Park (Pollino NP) represents the largest protected area in Italy, encompassing approximately 192,565 hectares across two regions: Basilicata and Calabria (Compagnucci et al., 2002). Owing to its topography, with elevation ranging from 52 to 2,267 m a.s.l., it is regarded as a transitional zone between temperate and Mediterranean climates (Blasi & Michetti, 2005). According to Todaro et al. (2007), coastal areas are typically characterised by a Mediterranean climate, with hot, dry summers, while mountainous regions experience cold, snowy winters and mild summers. The annual rainfall pattern varies significantly across this region, ranging from approximately 300 mm/year along the Ionian coast to nearly 2,000 mm/year on the Tyrrhenian side.

In addition, a marked altitudinal temperature gradient characterises the study area, with average temperatures at 2,000 m a.s.l. ranging from winter lows of -3.2 °C to summer peaks of 13.8 °C (Colangelo et al., 2021). Such conditions impose significant bioclimatic constraints, shaping specialised ecological niches as well as growth dynamics in high-elevation Mediterranean forests. Such environmental variations result in a rich biodiversity, including various forest types. More specifically, medium- and low-altitude forests are dominated by turkey oak (*Quercus cerris* L.), downy oak (*Quercus frainetto* Ten.), hornbeam (*Carpinus orientalis* Mill.), alder (*Alnus cordata* Loisel.), and various maple species. In contrast, at higher altitudes, beech (*Fagus sylvatica* L.), silver fir (*Abies alba* Mill.), and Bosnian pine (*Pinus heldreichii* Christ.) predominate. The Bosnian pine, in particular, forms highly distinctive populations with considerable ecological, cultural, and landscape value, which are emblematic of Pollino's natural heritage.

2.2 OGFs survey data

The present study was carried out across three old-growth mixed forests (Fig. 2.1) located within the Pollino NP, including Bosco Magnano (BM), Bosco Vaccarizzo (CA), and Cugno dell'Acero (TP). These sites, included as part of the Italian project "Building an Old-Growth Forest Network for Southern Apennine Parks", represent some of the most ecologically valuable forest ecosystems in this region.

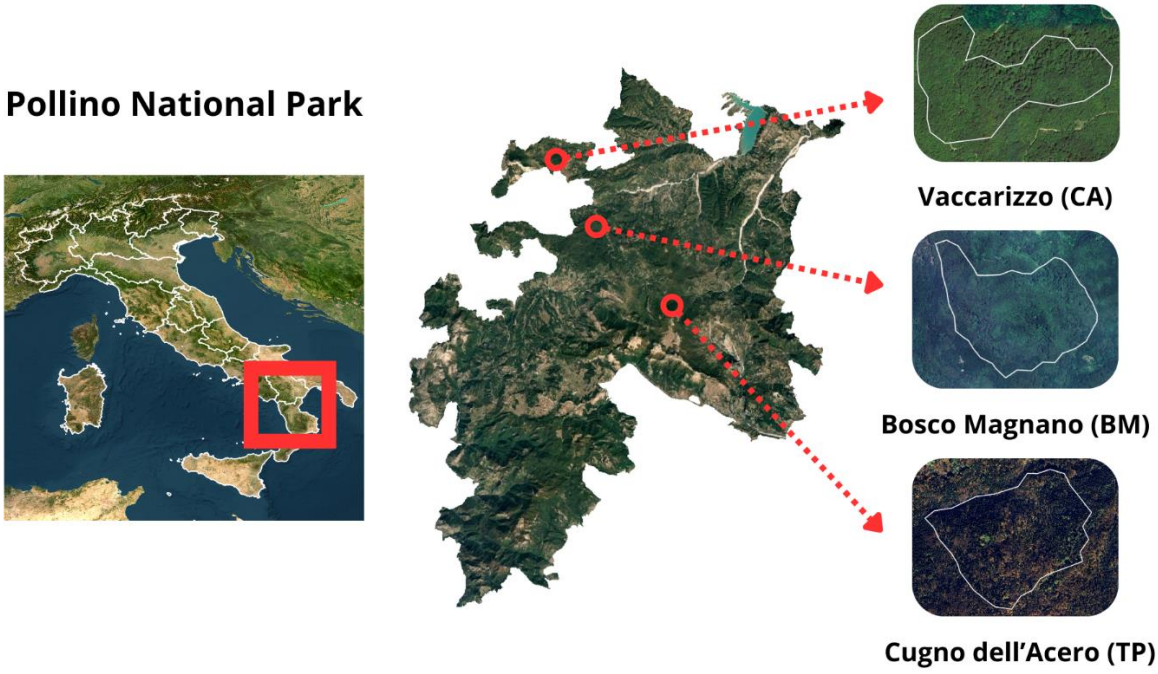

Figure 2.1. **Map showing Pollino National Park (southern Italy) and surveyed forest sites**. The inset map provides an overview of the park's location within the Italian peninsula. Detailed views of the three investigated forest stands — Bosco Vaccarizzo (CA), Bosco Magnano (BM), and Cugno dell'Acero (TP) — are shown by the surrounding panels. White lines indicate the old-growth forest boundaries designated as conservation zones.

Dominated by the occurrence of three main tree species, including European beech, silver fir, and turkey oak, these areas are characterised by structural and compositional features typically associated with late-stage forest succession.

To ensure data comparability, a 1-hectare sample area was defined within each of the investigated stands. The core areas were identified using a standardised protocol, as developed by the aforementioned project, and qualitative ecological criteria, including structural complexity, significant amounts of deadwood, dominance of native tree species, and the absence of recent human disturbance (Di Filippo et al., 2017).

Field surveys were conducted between 2015 and 2018, providing a consistent and robust reference dataset to characterise OGFs at the stand scale. Furthermore, the employment of a standardised four-stage sampling strategy ensured uniform data collection across all investigated sites. During the first stage, the core areas were systematically subdivided into 25 square microplots of 400 m² (Fig. 2.2), thereby establishing an explicit spatial framework for detailed field investigations. However, due to local topographic constraints, the effective sample area at the CA site was reduced to 0.36 ha.

Subsequently, floral composition and topographic attributes were also recorded. In the third stage, a comprehensive assessment of ground-level necromass was conducted, encompassing standing dead trees (DST), snags, downed dead trees (DDT), coarse woody debris (CWD), and stumps, all of which are recognised as key indicators in assessing forest structural complexity and natural disturbance regimes. Finally, a detailed inventory of living trees, shrubs, and regeneration layer was carried out, including all specimens with a diameter at breast height (DBH) of at least 5 cm and a height of 130 cm or more.

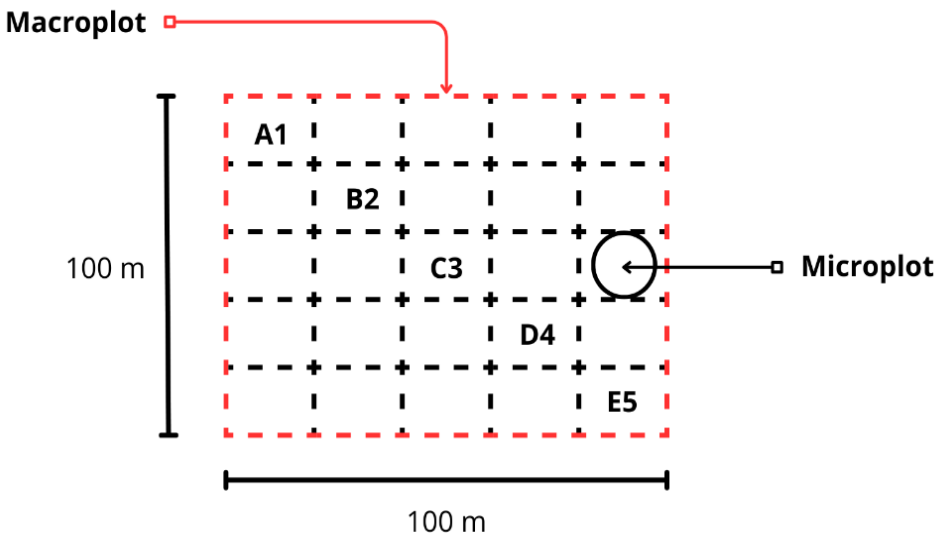

Figure 2.2. Conceptual scheme describing the field sampling design adopted according to the '*Building an Old-Growth Forest Network for Southern Apennine Parks*' project. Macro-plots (100 × 100 m; outlined in red) were subdivided into a standard grid of 20 × 20 m. Within each grid cell, forest structural attributes were recorded, and alphanumeric labels (A1–E5) were used to identify microplots within the core area.

3. Data analysis

A database of 24 easily measurable structural variables was derived from standard forest monitoring data (Chirici et al., 2011) and used to assess intra-stand forest complexity (Appendix S1, Tab. S2.1). The volumes of living trees, DST and DDT were estimated using double-entry equations based on the First National Forest Inventory. Conversely, deadwood components, including stumps, snags and CWD, were estimated according to the following equation (Eq. 2.1):

$$\text{(Equation 2.1)} \quad V = (\pi * h/3) * (R2 + r2 + (R * r)$$

Where V is the volume, h is the height, R is the major radius, and r is the minor radius.

3.1 Forest structure assessment

According to Sabatini et al. (2015), structural attributes were used to compute the Structural Heterogeneity Index (SHI) at the microplot scale. To verify their statistical distribution, a preliminary data inspection was performed.

All cases with kurtosis values greater than |2| were either corrected or excluded from the analysis. Additionally, variables with Pearson correlation coefficients exceeding 0.55 were also removed, reducing potential redundancy.

Two distinct tests were then implemented to evaluate the suitability of the retained variables for PCA: Kaiser–Meyer–Olkin and Bartlett. Suitable variables were then employed as inputs for the PCA analysis performed in RStudio (version 4.3.0) using the *FactoMineR* (Lê et al., 2008) and *factoextra* (Kassambara & Mundt, 2020) packages. To ensure a robust and comprehensive analysis, key variables along the first three PCA dimensions were selected and sorted into quartiles.

Each variable was then scaled to a 0–10 score and standardised by linear regression. SHI values were thus derived by summing all scores and expressed as percentages. Subsequently, K-means cluster analysis was implemented to classify forest patches by SHI.

3.2 LiDAR metrics and topographical data

ALS data was acquired by GEOCART S.p.A., a private Italian company specialising in remote sensing and geomatics. Data was collected using a multisensor airborne platform equipped with a GNSS/IMU navigation system for direct georeferencing and a Riegl Q560 laser scanner.

This technology, known as Full Waveform, represents one of the most significant laser scanner features, since it enables the acquisition of all backscattered echoes and improves penetration through tree canopies (Appendix S1, Table S2.2). Point clouds, characterised by an average density of approximately 8 points/m², were provided alongside intensity and class values. A preprocessing procedure was subsequently applied to all point clouds dating from 2013, and all relevant metrics were extracted in RStudio using a series of dedicated packages.

Initially, all point clouds were inspected to identify potential misclassification, missing points, or duplicates. Next, the ground points were isolated from vegetation returns by using both the *rasterise_terrain()* function and the iterative TIN algorithm (Roussel et al., 2020), thereby creating a Digital Terrain Model (DTM) with a resolution of 10 metres. Slope and aspect were then derived from the DTM employing the *terrain()* function available in the 'terra' package (Hijmans, 2020).

Vegetation heights, normalised adopting the *normalise_height()* function, were then processed based on the DTM, yielding a Canopy Height Model (CHM). To mitigate any potential bias, any value exceeding the 99th percentile was excluded from the subsequent analysis.

Finally, a suite of six forest height metrics, including minimum (zmin), maximum (zmax), mean (zmean), standard deviation (zsd), skewness (zskew), and kurtosis (zkurt), was derived using the *pixel_metrics()* function exclusively on cloud points above two metres. According to Lalechère et al. (2022), these metrics provide reliable insights to describe OGF ecosystems (Fuhr et al., 2022), as they reflect key factors such as tree height heterogeneity, light availability, and canopy gap dynamics.

3.3 Sentinel-2 multispectral data and preprocessing

Developed by the European Space Agency (ESA), Sentinel-2 (S2) consists of two satellites (Sentinel-2A and Sentinel-2B) equipped with multispectral sensors for high-resolution earth observation. These satellites offer global coverage every five days, revisiting each location every 10 days. Using 13 spectral bands, S2 captures images with spatial resolutions ranging from 10 m to 60 m. However, in this study, only bands with resolutions of 10 m and 20 m were considered (Tab. 2.1), providing sufficient spectral and spatial detail to monitor forest dynamics (Liu et al., 2018).

Table 2.1. Sentinel-2 spectral bands used in this study, including band designation, spectral region, central wavelength, and native spatial resolution.

Sentinel-2 band	Name	Central Wavelength (µm)	Spatial Resolution (m)
B2	Blue	0.490	10
B3	Green	0.560	10
B4	Red	0.665	10
B5	Red Edge	0.705	20
B6	Red Edge	0.740	20
B7	Red Edge	0.783	20
B8	Near IR	0.842	10
B8A	Near IR	0.865	20
B11	SWIR	1.610	20
B12	SWIR	2.190	20

Acquisition and processing of data from S2 were carried out in Google Earth Engine (GEE; Gorelick et al., 2017), applying two seasonal windows (Tab. 2.2) and setting a maximum cloud

cover threshold of 20% (Luo et al., 2025). Compared to single-date acquisitions frequently utilised by other studies, this strategy offered a more reliable predictive accuracy (Zlonis et al., 2022).

Table 2.2. Details of the seasonal Sentinel-2 image subsets employed in this study, including the acquisition periods, the number of images retained after cloud filtering, and the cloud cover threshold applied.

Season	Sensor	Start date	End date	Images collected	Cloud cover threshold
Summer	Sentinel-2	June 1, 2018	Aug 31, 2018	65	< 20%
Autumn	Sentinel-2	Sept 1, 2018	Nov 30, 2018	44	< 20%

All analyses involved the use of atmospherically corrected Level 2A surface reflectance data (COPERNICUS/S2_SR_HARMONISED). To remove contamination from cloud and cirrus, the QA60 band was applied, whilst the surface reflectance values were scaled according to the standard factor required to convert raw radiance to physically meaningful reflectance. Furthermore, to guarantee spatial consistency with LiDAR-derived metrics, all 20 m bands were resampled to 10 m through bilinear interpolation. Based on the pre-processed bands, three vegetation indices (VIs) were computed: Normalised Difference Vegetation Index (NDVI) (Eq. 2.2), Brightness Index (BI) (Eq. 2.3) and Enhanced Vegetation Index (EVI) (Eq. 2.4).

(Equation 2.2) $$NDVI=\frac{B8 - B4}{B8 + B4}$$

(Equation 2.3) $$BI=\frac{\sqrt{B4^2 + B3^2}}{2}$$

(Equation 2.4) $$EVI=2{,}5 * \frac{B8 - B4}{(B8 + 6 * B4)-(7{,}5 * B2 + 1)}$$

According to Munteanu et al. (2022), NDVI and BI are both effective in detecting features such as large trees, dead wood, canopy openings, as well as exposed soil (Lalechère et al., 2024; Zielewska-Büttner et al., 2020). Nevertheless, Yan et al. (2022) observed that NDVI tends to saturate in dense forest canopies, reducing its sensitivity to subtle changes. To address these limitations, the EVI index was also introduced (Spracklen & Spracklen, 2019). Moreover, based on the findings of Roy et al. (2016), seasonal composites were derived from cloud-free images by applying a median filter.

3.4 Long-term forest cover dynamics

A total of 40 years of Landsat surface reflectance data (1985–2024) was investigated to analyse forest canopy dynamics. Images were processed within the Google Earth Engine (GEE) cloud-computing environment using Landsat surface reflectance products from Landsat 5 Thematic Mapper (TM), Landsat 7 Enhanced Thematic Mapper Plus (ETM+) and Landsat 8 Operational Land Imager (OLI), obtained from the USGS Collection 2 Level-2 archive (U.S. Geological Survey, 2021).

To ensure phenological consistency and mitigate seasonal variability, this analysis focused exclusively on scenes captured within a defined growing season, ranging from April to October. Scenes with cloud cover exceeding 20% were also excluded. In addition, radiometric calibration was applied by employing the official scale factors, while clouds, cirrus and shadows were masked through the QA_PIXEL quality band. Nevertheless, given the failure of the Landsat 7 scan line corrector (SLC) during 2003, a time-stratified processing strategy was adopted to minimise the reliance on ETM+ observations (Appendix S1, Tab. S2.3). Missing data were reconstructed using a local spatio-temporal linear regression approach based on neighbouring observations, according to established gap-filling methodologies (Yin et al., 2017; Asare et al., 2020). NDVI and EVI were then derived for each cloud-free observation. Such indices were selected based on their widespread use within related research studies (Glenn et al., 2008; da Silva et al., 2020; Zhang et al., 2022).

Annual maximum composites were then calculated for both NDVI and EVI, and pixel-wise trends were investigated applying the Theil-Sen estimator (TS; Sen, 1968). TS represents an advanced non-parametric tool that effectively handles outliers, non-normal distributions, and missing data (Colditz et al., 2015; Mariano et al., 2018; Liu et al., 2021). Furthermore, to provide reliable delineation of forested areas, the ALOS PALSAR Forest/Non-Forest dataset (JAXA/ALOS/PALSAR/YEARLY/FNF4) was utilised to mask results (Shimada et al., 2014).

Finally, to validate long-term vegetation trends, an independent statistical assessment was conducted employing the non-parametric Mann–Kendall (MK) test (Mann, 1945; Kendall, 1948). According to Rustum et al. (2017), this combination is fundamental for evaluating environmental time series trends. Therefore, annual maximum NDVI and EVI time series were extracted and analysed in RStudio using the 'trend' package.

While the MK test was performed to identify statistically significant monotonic trends, TS was adopted to estimate trend magnitude and direction. To account for multiple testing across stands and indices, p-values were adjusted using the false discovery rate procedure (FDR; Benjamini & Hochberg, 1995; Wilks, 2006), thereby confirming the statistical support of the long-term TS-estimated trends.

3.5 Socio-ecological assessment

To consider the influence of socio-ecological pressures on forest ecosystems, our analysis included the Global Human Modification (GHM) index, derived from the GEE platform. More specifically, GHM provides a spatially explicit, cumulative measure of human impact on terrestrial biomes by combining several factors, such as built-up areas, agriculture, energy and mineral extraction, grazing, deforestation, road networks, and other disturbances (Theobald et al., 2023). Its values range from 0 (no human modification) to 1 (maximum modification), providing an intuitive representation of both intensity and spatial distribution of anthropogenic effects. Several studies have therefore adopted this index to represent landscape-scale changes, as well as to measure habitat integrity and ecosystem functioning (Theobald et al., 2020). Although specific socio-ecological data were lacking, GHM allowed a coherent and integrative assessment of human impact across various spatial scales. According to earlier studies, a strong correlation was found between anthropogenic disturbance gradients and vegetation dynamics, particularly in Mediterranean regions where historical land use practices have greatly impacted ecological systems (Venter et al., 2016; Williams et al., 2020).

3.6 Predictive model

To predict the potential 'old-growthness' degree within the investigated forest stands, a supervised machine learning approach, based on the Random Forest (RF) algorithm, was performed in GEE. In particular, the SHI-derived classes, representing low and high structural complexity, were designated as the response variable within the model. Meanwhile, other predictors were grouped into a multi-source raster stack - with a spatial resolution of 10 m - which included LiDAR-derived height metrics, topographic variables, S2 VIs, long-term VIs trends, and the GHM index. Training samples were obtained by extracting raster values from SHI-labelled polygons.

A space-based validation strategy was then adopted to account for spatial autocorrelation. First, samples were thinned using a 30 m grid-based filtering process; subsequently, a single sample was extracted from each grid cell, class, and forest plot. According to the conceptual approach proposed by Baumann et al. (2025), this distance should exceed the field microplot area.

A K-fold spatial cross-validation was also implemented, assigning folds by forest name (BM, TP, and CA), thereby ensuring spatial independence between the training and validation sets. Oversampling was used to balance classes only in the training subset, leaving the validation data unchanged. Then, the RF model was optimised by testing it with an increasing number of trees, before selecting the optimal configuration based on average accuracy across spatial folds.

Lastly, the RF model was trained utilising a stratified split on the spatially thinned samples, where 70% of observations were used for training and 30% for independent validation. Model performance was assessed on the validation set by evaluating overall accuracy (OA), Cohen's kappa coefficient (KA) and producers' and users' accuracy (PA and UA; Reinosch et al., 2025). Additionally, RF scorings were used to evaluate variable importance, quantifying the contribution of each predictor. A further assessment of the sampling design was done using Moran's test on the model residuals, applying the *moran.test* function in RStudio (Kumari et al., 2019). Residuals were computed as the difference between the observed SHI class and the RF-predicted probabilities, and were tested across neighbour distances ranging from 30 to 150 metres. Once trained, the model was implemented across the entire raster stack to derive SHI classifications and a continuous probability map.

4. Results

4.1 Forest structure patterns and SHI classes

By implementing the SHI procedure, 11 forest structural attributes were derived (Appendix S1, Tab. S2.4). After excluding highly skewed variables and redundant metrics, a suitable dataset was obtained to perform the multivariate analysis (KMO = 0.65). In addition, Bartlett's test further confirmed a substantial correlation between variables, yielding highly statistically significant results ($p < 0.001$). PCA showed that the first three dimensions accounted for 54.7% of the total variance.

Dim-1 (26.2%) was significantly associated with total necromass volume and dead wood components (Appendix S2, Fig. S2.1), while Dim-2 (18.3%) and Dim-3 (10.2%) reflected variations in terms of large tree abundance, living tree volume, and vertical structure diversity (Appendix S2, Fig. S2.2).

Furthermore, SHI scores expressed as percentages clearly delineated distinct structural gradients across all 59 examined microplots. Notably, TP exhibited higher median values than CA and BM, suggesting greater structural heterogeneity (Fig. 2.3). Also, K-means clustering (silhouette = 0.56) successfully defined two SHI classes reflecting low and high-microplot structural complexity (Appendix S2, Fig. S2.3).

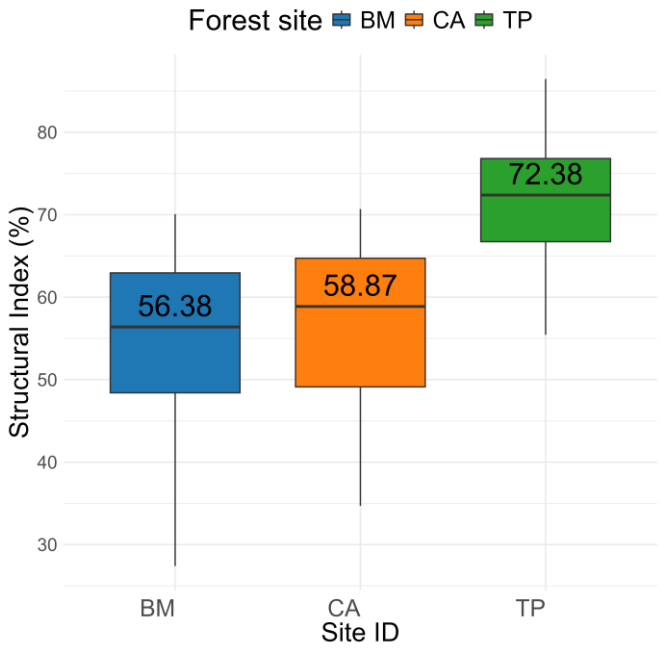

Figure 2.3. Structural heterogeneity index distribution across the three investigated forest stands: Bosco Magnano (BM), Vaccarizzo (CA) and Cugno dell'Acero (TP). The boxplots show SHI values derived from field microplots, highlighting their variability. Numeric labels indicate median SHI values at the stand level.

4.2 Seasonal vegetation indices and long-term trends

After filtering and pre-processing, 65 and 44 images from summer and autumn, respectively, were used to derive seasonal VIs composites. Likewise, long-term vegetation trends were assessed based on 431 cloud-free images acquired from Landsat collections.

More specifically, the pixel-wise trends, evaluated by the TS estimator, predominantly exhibited positive values across all investigated forest stands (Fig. 2.4). Furthermore, the stand-level validation analysis performed using the MK test verified statistically significant positive monotonic trends for NDVI at all three sites after applying the FDR correction ($q < 0.05$).

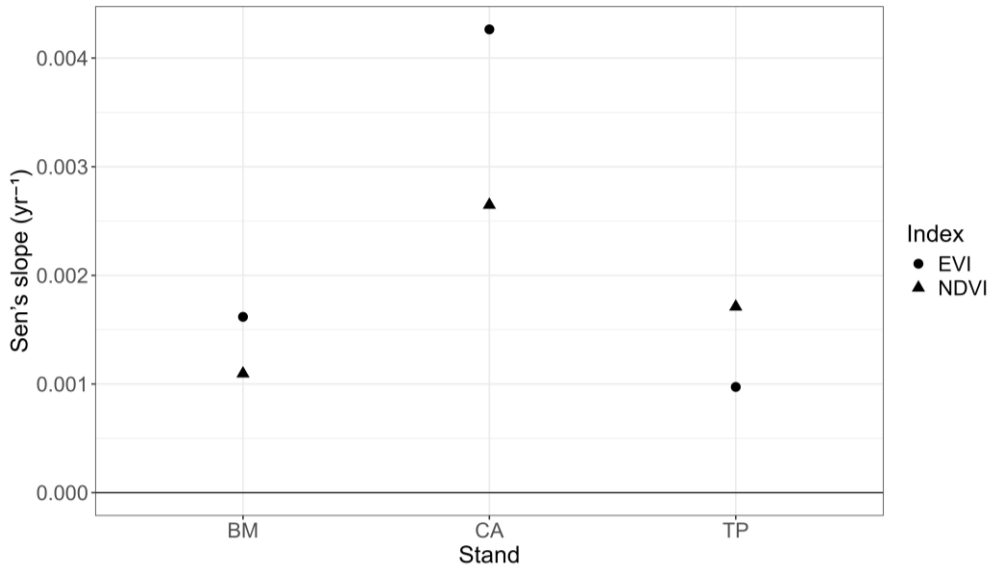

Figure 2.4. Stand-level Sen's slope estimates (yr^{-1}) derived from annual maximum NDVI and EVI Landsat time series for the three investigated forest stands. Points represent Sen's slope values for each index, indicating the magnitude and direction of long-term vegetation trends.

Our results revealed Kendall's tau (τ) values ranging from 0.53 to 0.75, along with TS estimates spanning from 0.0011 to 0.0026 yr^{-1} (Tab. 2.3). By contrast, statistically significant positive monotonic EVI trends were only detected at BM and CA sites ($q < 0.05$), as opposed to TP site, where these were not statistically significant ($q > 0.05$). However, the occurrence of predominantly positive and statistically significant long-term trends at the stand scale suggested that TS values accurately captured coherent vegetation dynamics, thereby supporting their use as continuous predictors within our model framework.

Table 2.3. Stand-level Mann–Kendall (MK) test results. Kendall's τ indicates the strength of monotonic trends, while *q*-values (*q*) represent false discovery rate (FDR)–adjusted significance levels.

Forest stand	EVI (τ)	EVI (*q*)	EVI trend	NDVI (τ)	NDVI (*q*)	NDVI trend
BM	0.238	< 0.05	Significant	0.526	< 0.0001	Significant
CA	0.605	< 0.0001	Significant	0.749	< 0.0001	Significant
TP	0.154	0.166	Not significant	0.662	< 0.0001	Significant

4.3 Model performance

The RF model achieved robust predictive performance in distinguishing low- and high-structural heterogeneity classes. After spatial thinning, 102 sample points were retained and analysed, comprising 37 low-SHI and 65 high-SHI observations. Model optimisation, based on K-fold spatial cross-validation, identified 90 trees as the optimal setup. The resulting model, which was trained using a 70/30 stratified sample split, achieved an overall accuracy (OA) of 0.84 and a Cohen's kappa (KA) of 0.68. Such findings revealed a significant agreement between the observed and predicted SHI classes. In addition, PA (producer's accuracy) reached a value of 0.92 for low and 0.80 for high SHI classes, whereas UA (user's accuracy) attained values of 0.73 and 0.94, respectively. Collectively, our results revealed notably high model reliability in identifying forest patches characterised by higher structural complexity (Fig. 2.5). Furthermore, the continuous probability map provided additional insights into the transition zones between forests exhibiting low and high structural complexity (Appendix S2, Fig. S2.4). At the site scale, high SHI areas covered 61.8% in BM, 62.5% in CA, and 91.9% in TP, reflecting significant differences across the investigated stands (Appendix S1, Tab. S2.5).

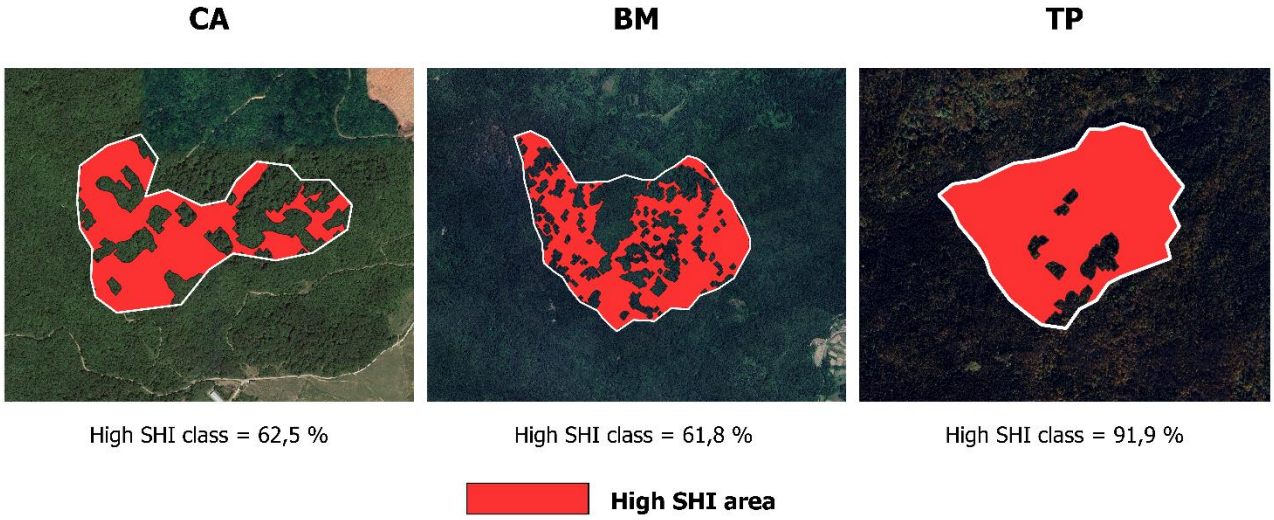

Figure 2.5. Spatial distribution of high Structural Heterogeneity Index (SHI). Red areas denote pixels classified as High SHI. White lines represent the officially established OGF's boundaries. Reported percentages indicate the proportion of each study area classified as high SHI.

Significant spatial correlation was identified at 30 m (p = 0.001) by Moran's I test; however, this disappeared beyond 40 m, thereby suggesting that spatial dependence was minimal beyond the neighbourhood scale (Table 2.4).

Table 2.4. Spatial autocorrelation analysis using Moran's I across increasing distance classes. Moran's score and its associated *p*-value are reported for each threshold. Statistical significance indicates the magnitude of the residual autocorrelation detected.

Distance (m)	Moran's I	*p*-value	
30	0.134	0.001	Significant
40	0.036	0.11	Not significant
50	- 0.003	0.41	Not significant
100	0.003	0.25	Not significant
150	0.005	0.22	Not significant

4.4 Variables importance

Variable importance analysis highlighted significant differences among the relative contributions of each predictor group (Fig. 2.6). In particular, vertical diversity represented by canopy height standard deviation (Zsd) emerged as a key factor in discerning low and high structural complexity classes. Subsequently, the seasonal Brightness Index (BI_sum and BI_aut) ranked second and fourth, respectively.

Additionally, the Global Human Modification Index (GHM) showed a strong association with structural complexity, highlighting the critical relationship between anthropogenic pressure and forest structure. Alongside these, seasonal Normalised Difference Vegetation Index metrics, including summer and autumn values (ndvi_sum and ndvi_aut), were also identified as crucial factors, further emphasising the significant impact of seasonal canopy stability and productivity patterns.

Among temporal predictors, multi-decadal functional trajectories — represented by Theil–Sen slopes of Enhanced Vegetation Index (EVI_sen) and Normalised Difference Vegetation Index (NDVI_sen) — were also among the main contributors. Their strong performance further suggests how long-term forest dynamics could provide a critical diagnostic feature in classifying stand-level heterogeneity.

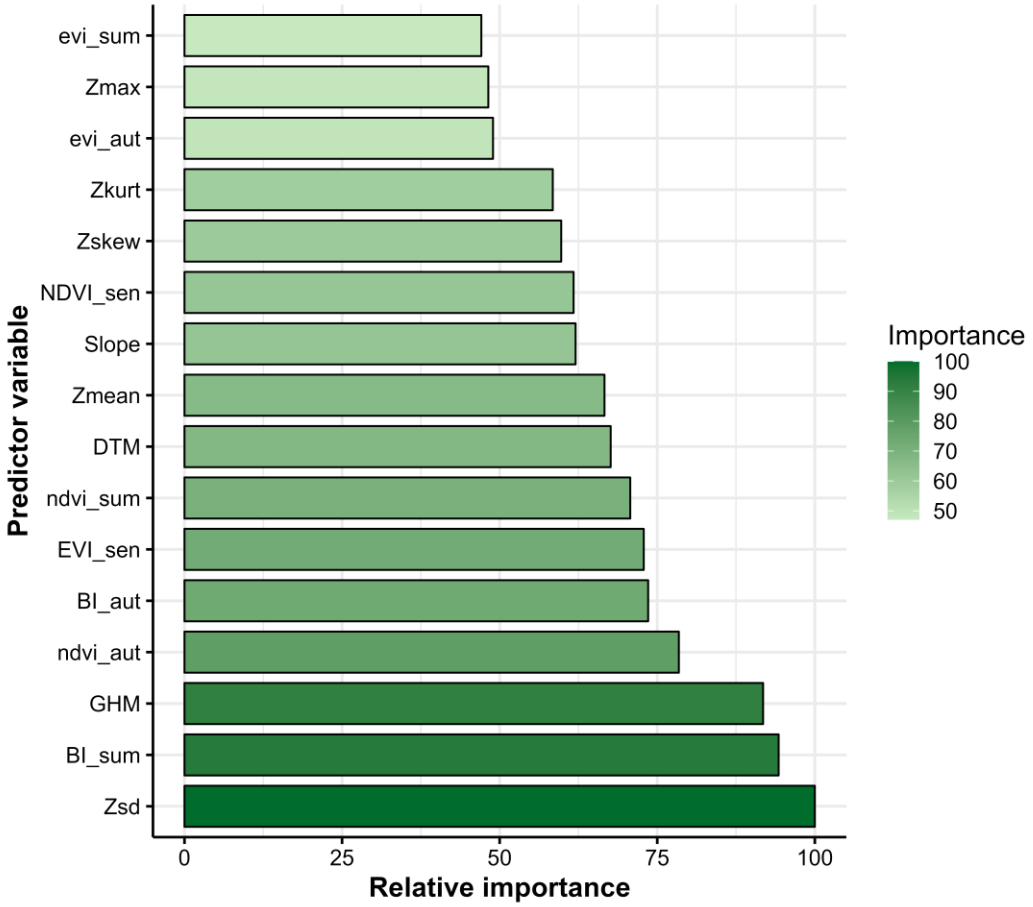

Figure 2.6. Relative importance of predictor variables derived from the random forest classifier model. Importance scores were standardised to a relative scale of 0-100. Variables were then ranked in ascending order, based on their importance, thereby highlighting their respective contributions to model performance.

Moreover, additional LiDAR metrics, including mean height (Zmean), skewness (Zskew), kurtosis (Zkurt), and maximum height (Zmax), classified as medium-ranking, provided further insight into the vertical forest structure. Although topographic variables, including elevation (DTM) and slope (Slope), offered supplementary contextual insights, summer and autumn EVI (evi_sum and evi_aut) were found to be comparatively less significant, indicating a more localised contribution when evaluated within a broader range of structural and multidecadal predictors.

5. Discussion

5.1 Structural heterogeneity as a crucial factor in defining old-growth forests

These findings emphasise the importance of adopting quantitative, structure-based approaches to refine OGF spatial interpretation as well as to identify forest patches which may be closer to late successional stages. Among LiDAR-derived metrics, canopy height standard deviation (Zsd) was the most significant, confirming that vertical heterogeneity provides straightforward and informative insights to classify forests with different structural properties.

According to Goetz et al. (2010) and Zolkos et al. (2013), height variability metrics strongly correlate with forest maturity, habitat diversity, and potentially with species richness, as it can capture multilayered canopies, gap dynamics, and large trees. Given their high significance in the model, these metrics align with ecological principles, consolidating LiDAR's effectiveness in remotely estimating forest structural complexity.

5.2 Seasonal multispectral metrics and forest characterisation

Seasonal multispectral metrics, including the Brightness Index (BI) and aggregated vegetation indices (NDVI and EVI), emerged as the second-most-effective predictors. In fact, by capturing phenological variations and stand-level reflectance heterogeneity, multi-season optical data could enhance forest characterisation, providing information not detectable by single-date images (Zhu & Woodcock, 2014; Pasquarella et al., 2016). In this context, BI might serve as a proxy to detect canopy gaps, shadowing, and structural discontinuities (Zielewska-Büttner et al., 2020).

Similarly, seasonal NDVI and EVI metrics can capture variations in canopy density and productivity during peak and later growth stages (Munteanu et al., 2022). These fluctuations typically occur alongside stand structure and successional stage differences.

5.3 Long-term vegetation trends as indicators of forest structure stability

Notably, this study employed a novel approach by using long-term trend metrics, expressed as Sen's slopes, for both NDVI (NDVI_sen) and EVI (EVI_sen). Time-series analyses have been widely utilised to investigate disturbance–recovery trajectories and long-term vegetation trends (Cohen et al., 2017). As a result, Theil Sen's slope (TS) could be used to interpret and track forest canopy responses to disturbances, recovery, and gradual structural changes.

Notably, in structurally complex stands characterised by high SHI values, weak or near-stable positive Sen's slopes may reflect long-term canopy stability resulting from limited disturbance events. Considering their significant contribution, it can be deduced that forest structural complexity not only describes the current state but also represents a continuous ecological process. This distinction is crucial in the Mediterranean context, where the widespread expansion of secondary forests can lead to an overestimation of forest maturity. Indeed, without considering long-term disturbance history, structural similarities in recovering stands may be confused as true successional maturity.

5.4 Stand-level validation and interpretation of trend significance

Stand-level validation using the Mann–Kendall (MK) test further corroborates these findings, confirming significant long-term productivity trends across the study area. Statistically significant values were observed for NDVI at all three sites; in contrast, significant EVI values were detected only in two of the three investigated stands.

The lack of statistical significance for EVI trends at the TP site does not imply an absence of change, but rather suggests stable long-term canopy dynamics. In fact, as expected for mature and OGF stands, long-term canopy dynamics tend to be characterised by gradual changes and stable structures (Pugh et al., 2019). In this context, weak positive greening trends may indicate sustained canopy stability and ecological continuity (Colangelo et al., 2021).

Comparable patterns were also observed in temperate forests, suggesting that these slow changes may be associated with biomass accumulation, gap-phase dynamics, or growth responses under climate change (Vacchiano et al., 2017).

5.5 How do human activity and the environmental context shape forest ecosystems?

Global Human Modification (GHM) proved to be one of the most significant predictors, highlighting how cumulative anthropogenic pressure can affect forest structural attributes, even in protected areas. At broad scales, these composite proxies effectively capture changes in both biodiversity and ecosystem integrity, particularly where local socio-ecological data are limited (Venter et al., 2016; Jacobson et al., 2019). This reinforces the importance of explicitly accounting for anthropogenic contexts, including topographical and climatic variables.

As shown by Cheng et al. (2023), topographic variables such as elevation (DTM) and slope (Slope) can also enhance model performance, providing insights about accessibility, microclimate, and disturbance regimes. Together, these factors play a pivotal role by shaping forest structures and modulating human impact in the long term.

5.6 Implications for conservation and old-growth forest mapping

This study successfully overcame conventional OGF designations by integrating structural (LiDAR), spectral (Sentinel-2), temporal (Landsat time series) and socio-ecological (GHM) data. Using this approach, old-growth potential could be spatially refined within designated protected areas. From a conservation perspective, this methodology enables the identification and prioritisation of core forest patches which most closely align with old-growth structural features. Overall, our findings highlight how integrated remote sensing approaches can effectively support both biodiversity conservation and forest management strategies, offering a compelling potential solution. It is important to note, however, that the transferability of the proposed framework should be interpreted at two distinct levels.

From a methodological standpoint, the entire workflow — integrating field-validated structural indices, multi-source remote sensing, and machine learning classification — is fully replicable across various forest ecosystems, provided that comparable data sources are available. At the predictive level, however, direct application of the trained model to biogeographically distinct contexts would require local recalibration, since several predictors — particularly LiDAR-derived canopy metrics, seasonal spectral indices, and the Global Human Modification Index — exhibit site-specific behaviour driven by local species composition, topographic configuration, and disturbance history. Consequently, future applications within different Mediterranean subregions or other European forest types should prioritise the re-training of the classifier on locally representative samples, while retaining the overall modelling architecture as a transferable scaffold.

6. Conclusion

The present research was conducted across three OGF sites within Pollino National Park. Although this may seem a restricted dataset, locating forest patches that simultaneously exhibit analogous species assemblages — co-dominated by European beech, turkey oak, and silver fir — within a comparable topographic and bioclimatic setting represents a substantial ecological constraint.

The convergence of these attributes — floristic composition, structural integrity, and limited anthropogenic pressure — within a single, well-defined protected area therefore constitutes an exceptional and rare scientific opportunity. This study proposed a robust methodological framework for refining the spatial delineation of forest patches with a higher relative old-growth status within officially designated areas. By adopting the Structural Heterogeneity Index (SHI) as a field-based proxy, considerable variation in forest structures was captured and modelled effectively using the Random Forest approach alongside multi-source remote sensing data.

Canopy height metrics, acquired using LiDAR technology, were identified as the most significant predictors. These results confirmed the pivotal role of vertical forest structure in accurately discerning forest areas characterised by different structural complexity.

Additional insights were also provided by seasonal Sentinel-2 vegetation indices, which highlighted canopy heterogeneity and phenological variability. Long-term trends derived from Landsat data, including NDVI and EVI, provided a temporal dimension capturing disturbance–recovery trajectories and ecological continuity. The Global Human Modification Index (GHM) further revealed how cumulative human pressures could potentially impact protected areas, thereby offering an alternative way to interpret and assess socio-ecological processes.

Clear differences were observed in the spatial distribution and frequency of high-SHI patches across all three examined sites. Stands at higher elevations, such as Cugno dell'Acero (TP), exhibited a greater prevalence of structurally complex patches. This pattern may be a direct result of its remote location and limited accessibility, which have likely discouraged intensive harvesting, ensuring minimal anthropogenic disturbance over time.

Conversely, stands at intermediate elevations, including Bosco Magnano (BM) and Vaccarizzo (CA), showed greater fragmentation and structural variability. Such findings support the

conclusions of previous studies, which emphasised how topography can play a crucial role in protecting natural forests from human-induced disturbances (Lindenmayer, 2016; Cudlín et al., 2017; Cheng et al., 2023). Although the number and spatial configuration of field plots were constrained by the adopted protocol's requirements, our findings highlighted that integrating structural, spectral, temporal, and socio-ecological predictors could enhance our understanding beyond the conventional OGF boundaries. Future work should therefore focus on optimising remote sensing analyses using an improved sampling design, as well as integrating repeated LiDAR acquisitions. Furthermore, more robust ecological interpretations could be achieved by including additional data, such as information on soil properties and biodiversity.

Extending this framework to other forest types and protected areas would provide a basis for exploring its broader application and allow the development of more rigorous scientific approaches. Ultimately, these findings provide a robust foundation for future research, revealing the potential of combining remote sensing and field-based aggregated indices to accurately identify forest patches with significant structural and ecological value, thereby supporting informed conservation strategies.

References

- Asare YM, Forkuo EK, Forkuor G, Thiel M (2020). *Evaluation of gap-filling methods for Landsat 7 ETM+ SLC-off image for LULC classification in a heterogeneous landscape of West Africa*. International Journal of Remote Sensing, 41(7), 2544–2564. DOI: https://doi.org/10.1080/01431161.2019.1693076
- Bae S, Levick SR, Heidrich L, Magdon P, Leutner BF, Wöllauer S, Müller J (2019). *Radar vision in the mapping of forest biodiversity from space*. Nature Communications, 10(1), 4757. DOI: https://doi.org/10.1038/s41467-019-12737-x
- Banskota A, Kayastha N, Falkowski MJ, Wulder MA, Froese RE, White JC (2014). *Forest monitoring using Landsat time series data: A review*. Canadian Journal of Remote Sensing, 40(5), 362-384. DOI: https://doi.org/10.1080/07038992.2014.987376
- Baumann E, Beierkuhnlein C, Preitauer A, Schmid K, Rudner M (2025). *Evaluating remote sensing data as a tool to minimize spatial autocorrelation in in-situ vegetation sampling*. Erdkunde, (H. 1), 25-40. DOI: https://doi.org/10.3112/erdkunde.2025.01.02
- Benjamini Y, Hochberg Y (1995). *Controlling the false discovery rate: a practical and powerful approach to multiple testing*. Journal of the Royal statistical society: series B (Methodological), 57(1), 289-300. DOI: https://doi.org/10.1111/j.2517-6161.1995.tb02031.x
- Blasi C, Michetti L (2005). *Biodiversity and climate*. Biodiversity in Italy contribution to the national biodiversity strategy (pp. 57–66). Rome, Italy: Palombi Editori. [online] Available at: chrome-extension://efaidnbmnnnibpcajpcglclefindmkaj/https://www.mase.gov.it/sites/default/files/archivio/biblioteca/protezione_natura/ecoregioni_italia_eng.pdf
- Brockerhoff EG, Barbaro L, Castagneyrol B, Forrester DI, Gardiner B, González-Olabarria JR, Jactel H (2017). *Forest biodiversity, ecosystem functioning and the provision of ecosystem services*. Biodiversity and Conservation, 26(13), 3005-3035. DOI: https://doi.org/10.1007/s10531-017-1453-2
- Bruening JM, Dubayah RO, Pederson N, Poulter B, Calle L (2024). *Definition criteria determine the success of old-growth mapping*. Ecological Indicators, 159, 111709. DOI: https://doi.org/10.1016/j.ecolind.2024.111709

- Burrascano S, Keeton WS, Sabatini FM, Blasi C (2013). *Commonality and variability in the structural attributes of moist temperate old-growth forests: A global review*. Forest Ecology and Management, 291, 458-479. DOI: https://doi.org/10.1016/j.foreco.2012.11.020
- Cheng K, Su Y, Guan H, Tao S, Ren Y, Hu T, Guo Q (2023). *Mapping China's planted forests using high resolution imagery and massive amounts of crowdsourced samples*. ISPRS Journal of Photogrammetry and Remote Sensing, 196, 356-371. DOI: https://doi.org/10.1016/j.isprsjprs.2023.01.005
- Cheng Z, Aakala T, Larjavaara M (2023). *Elevation, aspect, and slope influence woody vegetation structure and composition but not species richness in a human-influenced landscape in northwestern Yunnan, China*. Frontiers in Forests and Global Change, 6, 1187724. DOI: https://doi.org/10.3389/ffgc.2023.1187724
- Christensen M, Hahn K, Mountford EP, Ódor P, Standovár T, Rozenbergar D, Diaci J, Wijdeven S, Meyer P, Winter S, et al. (2005). *Dead wood in European beech (Fagus Sylvatica) forest reserves*. Forest Ecology and Management, 210, 267–282. DOI: https://doi.org/10.1016/j.foreco.2005.02.032
- Cohen WB, Healey SP, Yang Z, Stehman SV, Brewer CK, Brooks EB, Zhu Z (2017). *How similar are forest disturbance maps derived from different Landsat time series algorithms?.* Forests, 8(4), 98. DOI: https://doi.org/10.3390/f8040098
- Colangelo M, Camarero JJ, Gazol A, Piovesan G, Borghetti M, Baliva M, Ripullone F (2021). *Mediterranean old-growth forests exhibit resistance to climate warming*. Science of the total environment, 801, 149684. DOI: https://doi.org/10.1016/j.scitotenv.2021.149684
- Colditz RR, Ressl RA, Bonilla-Moheno, M. (2015, July). *Trends in 15-year MODIS NDVI time series for Mexico*. In 2015 8th International Workshop on the Analysis of Multitemporal Remote Sensing Images (Multi-Temp) (pp. 1-4). IEEE. DOI: 10.1109/Multi-Temp.2015.7245766
- Compagnucci F, Mazzoni F (2002). *Il Territorio dei Parchi Nazionali Italiani*. Quaderni di Ricerca, No. 172, Università degli Studi di Ancona Dipartimento di Economia, Ancona. [online] Available at: DOI: https://ideas.repec.org/p/anc/wpaper/172.html
- Concha VC, Caviedes J, Novoa FJ, Altamirano TA, Ibarra JT (2023). *Structural complexity is a better predictor than single habitat attributes of understory bird densities in Andean*

temperate forests. Ornithological Applications, 125(4), duad035. DOI: https://doi.org/10.1093/ornithapp/duad035

- Cudlín P, Klopčič M, Tognetti R, Máliš F, Alados CL, Bebi P, Wielgolaski FE (2017). *Drivers of treeline shift in different European mountains*. Climate Research, 73, 135-150.https://doi.org/10.3354/cr01465
- Di Filippo A, Biondi F, Piovesan G, Ziaco E (2017). *Tree ring-based metrics for assessing old-growth forest naturalness*. J Appl Ecol, 54: 737-749. DOI: https://doi.org/10.1111/1365-2664.12793
- Drusch M, Del Bello U, Carlier S, Colin O, Fernandez V, Gascon F, Bargellini P (2012). *Sentinel-2: ESA's optical high-resolution mission for GMES operational services*. Remote sensing of Environment, 120, 25-36. DOI: https://doi.org/10.1016/j.rse.2011.11.026
- Ducey MJ, Gunn JS, Whitman AA (2013). *Late-successional and old-growth forests in the northeastern United States: Structure, dynamics, and prospects for restoration*. Forests, 4(4), 1055-1086. DOI: https://doi.org/10.3390/f4041055
- Frey SJ, Hadley AS, Johnson SL, Schulze M, Jones JA, Betts MG (2016). *Spatial models reveal the microclimatic buffering capacity of old-growth forests*. Science Advances, 2(4), e1501392. DOI: https://doi.org/10.1126/sciadv.1501392
- Fuhr M, Lalechère E, Monnet JM, Bergès L (2022). *Detecting overmature forests with airborne laser scanning (ALS)*. Remote Sensing in Ecology and Conservation, 8(5), 731-743. DOI: https://doi.org/10.1002/rse2.274
- Glenn EP, Huete AR, Nagler PL, Nelson SG (2008). *Relationship between remotely-sensed vegetation indices, canopy attributes and plant physiological processes: What vegetation indices can and cannot tell us about the landscape*. Sensors, 8(4), 2136-2160. DOI: https://doi.org/10.3390/s8042136
- Goetz SJ, Steinberg D, Betts MG, Holmes RT, Doran PJ, Dubayah R, Hofton M (2010). *Lidar remote sensing variables predict breeding habitat of a Neotropical migrant bird*. Ecology, 91(6), 1569-1576. DOI: https://doi.org/10.1890/09-1670.1
- Gorelick N, Hancher M, Dixon M, Ilyushchenko S, Thau D, Moore R (2017). *Google Earth Engine: Planetary-scale geospatial analysis for everyone*. *Remote Sensing of Environment*, 202, 19-27. DOI: https://doi.org/10.1016/j.rse.2017.06.031

- Gunes G, Hens L (2007). *Ecotourism in old-growth forests in Turkey: The Kure mountains experience*. Mountain Research and Development, 27(3), 281-283. DOI: https://doi.org/10.1659/mrd.0926
- Hijmans RJ (2020) *Terra: Spatial Data Analysis. CRAN: Contributed Packages, The R Foundation*. DOI: https://doi.org/10.32614/cran.package.terra
- Hirschmugl M, Sobe C, Di Filippo A, Berger V, Kirchmeir H, Vandekerkhove K (2023). *Review on the possibilities of mapping old-growth temperate forests by remote sensing in Europe*. Environmental Modeling & Assessment, 28(5), 761-785. DOI: https://doi.org/10.1007/s10666-023-09897-y
- Jucker T, Bongalov B, Burslem DF, Nilus R, Dalponte M, Lewis SL, Coomes DA (2018). *Topography shapes the structure, composition and function of tropical forest landscapes*. Ecology letters, 21(7), 989-1000. DOI: https://doi.org/10.1111/ele.12964
- Kassambara A, Mundt F (2020) *Factoextra: Extract and Visualize the Results of Multivariate Data Analyses*. R Package Version 1.0.7. [online] Available at: https://CRAN.R-project.org/package=factoextra
- Kendall MG (1948). *Rank correlation methods*. Griffin, London. DOI: https://doi.org/10.2307/2333282
- Kirchmeir H, Vandekerkhove K, Di Filippo A, Prior A, Di Fiore L, Vanhaecht R (2023). *Mapping guideline and field survey protocol for the assessment of old-growth status and ecosystem services (biodiversity & carbon) in beech forests*. Internal Report Life Prognoses. [online] Available at: https://lifeprognoses.eu/wp-content/uploads/2023/07/Prognoses-mappingandfieldprotocol-final-June2023.pdf
- Kumari M, Sarma K, Sharma R (2019). *Using Moran's I and GIS to study the spatial pattern of land surface temperature in relation to land use/cover around a thermal power plant in Singrauli district, Madhya Pradesh, India*. Remote Sensing Applications: Society and Environment, 15, 100239. DOI: https://doi.org/10.1016/j.rsase.2019.100239
- Lalechère E, Bergès L, Vacher J, Monnet JM, Fuhr M (2022). *Building a network of overmature forests using airborne laser scanning and landscape graphs*. In IGARSS 2022-2022 IEEE International Geoscience and Remote Sensing Symposium (pp. 5901-5904). IEEE. DOI:10.1109/IGARSS46834.2022.9884614

- Lalechère E, Monnet JM, Breen J, Fuhr M (2024). *Assessing the potential of remote sensing-based models to predict old-growth forests on large spatiotemporal scales*. Journal of Environmental Management, 351, 119865. DOI: https://doi.org/10.1016/j.jenvman.2023.119865
- Lê S, Josse J, Husson F (2008). *"FactoMineR: A Package for Multivariate Analysis."* Journal of Statistical Software, 25(1), 1–18. DOI:10.18637/jss.v025.i01.
- Le Toan T, Quegan S, Davidson MWJ, Balzter H, Paillou P, Papathanassiou K, Ulander L (2011). *The BIOMASS mission: Mapping global forest biomass to better understand the terrestrial carbon cycle*. Remote sensing of environment, 115(11), 2850-2860. DOI: https://doi.org/10.1016/j.rse.2011.03.020
- Lindenmayer D. (2016). I*nteractions between forest resource management and landscape structure*. Current Landscape Ecology Reports, 1(1), 10-18. DOI: https://doi.org/10.1007/s40823-016-0002-0
- Liu C, Huang H, Sun F (2021). *A Pixel-Based Vegetation Greenness Trend Analysis over the Russian Tundra with All Available Landsat Data from 1984 to 2018*. Remote Sensing, 13(23), 4933. DOI: https://doi.org/10.3390/rs13234933
- Liu Y, Gong W, Hu X, Gong J (2018). *Forest type identification with random forest using Sentinel-1A, Sentinel-2A, multi-temporal Landsat-8 and DEM data*. Remote Sensing, 10(6), 946. DOI: https://doi.org/10.3390/rs11080929
- Luo D, Zhang HK, De Lemos H, Li J, Roy DP (2025). *A globally applicable deep learning model for Sentinel-2 cloud and shadow detection*. Science of Remote Sensing, 100278. DOI: https://doi.org/10.1016/j.srs.2025.100278
- Luyssaert S, Schulze ED, Börner A, Knohl A, Hessenmöller D, Law BE, Ciais P, Grace J (2008). *Old-growth forests as global carbon sinks*. Nature, 455(7210), 213–215. DOI: https://doi.org/10.1038/nature07276
- Maltamo M, Kallio E, Bollandsås OM, Næsset E, Gobakken T, Pesonen A (2013). *Assessing dead wood by airborne laser scanning*. Forestry Applications of Airborne Laser Scanning: Concepts and Case Studies, 375-395. DOI: https://doi.org/10.1007/978-94-017-8663-8_19
- Mann HB (1945). *Nonparametric tests against trend*. Econometrica: Journal of the econometric society, 245-259. DOI: https://doi.org/10.2307/1907187

- Mariano DA, dos Santos CA, Wardlow BD, Anderson MC, Schiltmeyer AV, Tadesse T, Svoboda MD (2018). *Use of remote sensing indicators to assess effects of drought and human-induced land degradation on ecosystem health in Northeastern Brazil*. Remote Sensing of Environment, 213, 129-143. DOI: https://doi.org/10.1016/j.rse.2018.04.048
- Marzahn P, Flade L, Sanchez-Azofeifa A (2020). *Spatial estimation of the latent heat flux in a tropical dry forest by using unmanned aerial vehicles*. Forests, 11(6), 604. DOI: https://doi.org/10.3390/f11060604
- Merce O, Borlea GF, Turcu DO (2014). *Definitions and structural attributes of the ecosystems from natural forests-short review*. [online] Available at: DOI: https://www.cabidigitallibrary.org/doi/full/10.5555/20143414979
- Munteanu C, Senf C, Nita MD, Sabatini FM, Oeser J, Seidl R, Kuemmerle T (2022). *Using historical spy satellite photographs and recent remote sensing data to identify high-conservation-value forests*. Conservation Biology, 36(2), e13820. DOI: https://doi.org/10.1111/cobi.13820
- Munteanu C, Senf C, Nita MD, Sabatini FM, Oeser J, Seidl R, Kuemmerle T (2022). *Using historical spy satellite photographs and recent remote sensing data to identify high-conservation-value forests*. Conservation Biology, 36(2), e13820. DOI: https://doi.org/10.1111/cobi.13820
- Paillet Y, Bergès L, Hjältén J, Ódor P, Avon C, Bernhardt-Römermann M, Bijlsma RJ, De Bruyn LUC, Fuhr M, Grandin ULF, et al. (2010). *Biodiversity differences between managed and unmanaged forests: Meta-analysis of species richness in Europe*. Conservation Biology, 24(1), 101–112. DOI: https://doi.org/10.1111/j.1523-1739.2009.01399.x
- Pasquarella VJ, Holden CE, Kaufman L, Woodcock CE (2016). *From imagery to ecology: leveraging time series of all available Landsat observations to map and monitor ecosystem state and dynamics*. Remote Sensing in Ecology and Conservation, 2(3), 152-170. DOI: https://doi.org/10.1002/rse2.24
- Pugh TA, Arneth A, Kautz M, Poulter B, Smith B (2019). *Important role of forest disturbances in the global biomass turnover and carbon sinks*. Nature geoscience, 12(9), 730-735. DOI: https://doi.org/10.1038/s41561-019-0427-2
- QGIS.org (2025). *QGIS Geographic Information System. QGIS Association*. [online] Available at: http://www.qgis.org

- R Core Team (2023). *R (4.3.1): A language and environment for statistical computing*. R Foundation for Statistical Computing, Vienna, Austria. [online] Available at: https://www.R-project.org
- Reinosch E, Backa J, Adler P, Deutscher J, Eisnecker P, Hoffmann K, Oehmichen K (2025). *Detailed validation of large-scale Sentinel-2-based forest disturbance maps across Germany*. Forestry: An International Journal of Forest Research, 98(3), 437-453. DOI: https://doi.org/10.1093/forestry/cpae038
- Rodrigues AC, Villa PM, Ferreira-Júnior WG, Schaefer CER, Neri AV (2021). *Effects of topographic variability and forest attributes on fine-scale soil fertility in late-secondary succession of Atlantic Forest*. Ecological Processes, 10(1), 62. DOI: https://doi.org/10.1186/s13717-021-00333-1
- Roussel J, Auty D, Coops NC, Tompalski P, Goodbody TRH, Sánchez Meador A, Bourdon JF, De Boissieu F, Achim A (2020). *"lidR: An R package for analysis of Airborne Laser Scanning (ALS) data"*. Remote Sensing of Environment, 251, 112061. DOI: https://doi.org/10.1016/j.rse.2020.112061
- Roy DP, Zhang HK, Ju J, Gómez-Dans JL, Lewis P, Schaaf CB, Sun Q, Huang H, Kovalskyy V (2016). *A general method to normalize Landsat reflectance data to nadir BRDF adjusted reflectance.* Remote Sensing of Environment, 176, 255-271. DOI: https://doi.org/10.1016/j.rse.2016.01.023
- Rustum R, Adeloye AJ, Mwale F (2017). *Spatial and temporal Trend Analysis of Long Term rainfall records in data-poor catchments with missing data, a case study of Lower Shire floodplain in Malawi for the Period 1953–2010*. Hydrology and earth system sciences discussions, 2017, 1-30. DOI: https://doi.org/10.5194/hess-2017-601
- Sabatini FM, Burrascano S, Keeton WS, Levers C, Lindner M, Pötzschner F, Kuemmerle T (2018). *Where are Europe's last primary forests?*. Diversity and distributions, 24(10), 1426-1439. DOI: https://doi.org/10.1111/ddi.12778
- Sabatini FM, Burrascano S, Lombardi F, Chirici G, Blasi C (2015). *An index of structural complexity for Apennine beech forests*. IForest, 8, 314-323. DOI: https://dx.doi.org/10.3832/ifor1160-008
- Sen PK (1968). *Estimates of the regression coefficient based on Kendall's tau*. Journal of the American statistical association, 63(324), 1379-1389.

- Shimada M, Itoh T, Motooka T, Watanabe M, Shiraishi T, Thapa R, Lucas R (2014). *New global forest/non-forest maps from ALOS PALSAR data (2007–2010)*. Remote Sensing of environment, 155, 13-31. DOI: https://doi.org/10.1016/j.rse.2014.04.014
- Spracklen BD, Spracklen DV (2019). *Identifying European old-growth forests using remote sensing: A study in the Ukrainian Carpathians*. Forests, 10(2), 127. DOI: https://doi.org/10.3390/f10020127
- Theobald DM, Kennedy C, Chen B, Oakleaf J, Baruch-Mordo S, Kiesecker J (2020). *Earth transformed: detailed mapping of global human modification from 1990 to 2017*. Earth System Science Data, 12(3), 1953-1972. DOI: https://doi.org/10.5194/essd-12-1953-2020
- Theobald DM, Kennedy C, Chen B, Oakleaf J, Baruch-Mordo S, Kiesecker J (2023). *Data for detailed temporal mapping of global human modification from 1990 to 2017 (v1.5) [Data set]*. Zenodo. DOI: https://doi.org/10.5281/zenodo.7534895
- Thomas RQ, Hurtt GC, Dubayah R, Schilz MH (2008). *Using lidar data and a height-structured ecosystem model to estimate forest carbon stocks and fluxes over mountainous terrain*. Canadian Journal of Remote Sensing, 34(sup2), S351-S363. DOI: https://doi.org/10.5589/m08-036
- Tinya F, Márialigeti S, Bidló A, Ódor P (2019). *Environmental drivers of the forest regeneration in temperate mixed forests*. Forest Ecology and Management, 433, 720-728. DOI: https://doi.org/10.1016/j.foreco.2018.11.051
- Todaro L, Andreu L, D'Alessandro CM, Gutiérrez E, Cherubini P, Saracino A (2007). Response of Pinus leucodermis to climate and anthropogenic activity in the National Park of Pollino (Basilicata, Southern Italy). Biological conservation, 137(4), 507-519. DOI: https://doi.org/10.1016/j.biocon.2007.03.010
- Tuominen J, Lipping T, Kuosmanen V, Haapanen R (2009). *Remote Sensing of Forest Health*. Geoscience and Remote Sensing. Pei-Gee Peter Ho (Ed.), ISBN: 978-953-307-003-2. [online] Available at: https://www.intechopen.com/chapters/9498
- U.S. Geological Survey (2021). *Landsat Collection 2 Level-2 Science Products: U.S.* Geological Survey Fact Sheet 2021–3055, 2 p., DOI: https://doi.org/10.3133/fs20213055
- Uhl B, Schall P, Bässler C (2025). *Achieving structural heterogeneity and high multi-taxon biodiversity in managed forest ecosystems: A European review*. Biodiversity and Conservation, 34(9), 3327-3358. DOI: https://doi.org/10.1007/s10531-024-02878-x

- Vacchiano G, Garbarino M, Lingua E, Motta R (2017). *Forest dynamics and disturbance regimes in the Italian Apennines*. Forest Ecology and Management, 388, 57-66. DOI: https://doi.org/10.1016/j.foreco.2016.10.033
- Venter O, Sanderson EW, Magrach A, Allan JR, Beher J, Jones KR, Watson JE (2016). *Sixteen years of change in the global terrestrial human footprint and implications for biodiversity conservation*. Nature communications, 7(1), 12558. DOI: https://doi.org/10.1038/ncomms12558
- Wilks D S (2006). *On "field significance" and the false discovery rate.* Journal of applied meteorology and climatology, 45(9), 1181-1189. DOI: https://doi.org/10.1175/JAM2404.1
- Yan J, Zhang G, Ling H, Han F (2022). *Comparison of time-integrated NDVI and annual maximum NDVI for assessing grassland dynamics*. Ecological Indicators, 136, 108611.https://doi.org/10.1016/j.ecolind.2022.108611
- Yin G, Mariethoz G, Sun Y, McCabe MF (2017). *A comparison of gap-filling approaches for Landsat-7 satellite data*. International Journal of Remote Sensing, 38(23), 6653-6679. DOI: https://doi.org/10.1080/01431161.2017.1363432
- Zhang Q, Zheng Z, Wu Z, Cao Z, Luo R (2022). *Using Multi-Source Geospatial Information to Reduce the Saturation Problem of DMSP/OLS Nighttime Light Data*. Remote Sensing, 14(14), 3264. DOI: https://doi.org/10.3390/rs14143264
- Zhu Z, Woodcock CE (2014). *Continuous change detection and classification of land cover using all available Landsat data*. Remote sensing of Environment, 144, 152-171. DOI: https://doi.org/10.1016/j.rse.2014.01.011
- Zielewska-Büttner K, Adler P, Kolbe S, Beck R, Ganter LM, Koch B, Braunisch V (2020). *Detection of standing deadwood from aerial imagery products: Two methods for addressing the bare ground misclassification issue*. Forests, 11(8), 801. DOI: https://doi.org/10.3390/f11080801
- Zlonis EJ, Deo R, Berdeen JB (2022). *LiDAR and multispectral imagery predict the occurrence of tree cavities suitable for a cavity-nesting duck*. Remote Sensing in Ecology and Conservation, 8(2), 191-207. DOI: https://doi.org/10.1002/rse2.236
- Zolkos SG, Goetz SJ, Dubayah R (2013). *A meta-analysis of terrestrial aboveground biomass estimation using lidar remote sensing*. Remote sensing of environment, 128, 289-298. DOI: https://doi.org/10.1016/j.rse.2012.10.017

Appendices – Chapter 2

Appendix S1. Supplementary Tables

Table S2.1. Forest structural variables derived from field-collected data and used to compute the Structural Heterogeneity Index (SHI). For each variable, the table provides the abbreviation, description, and corresponding unit of measurement.

Abbreviation	Variable	Unit of measurement
BA_living_tree	Basal area living tree	m^2
BASnagST	Basal area, Snag and Dead standing tree	m^2
Canopy_cover	Canopy cover	%
Vol_CWD	Volume Course Woody Debris	m^3
Density_living_tree	No. Living trees	No. trees
DensSnagST	No. Snag & Dead standing trees	No. trees
Vol_necromass	Volume Necromass	m^3
Vol_living_tree	Volume Living trees	m^3
N_dbh	No. Diameter class	No. classes
N_decay_classes	No. Decay classes	No. classes
Vol_SnagST	Volume Snag and Dead standing tree	m^3
n_dbh_40	No. Tree with DBH > 40	No. trees
n_dbh_50	No. Tree with DBH > 50	No. trees
n_dbh_70	No. Tree with DBH > 70	No. trees
Tree_rich	No. Tree species	No. tree species
Vol_stump	Volume Stump	m^3
Vol_ddt	Volume Dead downed tree	m^3
Dom_height	Average of the 5 highest trees	m
QMD	Quadratic mean diameter	cm
H_sd	Standard deviation Height	m
Gini	Gini index (basal area)	m^2
dlR	Dead live ratio	m^3
dbh_max	Max diameter	cm
dbh_min	Min diameter	cm

Table S2.2. Summary table of the LiDAR sensor's technical specifications and acquisition settings used for data collection, including precision and accuracy parameters.

LASER CHARACTERISTICS	
Wavelength	1550 nm
Type/class laser	Class 1
ACQUISITION METHODOLOGY	
Scanning Method	Polygonal rotating mirror
Maximum scanning angle	60 deg
Scan pattern	Parallel lines
Measurement	Full Waveform
PRECISION AND RESOLUTION	
Precision	10 mm
Accuracy	20 mm

Table S2.3. Landsat satellite collections used for long-term vegetation analysis, indicating sensor type and acquisition period.

Collection	Time window
Landsat 5 TM	1985–2006; 2008–2011
Landsat 7 ETM+	2007; 2012–2013
Landsat 8 OLI	2014–2024

Table S2.4. Variables representing the Structural Heterogeneity Index (SHI) have been grouped into ecological categories according to key old-growth forest attributes, as defined by the EU Biodiversity Strategy. Each category reflects a distinct feature of the naturalness, structural complexity and stand development.

Ecological domain	Variable (abbrev.)	Description	Unit	Relevance to old-growth status
Deadwood accumulation and ecological continuity	Vol_CWD	Volume of coarse woody debris	m^3	A significant amount of coarse woody debris provides essential habitat for saproxylic organisms. Coarse woody debris reflects natural mortality dynamics in late-successional and unmanaged stands and the accumulation of decaying material. It encompasses both standing and downed deadwood, capturing the long-term carbon storage and structural complexity associated with old-growth forests.
	Vol_ddt	Volume of dead downed trees		
	Vol_necromass	Total volume of necromass		
Tree size, structure and legacy trees	n_dbh_40	Number of trees with DBH > 40 cm	No. trees	The occurrence of large trees reflects extended growth periods, a lack of disturbance, and distinctive structural features typical of OGFs.
	n_dbh_70	Number of trees with DBH > 70 cm		
	QMD	Quadratic mean diameter	cm	
Multi-layered vertical structure	Dom_height	Mean height of the five tallest trees	m	Highly dominant trees and vertical heterogeneity both indicate stands in a late-successional stage, which is typical of old-growth ecosystems.
	H_sd	Standard deviation of tree height		
Stand developmental complexity	N_dbh	Number of diameter classes	No. classes	A wide diameter-class distribution suggests an uneven-aged structure, as well as continuous regeneration, which are two key features found in OGFs. In addition, high diversity of decay stages reflects sustained deadwood accumulation and long-term ecological processes.
	N_decay_classes	Number of decay classes		
Live biomass and stand maturity	Vol_living_tree	Volume of living trees	m^3	Late-successional forests that have experienced limited disturbance over an extended period tend to have high standing biomass.

Table S2.5. Total area and extent of forest patches classified as high Structural Heterogeneity Index (SHI). In particular, for each OGF, the total area, the high SHI area and the corresponding percentage are provided.

Site	OGF area (ha)	High SHI area (ha)	High SHI area (%)
BM	108.2	66.8	61.8
CA	20.9	13.1	62.5
TP	34.5	31.7	91.9

Appendix S2. Supplementary Figures

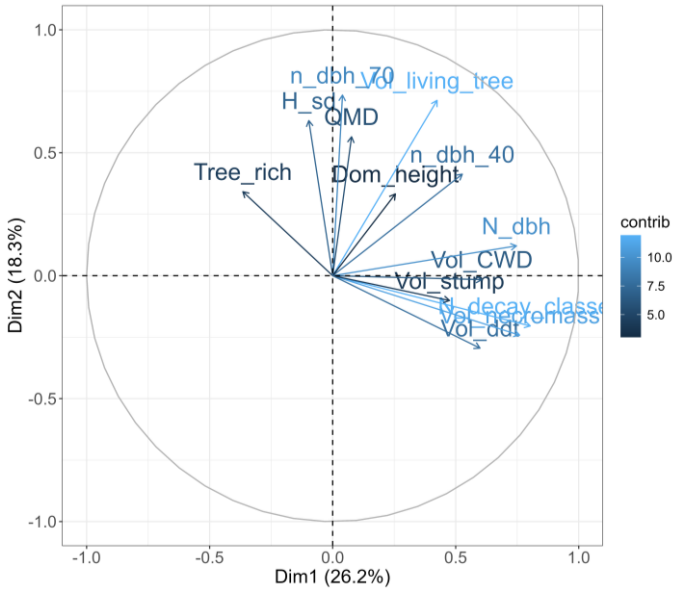

Figure S2.1. **Principal Component Analysis for Dimensions 1 and 2**. Dim1 reflects a gradient associated with forest structural complexity, influenced by variables such as tree size heterogeneity, deadwood volume, and decay-related attributes. In contrast, Dim2 is more strongly associated with vertical structure and stand density metrics, including dominant height, quadratic mean diameter, and large tree density.

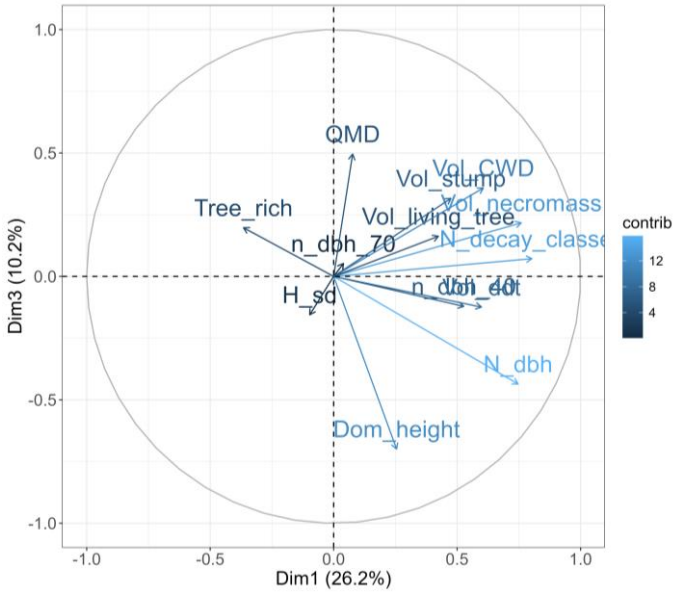

Figure S2.2. Principal Component Analysis for Dimensions 1 and 3. Dim1 is mainly defined by variables related to tree diameter distribution, standing and downed deadwood volume, necromass, and decay-class attributes; whereas Dim3 captures additional variance related to dominant tree dimensions and vertical stand structure, such as quadratic mean diameter and dominant height.

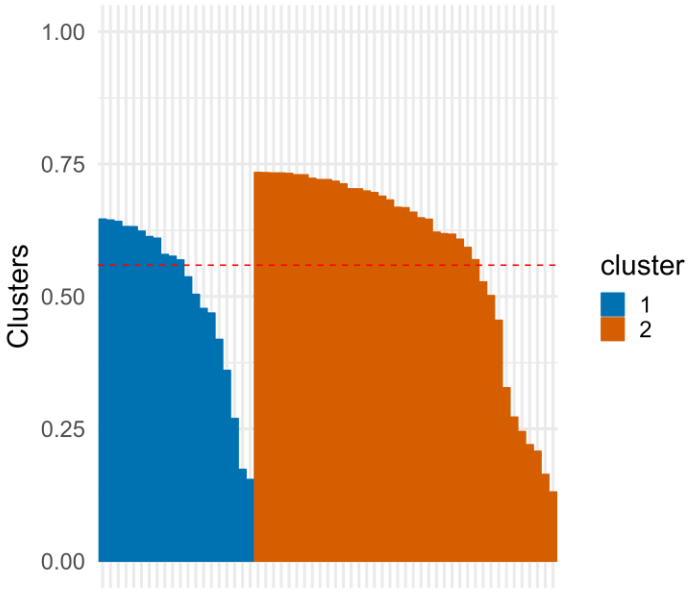

Figure S2.3. Silhouette coefficients obtained from k-means clustering applied to Structural Heterogeneity Index (SHI) values, used to identify optimal class separation between low and high structural complexity conditions. Blue and orange segments correspond to the two SHI clusters identified by the algorithm. The dashed red line represents the mean silhouette score across all samples, providing a metric for assessing the overall clustering quality.

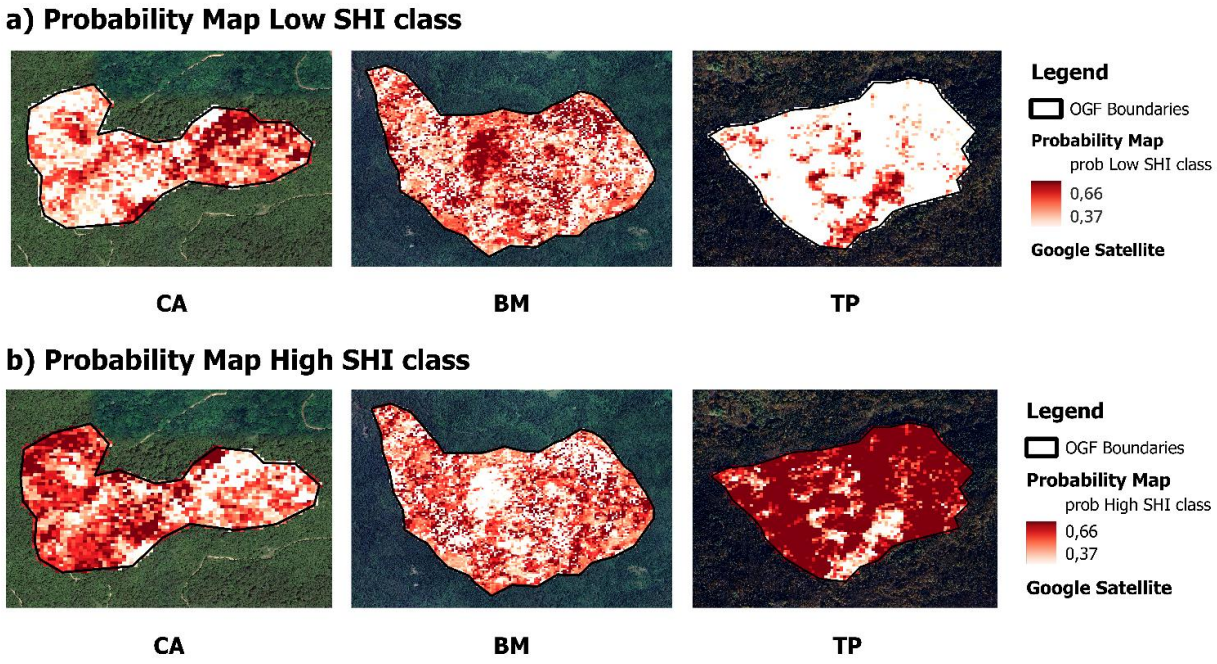

Figure S2.4. **Spatial distribution of predicted class probability, obtained from the Random Forest model, for (a) low Structural Heterogeneity Index (SHI) class and (b) high SHI class**. Pixel values represent the posterior probability assigned to each SHI class, with darker red tones reflecting higher probabilities. Official old-growth forest (OGF) boundaries are delineated in black.

Chapter 3: Satellite time series analysis of the long-term ecological dynamics in Mediterranean old-growth forests

Summary: *Building on earlier insights, Chapter 3 expands our analysis to provide a detailed investigation into long-term canopy dynamics. By studying a 40-year continuous Landsat time series, forest canopy greenness trends were examined and quantified using the Enhanced Vegetation Index (EVI). This enabled an effective investigation of multi-decadal trends in both Old-Growth Forests (OGFs) and ecologically comparable managed forests. A non-parametric trend estimation framework combined with block-level bootstrap inference was adopted to ensure robustness against spatial dependence, noise, and non-normal data distributions. Results consistently revealed a higher and more spatially stable long-term greenness trend within OGFs. Pure beech forests exhibited stronger and clearer contrasts compared to mixed stands, reflecting their differences in species composition, successional stage, and structural arrangement. When interpreted alongside previous findings, such results strongly suggest a significant relationship between forest structural complexity and long-term functional stability. Overall, this chapter highlights two key points: firstly, the pivotal role of OGFs as reference systems in ecosystem monitoring; and secondly, how long-term canopy greenness trajectories can offer an additional dimension when assessing forest status, resilience, and conservation value.*

Satellite-based assessment of long-term canopy dynamics within Mediterranean old-growth forests

Travascia D.[1], Hirschmugl M.[2], Zandler H.[2], Fiorentino C.[1], Schettino A.[3], Piovesan G.[4], Ripullone F.[1]

[1] *Department of Agricultural, Forest, Food and Environmental Sciences, University of Basilicata, Via dell'Ateneo Lucano 10, 85100 Potenza, Italy*

[2] *Department of Geography and Regional Sciences, University of Graz, Heinrichstr. 36, 8010 Graz, Austria*

[3] *Pollino National Park, Complesso monumentale Santa Maria della Consolazione, 85048 Rotonda, Italy*

[4] *Department of Ecological and Biological Sciences (DEB), University of Tuscia, Largo dell'Università, 01100 Viterbo, Italy*

Abstract

Old-growth forests (OGFs) play a crucial role in preserving biodiversity, storing carbon, and ensuring ecosystem resilience. However, their long-term functional dynamics are rarely considered in conjunction with their structural attributes. The present study analysed multi-decadal canopy greenness trends for six designated OGFs within Pollino National Park (Italy), comparing them with six ecologically comparable managed stands (NOGFs). Annual maximum Enhanced Vegetation Index (EVI) composites were derived from Landsat data spanning 1985–2024. Long-term trends were then quantified at pixel level by using the Theil–Sen slope (TS) estimator, as well as the modified Mann–Kendall (m-MK) test to determine their statistical significance. Block-level medians were computed to aggregate TS values into 100 x 100 m grid cells, addressing spatial dependence and reducing pseudo-replication. Differences between forest classes were assessed via block bootstrap resampling and Cliff's delta effect sizes. Across all sites, EVI TS magnitudes were generally low, suggesting weak monotonic trends. Nevertheless, OGFs exhibited a higher central tendency and a greater proportion of positive slopes than NOGFs, particularly in mixed and pure beech forests, where positive trends exceeded 90% of pixels. Block-level distributions revealed a systematic shift towards more positive EVI TS values in OGFs. Statistical analysis revealed significant differences between forest classes across all study sites (ΔEVI TS = 0.000331–0.001577), with stronger effects in pure beech stands. Results were also consistent when analysed at the forest-type level, where OGFs achieved higher long-term greening rates than managed sites, especially in beech-dominated stands. Overall, these findings highlighted how OGFs tend to exhibit more persistent greening trajectories and greater functional stability, thus underlining the effectiveness of combining robust trend estimators with satellite-derived vegetation indices to assess long-term ecological continuity in forest ecosystems.

1. Introduction

Old-growth forests (OGFs) represent stable ecological ecosystems developed over long periods with minimal human interference. Widely recognised as benchmarks for biodiversity conservation, ecosystem functioning and carbon storage, OGFs play a crucial role in addressing environmental and climate challenges (Luyssaert et al., 2008; Paillet et al., 2010; Burrascano et al., 2013). Furthermore, OGFs exhibit distinctive structural attributes, including old, large trees, multilayered canopies, and significant amounts of deadwood. These features, along with ecological continuity, are essential for their resilience against potential stressors (Frey et al., 2016; Colangelo et al., 2021). Therefore, to accurately assess their status, it is necessary to consider both their long-term dynamics and their current structure.

Canopy greenness, photosynthetic activity and biomass productivity have long been monitored using satellite-derived vegetation indices (Glenn et al., 2008; Banskota et al., 2014). In particular, the Enhanced Vegetation Index (EVI) has proven effective in analysing forest ecosystems characterised by high biomass and dense canopy cover. According to Zhang et al. (2022), EVI reduces background noise and saturation effects more effectively than the Normalised Difference Vegetation Index (NDVI). Its role in studying forest productivity, as well as phenology and responses to climate change, is thus crucial (Spracklen & Spracklen, 2019; Pasquarella et al., 2016).

Data from various satellite archives, particularly those from the Landsat programme, provide a valuable opportunity to study vegetation dynamics over several decades. By analysing these time series, gradual greening and browning trends can be identified, offering insights related to land use changes and forest status (Cohen et al., 2017; Marques et al., 2024). As demonstrated by previous studies (Zhang, 2015; Zibri et al., 2016; Meng et al., 2019; Balata et al., 2022), the analysis of vegetation index trends is a key method to distinguish ecosystem trajectories and their associated fluctuations, including vegetation succession, recovery, and resilience to climate change (Zhu & Woodcock, 2014; Kennedy et al., 2018). In this context, non-parametric estimators such as the Theil–Sen slope (TS) and the Mann–Kendall (MK) test represent standard techniques used to investigate long-term vegetation trends (Gutiérrez-Hernández & García, 2024). Furthermore, such tools are also widely adopted for their resilience to outliers, non-normal data distributions, and missing data (Sen, 1968; Eastman et al., 2013).

As demonstrated by Cipolla & Montaldo (2022), Wang et al. (2023) and Franquesa et al. (2025), their application in detecting monotonic vegetation trends across various natural ecosystems — including forests, grasslands, and wetlands — emerged effective, particularly when changes were subtle and gradual. Nevertheless, studies employing long-term trend analyses aimed at investigating OGFs' temporal dynamics remain limited. Therefore, current studies often rely on structural metrics from field inventories or proximal sensing, potentially overlooking the critical dimension of ecological continuity (Hirschmugl et al., 2023; Bruening et al., 2024).

This gap is particularly evident in Mediterranean regions, where complex land use histories and disturbances can result in forests achieving structural maturity yet failing to attain old-growth attributes (Burrascano et al., 2013; Sabatini et al., 2018). As Rodriguez et al. (2024) have shown, an increased stability over time can be observed within natural or protected forests. Undisturbed forest biomes tend to exhibit a more stable trajectory in vegetation indices when compared to managed stands (Shestakova et al., 2022).

To address these gaps, this study introduces a novel pair-wise analytical framework that, for the first time in a Mediterranean OGF context, combines long-term satellite-derived vegetation indices with non-parametric trend estimators and block-bootstrap inference to enable a statistically robust comparison of multi-decadal canopy dynamics between six designated OGFs and ecologically comparable managed reference stands within the Pollino National Park. These analyses were conducted using a 40-year annual maximum EVI derived from Landsat datasets. To ensure statistical robustness, long-term vegetation trends were examined through complementary methodologies. EVI trends were first quantified in terms of direction and magnitude by using the TS estimator. Subsequently, their statistical significance and spatial distribution were evaluated at the pixel level through an m-MK test accounting for temporal autocorrelation. Finally, a block-bootstrap resampling approach was employed to rigorously assess differences in the observed EVI trends within old-growth and managed forest pairs.

According to existing ecological theory, we hypothesise that OGFs will reveal distinct long-term vegetation dynamics. More specifically: (1) OGFs will exhibit more stable long-term EVI (Enhanced Vegetation Index) trajectories, showing reduced interannual variability; (2) managed stands will exhibit more pronounced EVI variability, reflecting disturbance-recovery cycles; and (3) these differences will vary in magnitude according to forest type.

By testing these hypotheses, this study provides a temporal perspective that complements structural and spatial assessments, offering a more complete picture of the functional status and conservation value of Mediterranean old-growth ecosystems.

2. Materials and methods

2.1 Study area

Pollino National Park (Pollino NP) is the largest protected area in Italy, covering approximately 192,565 hectares across the Calabria and Basilicata regions. Characterised by considerable biodiversity, this area is renowned for its notable altitudinal gradient as well as its complex geomorphology. According to Piovesan et al. (2019) and Palli et al. (2023), Pollino NP is considered a significant biogeographical transition area where the interaction between land use and climate over time played a key role in shaping forest composition and structure (Todaro et al., 2007; Rita et al., 2014).

Several earlier studies have also recognised the ecological importance of this protected area, emphasising its role in safeguarding unique forest ecosystems and rare endemic species (Burrascano et al., 2013; Rita et al., 2014; Colangelo et al., 2021). Such features make Pollino NP a suitable case study to investigate long-term forest dynamics within an ecosystem characterised by high ecological continuity and well-documented conservation value.

2.2 Pair-wise stand selection

Six designated OGFs were selected within the Pollino NP according to the objectives of the present study (Fig. 3.1). These sites were all characterised by attributes typically associated with old-growth ecosystems, including minimal human disturbance (Burrascano et al., 2013; Rita et al., 2014; Colangelo et al., 2021), occurrence of large, old trees (Piovesan et al., 2018), large amounts of deadwood (Burrascano et al., 2018), as well as high structural complexity. More specifically, the selected OGFs included two main forest types. Mixed mountain forests, dominated by European beech (*Fagus sylvatica L.*), turkey oak (*Quercus cerris L.*) and/or silver fir (*Abies alba Mill.*), represented by Vaccarizzo (CA), Bosco Magnano (BM) and Cugno dell'Acero (TP).

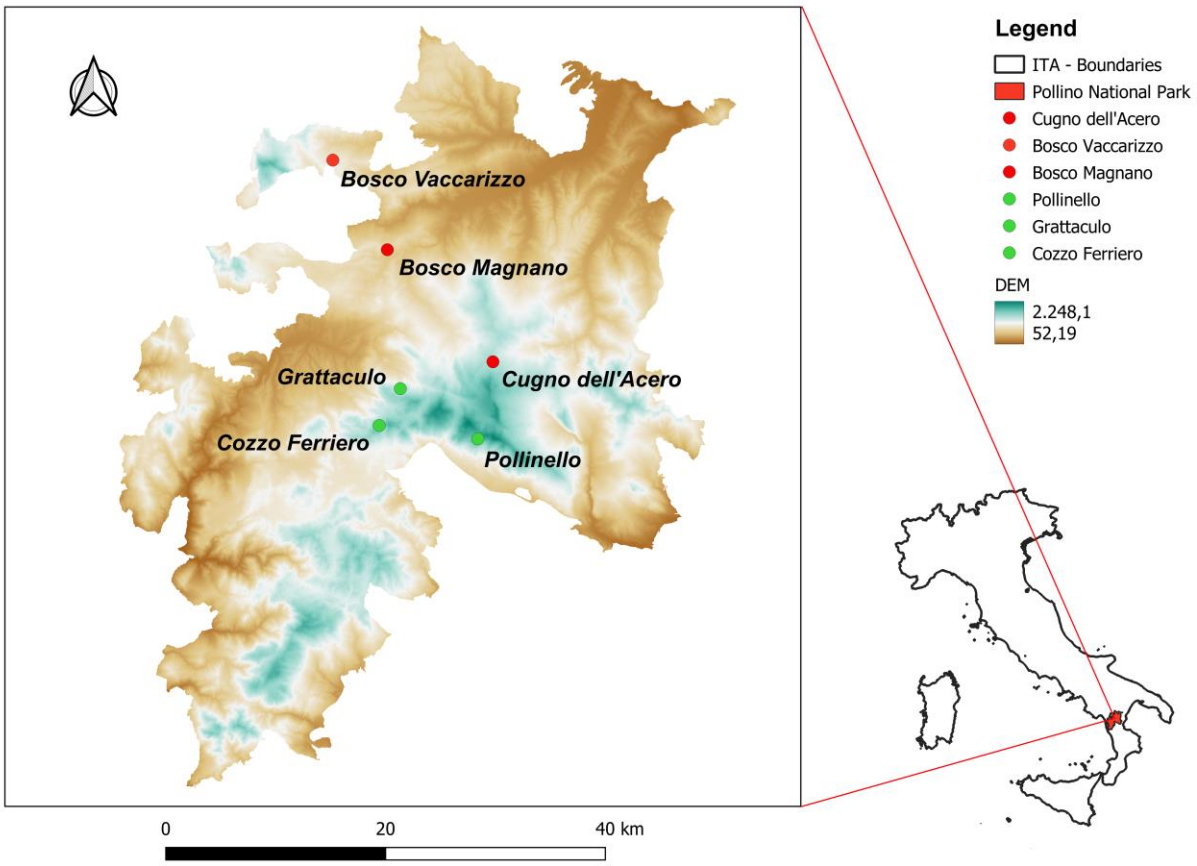

Figure 3.1. Study area and surveyed forest sites. Park boundaries are plotted on a digital elevation model (DEM), highlighting the spatial distribution of the six stands designated as old-growth forests (OGFs). Red dots represent mixed forest sites — Bosco Vaccarizzo, Bosco Magnano and Cugno dell'Acero — while green dots correspond to pure beech forest sites — Pollinello, Grattaculo and Cozzo Ferriero.

According to Castellaneta et al. (2023), such forests are characterised by heterogeneous canopies and uneven stand structures developed over several decades. In contrast, pure beech forests, such as Pollinello (PO), Cozzo Ferriero (RO) and Grattaculo (VIG), were included in the second group (Tab. 3.1). These sites commonly exhibit later successional stages, old trees and considerable resilience to natural disturbances (Iovino et al., 2010).

In particular, the PO and RO sites were included in the European network of ancient beech forests and are recognised by UNESCO as World Heritage Sites, providing further evidence of their scientific and cultural value.

Table 3.1. An overview concerning the investigated OGF sites, including site identification, forest name, forest type, dominant tree species, elevation, and the corresponding Site of Community Importance (SCI) code**.**

Forest name	Site ID	Forest type	Dominant tree species	Elevation (m)	Area (ha)	SCI code
Bosco Magnano	BM	Mixed	*Fagus sylvatica* L., Quercus cerris L.	850	18	IT9210070
Vaccarizzo	CA	Mixed	*Fagus sylvatica* L., *Abies alba* Mill.	950	21	IT9210040
Cugno dell'Acero	TP	Mixed	*Abies alba Mill., Fagus sylvatica L.*	1400	83	IT9210075
Grattaculo	VIG	Pure beech	*Fagus sylvatica* L.	1750	54	1133qui-082
Cozzo Ferriero	RO	Pure beech	*Fagus sylvatica* L.	1750	70	IT9210125
Pollinello	PO	Pure beech	*Fagus sylvatica* L.	1950	20	1133ter-045

Furthermore, following guidelines defined by the Pollino NP authorities (Tab. 3.2), six managed reference stands (NOGF) were selected as comparative sites. Specifically, the NOGFs were chosen based on a set of predefined criteria to ensure their ecological comparability with the OGF sites; critical factors, such as elevation, slope and forest type, were explicitly considered.

Table 3.2. Managed stand details. Summary of the environmental and geographical properties of managed forest stands, including the distance to their respective old-growth reference stands.

Site ID	Coordinates		Municipality	Forest type	Elevation (m)	Area (ha)	Dist. to paired OGF (km)
	Lat	*Long*					
BM - M	40.051	16.112	S. Severino Lucano	Mixed	800	33	0,9
CA - M	40.127	16.032	Carbone	Mixed	1050	17	1,4
TP - M	39.966	16.221	Terranova	Mixed	1450	45	0,8
VIG - M	39.933	16.125	Viggianello	Pure beech	1550	75	0,6
RO - M	39.915	16.103	Rotonda	Pure beech	1650	107	0,5
PO - M	39.919	16.180	Chiaromonte	Pure beech	1700	144	2,5

2.3 Satellite time-series processing

To analyse long-term forest dynamics, a continuous time series covering 40 years (1985–2024) was processed using Landsat surface reflectance data through the Google Earth Engine (GEE) environment (Gorelick et al., 2017). To ensure temporal continuity and radiometric consistency across all observations, surface reflectance products from Landsat 5 (Thematic Mapper, TM),

Landsat 7 (Enhanced Thematic Mapper Plus, ETM+) and Landsat 8 (Operational Land Imager, OLI) were utilised (U.S. Geological Survey, 2021).

Images were acquired during the main growing season, from April to October, and only those with cloud cover less than 20% were retained. Radiometric calibration was then applied using official scale factors, while clouds, cirrus and shadows were masked based on the QA_PIXEL bit mask. To mitigate any artefacts derived from the failure of Landsat 7's scan line corrector (SLC), a time-stratified approach was adopted (Tab. 3.3). Specifically, missing data were reconstructed to preserve temporal continuity using local spatio-temporal linear regression based on temporally adjacent observations (Yin et al., 2017; Asare et al., 2020).

Table 3.3. Temporal distribution of satellite data sources. Summary of the Landsat satellite collections and their respective time windows utilised to reconstruct vegetational index trajectories from 1985 to 2024.

Collection	Time window
Landsat 5 TM	1985–2006; 2008–2011
Landsat 7 ETM+	2007; 2012–2013
Landsat 8 OLI	2014–2024

Forest canopy status was then estimated using the Enhanced Vegetation Index (EVI). As opposed to the Normalised Difference Vegetation Index (NDVI), EVI mitigates the impact of background and atmospheric noise while preserving sensitivity to high biomass and closed canopy conditions typically observed in late-successional and old-growth ecosystems (Glenn et al., 2008; Zhang et al., 2022). Maximum annual EVI composites were then derived to represent peak canopy greenness and minimise residual cloud and short-term phenological variability. Long-term EVI trends at the pixel scale were quantified using the Theil–Sen slope estimator (TS; Sen, 1968), a robust non-parametric method commonly employed in ecological time series analysis. TS estimates temporal trends based on the median of all pairwise slopes within the time series (Eq. 3.1).

$$\text{(Equation 3.1)} \qquad \beta = \text{Median}\left(\frac{Xj - Xi}{tj - ti}\right) \qquad \text{for all pairs (i, j)}$$

Where: $Xj - Xi$ represents the difference between the observed values at two time points; and $tj - ti$ refers to the time difference between two observations, where tj occurs after ti.

According to median slope estimation, TS provides a robust approach, ensuring greater resilience to outliers, non-normal data distributions and missing values. According to Gutiérrez-Hernández and García (2024), TS can tolerate a significant proportion of biased data without affecting its reliability or accuracy in long-term monitoring applications. Further, by focusing on monotonic trends derived from annual maximum EVI values, TS emphasises long-term canopy changes, reducing sensitivity to interannual variability.

Such characteristics are crucial in analysing gradual ecological processes, including forest degradation, recovery, and long-term dynamics (Colditz et al., 2015; Mariano et al., 2018). All trend estimates were finally spatially constrained to capture EVI trends exclusively related to forest areas (Shimada et al., 2014) by applying the forest mask acquired from the ALOS PALSAR Forest/Non-Forest dataset (JAXA/ALOS/PALSAR/YEARLY/FNF4).

2.4 Monotonic trend detection

To ensure a reliable interpretation of the TS results, an assessment of monotonic trend significance was conducted. Long-term trends were then assessed using the modified Mann–Kendall (m-MK) test, implemented in RStudio through the 'Kendall' package (McLeod, 2025). The m-MK test was adopted for its robustness in analysing ecological time series, as outlined by Hu et al. (2020). In contrast to the standard Mann–Kendall test (Mann, 1945; Kendall, 1948), this non-parametric technique remains unaffected by non-normal distributions or serial correlation. Its effectiveness in addressing these statistical challenges, as well as missing data, makes it well-suited to multi-decadal satellite observations.

Before performing trend analysis, annual maximum EVI time series were filtered using the median absolute deviation (MAD) procedure. According to Verbesselt et al. (2016), this process reduces any influence from extreme values potentially associated with residual atmospheric contamination, sensor artefacts or short-term disturbances. Subsequently, to evaluate the statistical significance of these trends, the MK-S statistic was derived by applying Equation 3.2.

$$\text{(Equation 3.2)} \qquad S = \Sigma i=1^{(n-1)} \Sigma j=i+1^{n} \; sign\,(Xj - Xi)$$

where *Xi* and *Xj* represent EVI observations at times *i* and *j*, respectively, and *sign* denotes the sign function. In particular, the S statistic variance was first computed assuming stochastic independence among observations; then, it was adjusted using the Yue and Wang (2004) correction factor, derived from the effective sample size of the trend-free series' autocorrelation structure. After that, corrected Z statistics and two-sided p-values were also derived to identify pixels with statistically detectable monotonic trends. Finally, the proportion of significant monotonic trends was quantified and expressed as a percentage within each study area, thus assessing the suitability of stand-level TS aggregation for subsequent analysis.

2.5 Spatial aggregation and data analysis

Long-term forest dynamics, expressed as EVI TS, were extracted at the pixel level for both OGF and NOGF, using the 'terra' package (Hijmans, 2025), available in RStudio (R 4.3.1). All extracted values below the 1st and above the 99th percentile were subsequently excluded to ensure a more accurate result. Then, a descriptive exploratory analysis at the pixel scale was conducted. However, raster-derived data are not independent and cannot be used in further analysis. To address this issue and prevent pseudo-replication, a block-wise spatial aggregation approach (Fig. 3.2) was adopted (Tian et al., 2025).

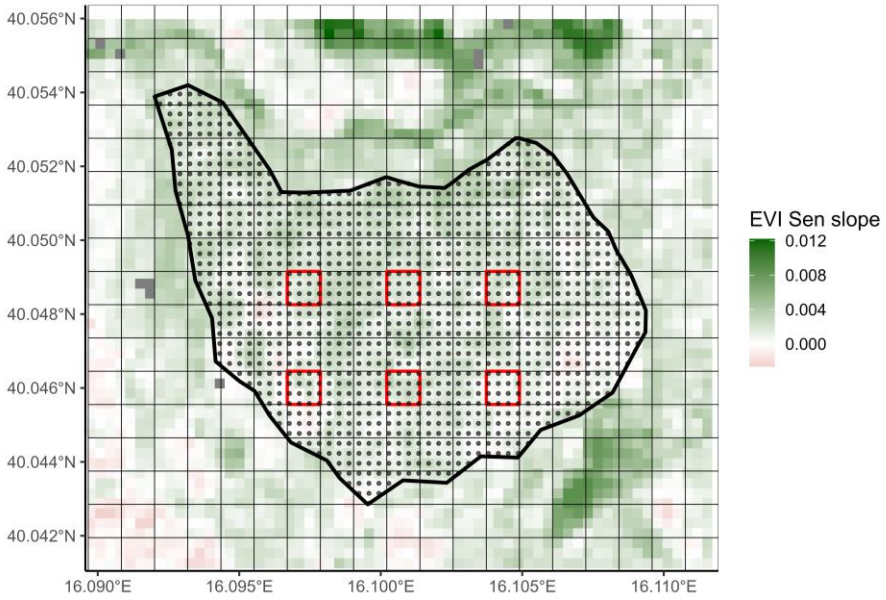

Figure 3.2. Block spatial aggregation applied to EVI Theil-Sen slope values within the 'Bosco Magnano' site. Here, the basemap shows EVI TS values derived from the Landsat time series (1985–2024). Black polygons denote the forest boundaries. The regular grid shows the spatial blocks of 100 × 100 m used for aggregation. Black dots

represent individual pixels included in the analysis, while red squares show how median EVI-TS values were computed for each grid cell.

For each forest type, study areas were divided into a regular grid of 100 × 100 m and pixels were allocated to their respective grid cell. Based on these grid cells, median EVI TS values were derived for each OGF and NOGF area, providing a robust summary of local trend patterns (Hartwig et al., 2020).

The Moran's I test (Fan & Myint, 2014; Naseri et al., 2026) was subsequently performed to assess spatial autocorrelation across a range of spatial scales (k = 4, 8 and 12 nearest neighbours). Then, a paired-site approach was adopted to compare forest classes according to their type. Differences in long-term EVI trends were examined through a block bootstrap approach (Johnston & Faulkner, 2021). Within each forest class, block median EVI TS were sampled with replacement and differences in mean EVI TS (Eq. 3.3) were estimated across 1,000 iterations.

$$\Delta = EVI_{OGF} - EVI_{NOGF} \quad \text{(Equation 3.3)}$$

Where EVI_{OGF} and EVI_{NOGF} represent the mean EVI TS median from OGFs and managed stands, while Δ represents the estimated difference.

Empirical 95% confidence intervals and one- and two-sided bootstrap *p*-values were hence derived from the resulting distributions, providing a non-parametric assessment of long-term variations in forest dynamics (Zeng et al., 2023; Glowienka & Kucza, 2025). Moreover, a global comparison, grouping forests by type, was conducted. Finally, Cliff's delta was also estimated to provide supplementary insights and quantify the magnitude of the observed differences.

3. Results

3.1 Spatial distribution of Long-Term EVI trends

Analysing EVI time series from Landsat data provided spatially detailed estimates of long-term forest trends across our study areas. The robustness of the long-term trend analysis was further supported by a dense temporal dataset comprising consistent annual observations (Appendix S2, Fig. S3.1). As shown in Figure 3.3, EVI TS varied moderately within the study area.

Notably, positive trends emerged across a significant portion of Pollino NP; meanwhile, subtle negative trends appeared in more isolated areas.

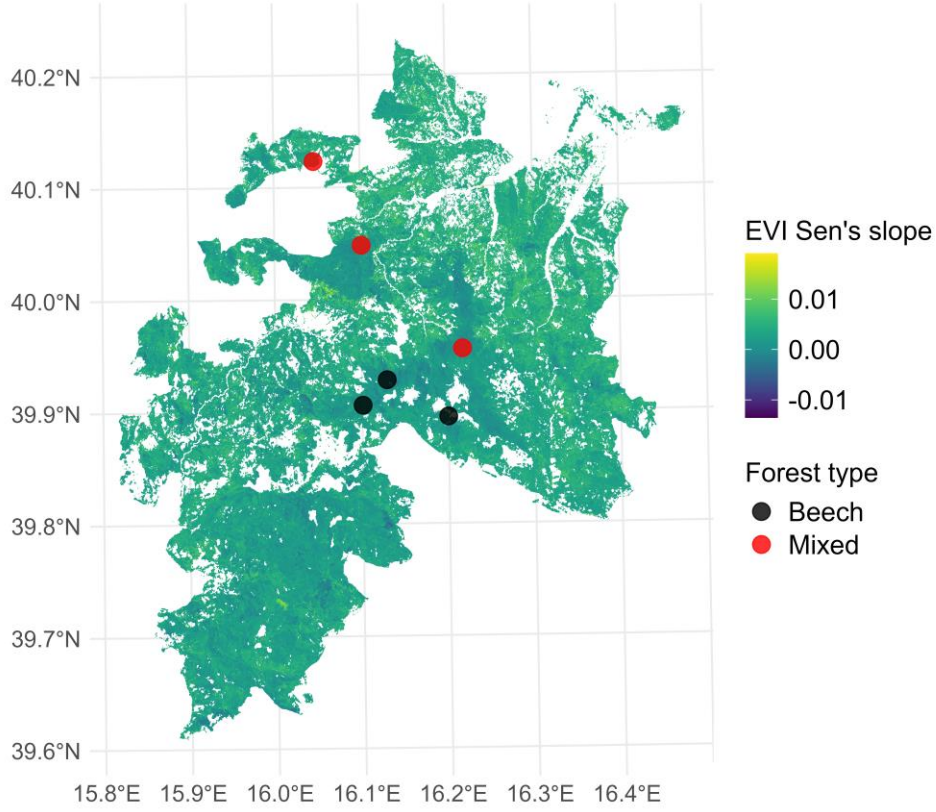

Figure 3.3. Spatial distribution of long-term EVI trends within the Pollino National Park. The background map shows Sen's slope values derived from the Enhanced Vegetation Index (EVI). Positive values (green and yellow) represent increasing vegetation greenness over time, while negative values (blue and purple) represent decreasing trends. Red and black points represent mixed and beech forests, respectively.

Likewise, at the stand scale, EVI TS values were generally low in all the investigated sites. However, considerable variations in forest types as well as within classes were observed (Tab. 3.4). More specifically, in pure beech forests, OGFs exhibited higher EVI TS values (0.001725) than

managed stands (0.000510). Analogous trends were also observed in mixed forest stands, where OGFs exhibited greater median EVI TS values (0.001607) when compared to managed sites (0.000914).

Table 3.4. Descriptive statistics of Sen's slope values (1985–2024) at the pixel level (n) for mixed and pure beech forests. Data are grouped by forest class (managed vs. OGF) and show the mean, median, standard deviation (SD), and interquartile range (q25 and q75) of long-term canopy trajectories.

Forest type	Forest class	n (pixels)	Mean slope	Median slope	SD	q25	q75
Mixed	Managed	1,047	0.001091	0.000914	0.001257	0.000259	0.001748
	OGF	1,781	0.001768	0.001607	0.001147	0.000984	0.002382
Pure beech	Managed	3,561	0.000448	0.000510	0.001216	−0.000475	0.001353
	OGF	4,600	0.001789	0.001725	0.001362	0.000977	0.002599

These results, therefore, highlighted how these differences were primarily driven by shifts in central tendency rather than dispersion. Furthermore, examining patterns in EVI directionality (Tab. 3.5) provided additional insights. In pure beech stands, OGFs exhibited a higher proportion of positive EVI TS values (90.9%), contrasting with the 62.6% observed in managed stands. Similarly, in mixed forest areas, OGFs showed stronger positive trends (96.2%) than managed stands (83.1%). Overall, these results provide a detailed and comprehensive assessment of long-term EVI dynamics, showing mainly positive and stable trends within the OGF class across both forest types.

Table 1.5. Proportion of the positive and negative EVI Sen Slope values in old-growth and managed forests, stratified by forest type. Values represent the percentage of pixels exhibiting greening (positive) or browning (negative), derived from annual maximum EVI time series (1985–2024).

Forest type	Forest class	Positive slopes (%)	Negative slopes (%)
Mixed	Managed	83.1	16.9
	OGF	96.2	3.7
Pure beech	Managed	62.6	37.4
	OGF	90.9	9.0

3.2 Pixel-wise trend significance and spatial support for stand-level analysis

The spatial distribution of statistically significant monotonic trends ($p < 0.05$) varied across all study sites according to forest type and class. However, OGFs consistently exhibited a higher and more extensive proportion of significant pixels than their NOGF counterparts (Tab. 3.6). In pure beech stands, OGFs exhibited substantial spatial coherence.

While PO exhibited significant trends across 73.4% of its area, RO and VIG revealed more moderate, yet still widespread, proportions of 45.2% and 15.0%, respectively. By contrast, managed beech forests showed lower and more heterogeneous spatial support, with significant trends only covering 11.2% (VIG-M) to 31.6% (RO-M) of their total area. Similar patterns were also observed in mixed forests, though with greater variability. Old-growth mixed stands showed a high degree of spatial coherence, with significant trends at CA (99.1%) and BM (50.2%), while TP (21.6%) showed a more localised trend. Managed mixed areas, conversely, exhibited an expanded range. Relatively higher proportions were observed in CA-M (75.4%) and BM-M (37.7%), while TP-M (15.1%) showed notably lower spatial support.

Table 3.2. Summary statistics of pixel-wise trend significance derived from the m-MK test applied to annual maximum EVI time series, stratified by forest type, management class, and site. For each stand, the table includes: total area, number of analysed pixels, proportion of pixels exhibiting statistically significant monotonic trends, as well as the median values of both Kendall's τ and corresponding Z statistics to characterise the central tendency of trend direction and strength.

Forest Type	Site	Forest class	Area (ha)	Pixels (n)	Significant pixels ($p < 0.05$)	Median Kendall's τ	Median Z
Pure beech	RO	OGF	98.30	1,082	45.2%	0.197	1.71
	VIG		54.83	605	15.0%	0.101	0.90
	PO		270,63	3,007	73.4%	0.368	3.11
	RO-M	Managed	107.45	1,194	31.6%	0.146	1.30
	VIG-M		75.17	833	11.2%	−0.033	−0.27
	PO-M		144.73	1,608	17.5%	0.034	0.29
Mixed	BM	OGF	108.24	1,204	50.2%	0.218	1.97
	TP		34.53	384	21.6%	0.145	1.23
	CA		20.91	231	99.1%	0.528	4.77
	BM-M	Managed	33.54	374	37.7%	0.188	1.69
	TP-M		45.59	504	15.1%	0.028	0.24
	CA-M		17.51	191	75.4%	0.385	3.48

Overall, our findings confirm the existence of statistically significant monotonic EVI trends across the investigated forest stands. In addition, OGF areas exhibited clear spatial coherence, in contrast to the more fragmented and variable trends observed in managed stands.

3.3 Block-level aggregation and descriptive comparison of EVI trends

Aggregating EVI TS values at the block level substantially reduced spatial autocorrelation while preserving consistent spatio-temporal trends in long-term forest dynamics. Moran's I coefficients, derived using block-level median values, revealed decreasing rates as neighbourhood size

increased (Appendix S1, Tab. S3.1). Across all forest types, EVI TS values generally exhibited low magnitudes and weak long-term monotonic trends (Tab. 3.7). Nevertheless, a clear and significant distinction between forest classes emerged in both forest types.

Table 3.7. EVI Sen's slope: block-level descriptive statistics. Block-level descriptive statistics of the median EVI Sen's slope for OGFs and NOGFs, grouped by forest type.

Forest type	Forest class	No. of blocks	Mean median slope	Median slope	SD
Mixed	Managed	127	0.001125	0.000939	0.001202
	OGF	199	0.001821	0.001582	0.001094
Pure beech	Managed	380	0.000462	0.000515	0.001101
	OGF	533	0.001771	0.001712	0.001268

OGFs in pure beech stands exhibited higher median EVI trends (Appendix S2, Fig. S3.4). Likewise, in mixed forest ecosystems, OGFs had higher median block-level values compared to managed reference sites. Additionally, EVI TS density distributions showed a systematic shift towards higher, more positive values within OGFs for both forest types (Fig. 3.4). These findings emphasise the significant differences between OGFs and managed stands, mainly characterised by changes in central tendency.

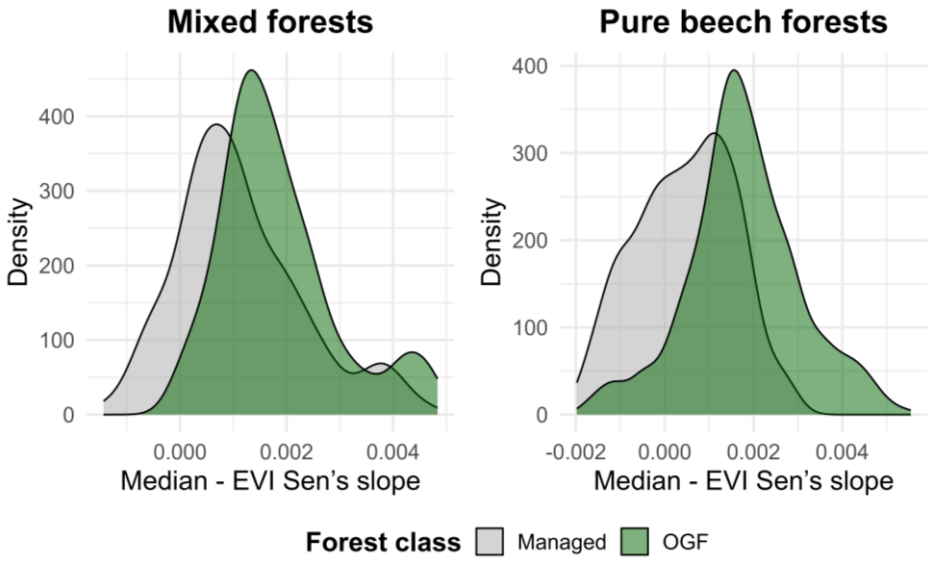

Figure 3.4. Kernel density distributions of block-level median EVI Sen's slope for mixed forests and pure beech forests. Density curves compare OGF and managed stands, highlighting differences in the magnitude and distribution of long-term forest trends.

3.4 Bootstrap inference and magnitude of inter-class differences

Block bootstrap analysis also produced significant findings, revealing higher median EVI TS values across all investigated OGFs (Fig. 3.5). While these differences were consistent in direction, their magnitude varied significantly, suggesting substantial heterogeneity in long-term forest dynamics at the stand level.

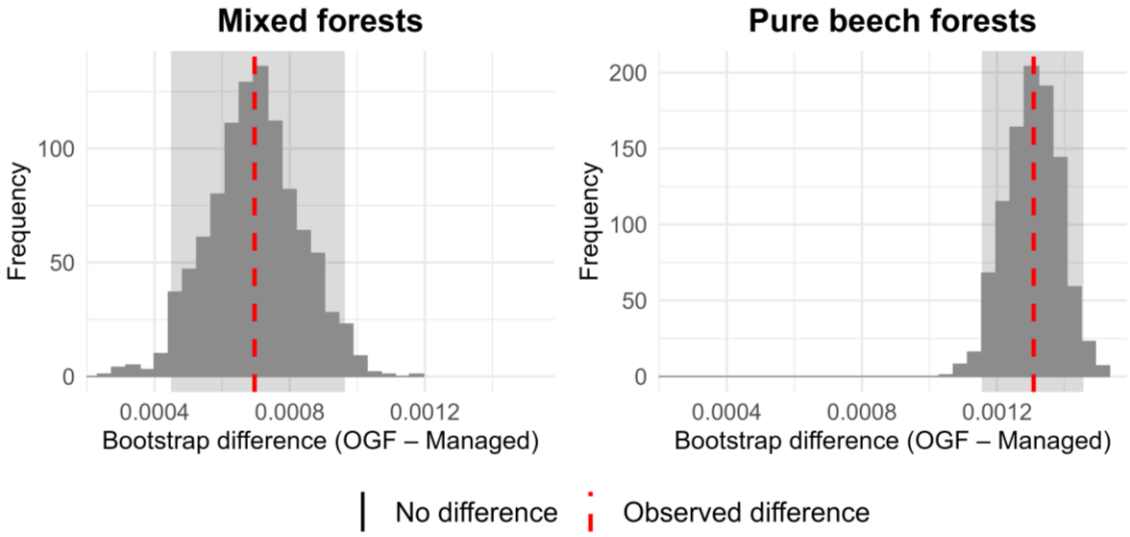

Figure 3.5. Bootstrap distributions of differences in mean EVI TS values between OGF and NOGF, for mixed forests and pure beech forests. The distributions were based on 1,000 bootstrap iterations using block medians EVI TS. The dashed lines mark the observed difference between the OGF and NOGF, while the shaded areas represent the 95% confidence interval.

However, within mixed forest stands, class differences were relatively moderate, especially at the BM site. Simultaneously, increasingly significant differences emerged in TP and CA, as reflected by their larger effect sizes (Tab. 3.8).

Table 3.8. Results from block bootstrap analyses. Reported values represent the difference in mean block-level median EVI Sen's slope (OGF-NOGF), with 95% bootstrap confidence intervals. Effect size is expressed as Cliff's δ.

Site ID	Forest type	Blocks (OGF)	Blocks (NOGF)	Δ EVI Sen's slope	95% CI	*p* (two-sided)	Cliff's δ
BM	Mixed	125	42	0.000331	0.000103–0.000530	0.002	0.31
TP	Mixed	44	57	0.000913	0.000702–0.001113	<0.001	0.77
CA	Mixed	30	28	0.001001	0.000492–0.001513	<0.001	0.54
RO	Pure beech	123	128	0.000668	0.000302–0.000999	<0.001	0.26
VIG	Pure beech	76	90	0.001168	0.000864–0.001461	<0.001	0.60
PO	Pure beech	334	162	0.001577	0.001382–0.001786	<0.001	0.69

Clear differences were, however, consistently detected between pure beech forest classes. All beech sites revealed a clear distinction between OGFs and managed stands, as evidenced by limited overlap in their bootstrap confidence intervals. PO showed the most pronounced contrast, highlighting significant variations in its long-term canopy dynamics. Such findings were further reinforced through global block bootstrap analyses conducted at the forest type level (Tab. 3.9). By aggregating block-level medians according to forest type and class, greater long-term EVI trends were still evident among OGF sites, especially in pure beech stands.

Table 3.9. Results from global block bootstrap analyses conducted within each forest type. Results are based on block-level median EVI Sen's slope values aggregated across all study sites within each forest type. Reported values represent the difference in mean block medians (OGF-NOGF), with 95% bootstrap confidence intervals and associated effect sizes (Cliff's δ).

Forest type	Blocks (OGF)	Blocks (NOGF)	Δ EVI Sen's slope	95% CI	p (two-sided)	Cliff's δ
Mixed forests	199	127	0.000696	0.000448–0.000963	<0.001	0.37
Pure beech forests	533	380	0.001308	0.001155–0.001456	<0.001	0.57

4. Discussion

This study successfully employed Theil–Sen slope (TS) estimators and block bootstrap techniques to analyse long-term forest trends within OGFs and managed reference stands (NOGFs). This approach was crucial in capturing robust long-term trends from satellite data, given its resilience to outliers, non-normal data distributions, and missing data, all of which are common in multi-decadal time series (Zhu & Woodcock, 2014; Gutiérrez-Hernández & García, 2024). Block bootstrapping also addressed spatial autocorrelation and data dependency, thereby enhancing the reliability and robustness of the comparison between OGFs and NOGFs. Moran's I coefficients, ranging from 0.2 to 0.8 depending on forest type and spatial scale adopted, revealed moderate to strong spatial autocorrelation.

While these results generally hold statistical significance, their inclusion remains acceptable considering the natural spatial dependencies occurring in forest ecosystems (Dormann et al., 2007). Furthermore, adopting the block-level aggregation approach mitigated pseudo-replication, improving the ecological relevance of our analysis (Fan & Myint, 2014; Shi et al., 2022). Although spatial and temporal data dependencies posed challenges, this methodological approach ensured reliable comparisons in long-term forest dynamics.

4.1 Monotonic canopy trends and their spatial distribution

The modified Mann-Kendall (m-MK) test revealed fundamental differences in the spatial dynamics of long-term trends in both forest types (Appendix S2 and Figures S3.2–S3.3). Statistically significant monotonic trends were consistently observed across large areas of old-growth forest (OGF) stands. Such evidence could suggest that detected long-term trends represent a process occurring at the stand scale rather than a series of localised, independent signals. By contrast, managed forests exhibited more fragmented patterns, indicating that long-term temporal signals could be locally interrupted or spatially heterogeneous.

Our findings revealed a potential link between the observed spatial patterns and various ecological factors, including forest successional stages, structural stability and reduced human interference, all of which are typical in old-growth ecosystems. Mature, multi-layered canopies are indeed renowned for their buffering capacity against short-term climatic fluctuations and local disturbances, which promote temporally consistent productivity signals (Musavi et al., 2017; Anderegg et al., 2020). Conversely, silvicultural practices such as selective harvesting and thinning can introduce irregularities in the canopy response, which may impact continuous monotonic trends (Senf et al., 2018; Pugh et al., 2019).

In this context, several methodological considerations should be acknowledged. Firstly, the m-MK test was specifically developed to detect monotonic trends. However, its ability to capture complex vegetation dynamics is limited when trend reversals occur during the study period. For instance, when a pixel shifts from initial greening to browning (or vice versa), the S statistic could potentially approach zero, resulting in a misclassification as stable or non-significant processes (Jones et al., 2022). Secondly, although temporal autocorrelation was corrected, residual spatial dependencies could still influence local patterns, particularly in dense canopies (Wilks, 2016).

Therefore, the absence of statistical significance at a specific location does not necessarily imply stasis; such non-significant pixels may, in fact, still contribute to the ecosystem's functioning through compensatory processes (Wu et al., 2020). Consequently, reported proportions should be interpreted as a measure of consistent, unidirectional change, rather than as a comprehensive index representing all temporal EVI variations.

For these reasons, our analytical framework interpreted pixel-wise significance as a reliable indicator of spatial patterns and not as an absolute measure of spatial change. These hypotheses were also supported by the large number of significant trends identified across all investigated sites, thereby justifying the aggregation of TS values at the stand scale.

4.2 Forest structure, species traits, and long-term EVI trajectories

As hypothesised, our study revealed significant differences in long-term EVI trends between OGFs and their paired NOGFs. According to Zhang et al. (2022) and Hirschmugl et al. (2023), OGFs are expected to exhibit more stable greening trajectories due to their high structural complexity, biodiversity, and ecological continuity. Consistent trends observed across all OGFs, particularly in pure beech stands, may therefore imply that increased structural complexity enhances resilience to climatic stressors by establishing more stable microclimatic conditions. By contrast, managed forests (NOGFs) exhibited more variable EVI trends, presumably due to past and/or recent human-induced disturbances (Spracklen & Spracklen, 2019; Rodriguez et al., 2024).

The results highlight the importance of shade-tolerant, late-successional species in sustaining stable canopies (Piovesan et al., 2005; Leuschner & Ellenberg, 2017). Specifically, European beech trees contribute to long-term stability by establishing a resilient forest structure that persists despite climate change and historical land-use practices (Fuchs et al., 2024). Conversely, mixed forests, characterised by increased biodiversity, showed weaker distinctions between OGFs and NOGFs. According to Zhang (2015) and Versace et al. (2021), species with contrasting ecological requirements, such as turkey oak and silver fir, may introduce greater variability in canopy structure and phenology, potentially influencing TS EVI trajectories.

4.3 Old-growth forests as functional benchmarks of ecosystem stability

The observed differences in EVI trends provided a clear distinction between old-growth and managed stands, mirroring wider ecological patterns related to forest structure and dynamic processes. Defined by their high structural complexity, multi-age cohorts, and irregular canopy gaps, OGFs can sustain stable productivity and functionality over time (Ehbrecht et al., 2021). The observed differences in EVI trends provided a clear distinction between old-growth and managed stands, mirroring wider ecological patterns related to forest structure and dynamic processes.

Defined by their high structural complexity, multi-age cohorts, and irregular canopy gaps, OGFs can sustain stable productivity and functionality over time (Ehbrecht et al., 2021). Such features also enhance their resilience to environmental stressors, including climate change and extreme weather events (Barredo et al., 2023; Adhikari et al., 2025), especially in the Mediterranean basin (Colangelo et al., 2021; Solano et al., 2025). In addition, OGFs provide essential ecosystem services such as carbon storage, biodiversity protection, and habitat provision, which are reinforced by their intricate structure and ecological continuity (Luyssaert et al., 2008; Besnard et al., 2025; Seidel & Boettger, 2023).

This distinct divergence highlighted the indispensable role of OGFs as ecological baselines. Functioning as near-natural reference systems, these forests provide a unique opportunity to examine the effects of climate-driven stressors while excluding the impacts of historical forest management practices. Understanding these primary ecosystems is crucial not only to recognise their intrinsic adaptive abilities, but also to model forest resilience under diverse future climate scenarios (Maes et al., 2020).

Furthermore, according to DellaSala et al. (2022), our findings support the hypothesis that OGFs provide more stable and sustained ecosystem services, reflecting their complexity, biodiversity, and undisturbed successional dynamics. Overall, our research emphasises an urgent need towards forest management and restoration strategies which closely mimic natural processes, aiming to enhance their stability and resilience (Messier et al., 2019; Larsen et al., 2022).

5. Conclusions

This research provides empirical evidence of distinct multi-decadal trajectories in canopy dynamics, distinguishing old-growth forests (OGFs) from managed counterparts. Longitudinal analysis of a 40-year Enhanced Vegetation Index (EVI) time series revealed sustained, statistically significant greening trends in OGFs, particularly within beech-dominated sites. This observed spectral stability supports the hypothesis that OGFs maintain superior ecological resilience and biomass accumulation rates over secular timescales (Markuljaková et al., 2025).

The robustness of these findings was also underscored by a high degree of spatial consistency; the prevalence of significant monotonic trends across extensive areas validates the reliability of aggregated EVI values at the stand scale.

This cross-scale stability was most pronounced in pure beech forests, where late-successional structural attributes and species composition appear to govern long-term canopy dynamics (Govedar et al., 2024). By maintaining a consistent spectral signature, these patterns highlight OGFs' ability to preserve ecological continuity (Lindner et al., 2010).

In contrast, managed stands exhibited weaker, more variable, and fragmented trend patterns. While OGF stability aligns with the intricate structural complexity and negligible disturbance rates typical of primary ecosystems (Barbati et al., 2012), the reduced spatial coherence in managed stands reveals disjointed canopy dynamics. This heterogeneity likely arises from past silvicultural interventions. In particular, the occurrence of these fragmented signatures after accounting for spatial autocorrelation further confirmed them as genuine ecological consequences of forest management, representing a landscape-scale divergence from the integrated trajectories observed in OGFs.

From a methodological perspective, this study successfully integrates Theil–Sen (TS) estimates and the block bootstrap resampling technique to effectively analyse high-density satellite time series. By addressing critical challenges such as spatial autocorrelation, non-normality, and pseudo-replication, this framework enables the identification of fine-scale functional dynamics. Rather than merely filtering data, the modified Mann–Kendall (m-MK) test validated the spatial consistency of trends, providing a robust empirical basis for stand-level data aggregation.

These findings suggest that canopy greenness stability can serve as a proxy for ecological integrity and resilience, offering a replicable, spatially explicit metric for identifying high-conservation-value forests (Muise, 2025).

Nonetheless, some limitations should be acknowledged. The present study was conducted across six OGF sites within Pollino National Park, paired with six ecologically comparable managed reference stands. Despite the apparent limitation in sample size, establishing paired OGF and managed stands sharing analogous species composition and bioclimatic context within a single protected area represents a considerable ecological constraint — especially in Pollino National Park, where steep altitudinal gradients, contrasting exposures, as well as the shift between temperate and Mediterranean climate regimes result in highly heterogeneous scenarios across small distances.

Furthermore, while EVI effectively captures canopy photosynthetic activity, it does not directly reflect sub-canopy processes or forest structural complexity below the dominant layer (Fassnacht et al., 2024). Finally, although the m-MK test reliably detects monotonic trends, it may be insensitive to non-linear or threshold-driven dynamics, resulting in an incomplete representation of ecological processes.

To bridge the gap between spectral stability and three-dimensional architecture, future research should integrate long-term vegetation trends with LiDAR-derived structural metrics. Incorporating high-resolution climatic variables would further elucidate the synergistic effects of climate change and management on forest ecosystem health. Overall, this study highlights the importance of combining multi-decadal remote sensing data with robust statistical modelling to understand functional differences between natural and managed systems, providing a transferable framework to monitor these critical ecosystems.

References

- Adhikari Y, Bachstein N, Gohr C, Blumröder JS, Meier C, Ibisch PL (2024). *Old-growth beech forests in Germany as cool islands in a warming landscape*. Scientific Reports, 14(1), 30311. DOI: https://doi.org/10.1038/s41598-024-81209-0
- Asare YM, Forkuo EK, Forkuor G, Thiel M (2020). *Evaluation of gap-filling methods for Landsat 7 ETM+ SLC-off image for LULC classification in a heterogeneous landscape of West Africa*. International Journal of Remote Sensing, 41(7), 2544–2564. DOI: https://doi.org/10.1080/01431161.2019.1693076
- Balata D, Gama I, Domingos T, Proença V (2022). *Using satellite NDVI time-series to monitor grazing effects on vegetation productivity and phenology in heterogeneous Mediterranean forests*. Remote Sensing, 14(10), 2322. DOI: https://doi.org/10.3390/rs14102322ù
- Banskota A, Kayastha N, Falkowski MJ, Wulder MA, Froese RE, White JC (2014). *Forest monitoring using Landsat time series data: A review*. Canadian Journal of Remote Sensing, 40(5), 362-384. DOI: https://doi.org/10.1080/07038992.2014.987376
- Barbati A, Salvati R, Ferrari B, Di Santo D, Quatrini A, Portoghesi L, Nocentini S (2012). *Assessing and promoting old-growthness of forest stands: lessons from research in Italy*. Plant Biosystems-An International Journal Dealing with all Aspects of Plant Biology, 146(1), 167-174. DOI: https://doi.org/10.1080/11263504.2011.650730
- Barbeta A, Miralles DG, Mendiola L, Gimeno TE, Sabaté S, Carnicer J (2023). *Disentangling the role of Forest structure and functional traits in the thermal balance of the Mediterranean–temperate ecotone*. Journal of Geophysical Research: Biogeosciences, 128(6), e2022JG007264. DOI: https://doi.org/10.1029/2022JG007264
- Barredo JI, Brailescu C, Teller A, Sabatini FM, Mauri A, Janouskova K (2021). *Mapping and assessment of primary and old-growth forests in Europe*. Amt fur Veroffentlichungen der EU, Luxemburg. DOI: 10.2760/797591
- BARREDO JI, MANSUY N, MUBAREKA SB (2023). *Primary and old-growth forests are more resilient to natural disturbances–Perspective on wildfires*. [online] Available at: https://publications.jrc.ec.europa.eu/repository/handle/JRC133970
- Besnard S, Heinrich VH, Carvalhais N, Ciais P, Herold M, Luijkx I, Yang H (2025). *Global covariation of forest age transitions with the net carbon balance*. Nature Ecology & Evolution, 9(10), 1848-1860. DOI: https://doi.org/10.1038/s41559-025-02821-5

- Bruening JM, Dubayah RO, Pederson N, Poulter B, Calle L (2024). *Definition criteria determine the success of old-growth mapping*. Ecol. Indic. 159, 111709. DOI: https://doi.org/10.1016/j.ecolind.2024.111709
- Burrascano S, Keeton WS, Sabatini FM, Blasi C (2013). *Commonality and variability in the structural attributes of moist temperate old-growth forests: A global review*. Forest Ecology and Management, 291, 458-479. DOI: https://doi.org/10.1016/j.foreco.2012.11.020
- Burrascano S, Ripullone F, Bernardo L, Borghetti M, Carli E, Colangelo M, Blasi C (2018). *It's a long way to the top: Plant species diversity in the transition from managed to old-growth forests*. Journal of Vegetation Science, 29(1), 98-109. DOI: https://doi.org/10.1111/jvs.12588
- Castellaneta M, Schettino A, Travascia D, Lapolla A, Colangelo M, Marchianò V, Ripullone F (2023). *I boschi vetusti nel Parco del Pollino: situazione attuale e prospettive future*. Forest@-Journal of Silviculture & Forest Ecology, 20. DOI: 10.3832/efor4303-020
- Cipolla SS, Montaldo N (2022). *On the impacts of historical and future climate changes to the sustainability of the main Sardinian forests*. Remote Sensing, 14(19), 4893. DOI: https://doi.org/10.3390/rs14194893
- Cohen WB, Healey SP, Yang Z, Stehman SV, Brewer CK, Brooks EB, Zhu Z (2017). *How similar are forest disturbance maps derived from different Landsat time series algorithms?*. Forests, 8(4), 98. DOI: https://doi.org/10.3390/f8040098
- Colangelo M, Camarero JJ, Gazol A, Piovesan G, Borghetti M, Baliva M, Ripullone F (2021). *Mediterranean old-growth forests exhibit resistance to climate warming*. Science of the total environment, 801, 149684. DOI: https://doi.org/10.1016/j.scitotenv.2021.149684
- Colditz RR (2015). *An evaluation of different training sample allocation schemes for discrete and continuous land cover classification using decision tree-based algorithms*. Remote Sensing, 7(8), 9655-9681. DOI: https://doi.org/10.3390/rs70809655
- DellaSala DA, Mackey B, Norman P, Campbell C, Comer PJ, Kormos CF, Rogers B (2022). *Mature and old-growth forests contribute to large-scale conservation targets in the conterminous United States*. Frontiers in Forests and Global Change, 5, 979528. DOI: https://doi.org/10.3389/ffgc.2022.979528
- Dormann CF, McPherson JM, Araújo MB, Bivand R, Bolliger J, Carl G, Wilson R (2007). *Methods to account for spatial autocorrelation in the analysis of species distributional data: a review*. *Ecography*, 609-628. DOI: https://doi.org/10.1111/j.2007.0906-7590.05171.x

- Eastman JR, Sangermano F, Machado EA, Rogan J, Anyamba A (2013). *Global trends in seasonality of normalized difference vegetation index (NDVI), 1982–2011*. Remote Sensing, 5(10), 4799-4818. DOI: https://doi.org/10.3390/rs5104799
- Ehbrecht M, Seidel D, Annighöfer P, Kreft H, Köhler M, Zemp DC, Ammer C (2021). *Global patterns and climatic controls of forest structural complexity*. Nature communications, 12(1), 519. DOI: https://doi.org/10.1038/s41467-020-20767-z
- Fan C, Myint S (2014). *A comparison of spatial autocorrelation indices and landscape metrics in measuring urban landscape fragmentation*. Landscape and Urban Planning, 121, 117-128. DOI: https://doi.org/10.1016/j.landurbplan.2013.10.002
- Fassnacht FE, White JC, Wulder MA, Næsset E (2024). *Remote sensing in forestry: current challenges, considerations and directions*. Forestry: An International Journal of Forest Research, 97(1), 11-37. DOI: https://doi.org/10.1093/forestry/cpad024
- Franquesa M, Adell-Michavila M, Vicente-Serrano SM (2025). *Long-term vegetation dynamics in Spain's National Park Network: insights from remote sensing data*. Environmental Monitoring and Assessment, 197(7), 767. DOI: https://doi.org/10.1007/s10661-025-14233-w
- Frey SJ, Hadley AS, Johnson SL, Schulze M, Jones JA, Betts MG (2016). *Spatial models reveal the microclimatic buffering capacity of old-growth forests*. Science Advances, 2(4), e1501392. DOI: https://doi.org/10.1126/sciadv.1501392
- Fuchs Z, Vacek Z, Vacek S, Cukor J, Simunek V, Stefancik I, Králíček I (2024). *European beech (Fagus sylvatica L.): A promising candidate for future forest ecosystems in Central Europe amid climate change*. Central European Forestry Journal, volume 70, issue: 2. DOI: 10.2478/forj-2023-0020
- Gilhen-Baker M, Roviello V, Beresford-Kroeger D, Roviello GN (2022). O*ld growth forests and large old trees as critical organisms connecting ecosystems and human health*. A review. *Environmental Chemistry Letters*, *20*(2), 1529-1538. DOI: https://doi.org/10.1007/s10311-021-01372-y
- Glenn EP, Huete AR, Nagler PL, Nelson SG (2008). *Relationship between remotely-sensed vegetation indices, canopy attributes and plant physiological processes: What vegetation indices can and cannot tell us about the landscape*. Sensors, 8(4), 2136-2160. DOI: https://doi.org/10.3390/s8042136

- Głowienka E, Kucza M (2025). *Persistent Urban Park Cooling Effects in Krakow: A Satellite-Based Analysis of Land Surface Temperature Patterns (1990–2018)*. Remote Sensing, 17(21), 3608. DOI: https://doi.org/10.3390/rs17213608
- Gorelick N, Hancher M, Dixon M, Ilyushchenko S, Thau D, Moore R (2017). *Google Earth Engine: Planetary-scale geospatial analysis for everyone*. *Remote Sensing of Environment*, 202, 19-27. DOI: https://doi.org/10.1016/j.rse.2017.06.031
- Govedar Z, Anikić N (2024). *Vegetation indices monitoring by using copernicus data in the old-growth forests of the Republic of Srpska/Bosnia and Herzegovina*. Frontiers in Forests and Global Change, 7, 1354769. DOI: https://doi.org/10.3389/ffgc.2024.1354769
- Gutiérrez-Hernández O, García LV (2024). *Robust trend analysis in environmental remote sensing: a case study of cork oak forest decline*. Remote Sensing, 16(20), 3886. DOI: https://doi.org/10.3390/rs16203886
- Hartwig FP, Smith GD, Schmidt AF, Sterne JAC, Higgins JPT, Bowden J (2020). *The median and the mode as robust meta-analysis estimators in the presence of small-study effects and outliers*. Research Synthesis Methods, 11(3), 397-412. DOI: https://doi.org/10.1002/jrsm.1402
- Hijmans R (2025). terra: Spatial Data Analysis. R package version 1.8-91. [online] Available at: https://github.com/rspatial/terra
- Hirschmugl M, Sobe C, Di Filippo A, Berger V, Kirchmeir H, Vandekerkhove K (2023). *Review on the possibilities of mapping old-growth temperate forests by remote sensing in Europe*. Environmental Modeling & Assessment, 28(5), 761-785. DOI: https://doi.org/10.1007/s10666-023-09897-y
- Hu Z, Liu S, Zhong G, Lin H, Zhou Z (2020). *Modified Mann-Kendall trend test for hydrological time series under the scaling hypothesis and its application*. Hydrological Sciences Journal, 65(14), 2419-2438. DOI: https://doi.org/10.1080/02626667.2020.1810253
- Iovino F, Marziliano PA, Menguzzato G, Nicolaci A (2010). S*trutture delle faggete vetuste del Cilento e del Pollino*. L'Italia forestale e montana, 65(6), 657-678. DOI: https://doi.org/10.4129/ifm.2010.6.01
- Johnston MG, Faulkner C (2021). *A bootstrap approach is a superior statistical method for the comparison of non-normal data with differing variances*. The New Phytologist, 230(1), 23-26. DOI: https://doi.org/10.1111/nph.17159

- Kendall MG (1948). *Rank correlation methods*. Griffin, London. DOI: https://doi.org/10.2307/2333282
- Kennedy RE, Ohmann J, Gregory M, Roberts H, Yang Z, Bell DM, Seidl R (2018). *An empirical, integrated forest biomass monitoring system*. Environmental Research Letters, 13(2), 025004. DOI: 10.1088/1748-9326/aa9d9e
- Larsen JB, Angelstam P, Bauhus J, Carvalho JF, Diaci J, Dobrowolska D, Schuck A (2022). Closer-to-Nature Forest Management. From Science to Policy 12 (Vol. 12, pp. 1-54). EFI European Forest Institute. [online] Available at: https://iris.unito.it/bitstream/2318/1866375/1/EFI_fstp_12_2022.pdf
- Leuschner C, Ellenberg H (2017). *Beech and mixed beech forests*. In *Ecology of Central European Forests: Vegetation Ecology of Central Europe, Volume I* (pp. 351-441). Cham: Springer International Publishing. DOI: https://doi.org/10.1007/978-3-319-43042-3_5
- Lindner M, Maroschek M, Netherer S, Kremer A, Barbati A, Garcia-Gonzalo J, Marchetti M (2010). *Climate change impacts, adaptive capacity, and vulnerability of European forest ecosystems*. Forest ecology and management, 259(4), 698-709. DOI: https://doi.org/10.1016/j.foreco.2009.09.023
- Luyssaert S, Schulze ED, Börner A, Knohl A, Hessenmöller D, Law BE, Grace J (2008). *Old-growth forests as global carbon sinks*. Nature, 455(7210), 213-215. DOI: https://doi.org/10.1038/nature07276
- Maes J, Teller A, Erhard M, Condé S, Vallecillo S, Barredo JI, Santos-Martín F (2020). *Mapping and assessment of ecosystems and their services: An EU ecosystem assessment: Supplement (Indicator fact sheets)*. JRC Science for Policy Report. [online] Available at: https://publications.jrc.ec.europa.eu/repository/handle/JRC120383
- Mann HB (1945). *Nonparametric tests against trend*. Econometrica: Journal of the econometric society, 245-259. DOI: https://doi.org/10.2307/1907187
- Mariano DA, dos Santos CA, Wardlow BD, Anderson MC, Schiltmeyer AV, Tadesse T, Svoboda MD (2018). *Use of remote sensing indicators to assess effects of drought and human-induced land degradation on ecosystem health in Northeastern Brazil*. Remote Sensing of Environment, 213, 129-143. DOI: https://doi.org/10.1016/j.rse.2018.04.048

- Markuljaková K, Svitok M, Mikoláš M, Hofmeister J, Keeton WS, Alhström A, Svoboda M (2025). *Old-growth mixed beech-dominated forests continue accumulating carbon with advancing age*. Forest Ecosystems, 100411. DOI: https://doi.org/10.1016/j.fecs.2025.100411
- Marques EQ, Silvério DV, Galvão LS, Aragão LE, Uribe MR, Macedo MN, Brando PM (2024). *Assessing the effectiveness of vegetation indices in detecting forest disturbances in the southeast Amazon*. Scientific Reports, 14(1), 27287. DOI: https://doi.org/10.1038/s41598-024-77924-3
- McLeod A (2025). *Kendall: Kendall Rank Correlation and Mann-Kendall Trend Test*. R package version 2.2.2. [online] Available at: https://CRAN.R-project.org/package=Kendall
- Meng Y, Liu X, Wu L, Liu M, Zhang B, Zhao S (2019). *Spatio-temporal variation indicators for landscape structure dynamics monitoring using dense normalized difference vegetation index time series*. Ecological Indicators, 107, 105607. DOI: https://doi.org/10.1016/j.ecolind.2019.105607
- Messier C, Bauhus J, Doyon F, Maure F, Sousa-Silva R, Nolet P, Puettmann K (2019). *The functional complex network approach to foster forest resilience to global changes*. Forest Ecosystems, 6(1), 1-16. DOI: https://doi.org/10.1186/s40663-019-0166-2
- Muise ER (2025). *Assessing forest ecological integrity and protected area effectiveness in British Columbia with satellite remote sensing* (Doctoral dissertation, University of British Columbia). DOI: https://dx.doi.org/10.14288/1.0449966
- Naseri MH, Shataee Jouibary S, Habashi H (2026). *Spatiotemporal analysis of the forest tree dieback patterns using aerial remote sensing data and clustering pattern indices*. Trees, 40(1), 8. DOI: https://doi.org/10.1007/s00468-025-02717-8
- Paillet Y, Bergès L, Hjältén J, Ódor P, Avon C, Bernhardt-Römermann M, Bijlsma RJ, De Bruyn LUC, Fuhr M, Grandin ULF, et al. (2010). *Biodiversity differences between managed and unmanaged forests: Meta-analysis of species richness in Europe*. Conservation Biology, 24(1), 101–112. DOI: https://doi.org/10.1111/j.1523-1739.2009.01399.x
- Palli J, Cagnetti C, Emanuel C, Ferrari S, Filibeck G, Forte TAGW, Piovesan, G. (2023). *The environmental dimension of ecotourism in Italian protected areas: A comparison of two bio-geographical regions based on the assessment of accredited hiking guides*. Journal of Ecotourism, 22(1), 164-186. DOI: https://doi.org/10.1080/14724049.2022.2080215

- Pasquarella VJ, Holden CE, Kaufman L, Woodcock CE (2016). *From imagery to ecology: leveraging time series of all available Landsat observations to map and monitor ecosystem state and dynamics*. Remote Sensing in Ecology and Conservation, 2(3), 152-170. DOI: https://doi.org/10.1002/rse2.24
- Piovesan G, Biondi F, Baliva M, De Vivo G, Marchianò V, Schettino A, Di Filippo A (2019). *Lessons from the wild*. Ecology, 100(9), 1-4. DOI: https://doi.org/10.1002/ecy.2737
- Piovesan G, Biondi F, Baliva M, Saba EP, Calcagnile L, Quarta G, Di Filippo A (2018). *The oldest dated tree of Europe lives in the wild Pollino massif*. Ecology, 99(7), 1682-1684. DOI: https://www.jstor.org/stable/26625780
- Piovesan G, Di Filippo A, Alessandrini AEA, Biondi F, Schirone B (2005). *Structure, dynamics and dendroecology of an old‐growth Fagus forest in the Apennines*. Journal of Vegetation Science, 16(1), 13-28. DOI: https://doi.org/10.1111/j.1654-1103.2005.tb02334.x
- R Core Team (2023) *R (4.3.1): A Language and Environment for Statistical Computing*. R Foundation for Statistical Computing, Vienna. [online] Available at: https://www.R-project.org/
- Ripullone F, Gentilesca T, Lauteri M, Rita A, Rivelli AR, Schettino A, Borghetti M (2016). *Apical dominance ratio as an indicator of the growth conditions favouring Abies alba natural regeneration under Mediterranean environment*. European journal of forest research, 135(2), 377-387. DOI: https://doi.org/10.1007/s10342-016-0941-3
- Rita A, Gentilesca T, Ripullone F, Todaro L, Borghetti M (2014). *Differential climate–growth relationships in Abies alba Mill. and Fagus sylvatica L. in Mediterranean mountain forests*. Dendrochronologia, 32(3), 220-229. DOI: https://doi.org/10.1016/j.dendro.2014.04.001
- Rodriguez PS, Schwantes AM, Gonzalez A, Fortin MJ (2024). *Monitoring changes in the enhanced vegetation index to inform the management of forests*. Remote Sensing, 16(16), 2919. DOI: https://doi.org/10.3390/rs16162919
- Sabatini FM, Burrascano S, Keeton WS, Levers C, Lindner M, Pötzschner F, Kuemmerle T (2018). *Where are Europe's last primary forests?*. Diversity and distributions, 24(10), 1426-1439. DOI: https://doi.org/10.1111/ddi.12778
- Sabatini FM, Keeton WS, Lindner M, Svoboda M, Verkerk PJ, Bauhus J, Kuemmerle T (2020). *Protection gaps and restoration opportunities for primary forests in Europe*. Diversity and Distributions, 26(12), 1646-1662. DOI: https://doi.org/10.1111/ddi.13158

- Seidel D, Boettger FA (2023). *How biomass and other tree architectural characteristics relate to the structural complexity of a beech-pine forest*. iForest-Biogeosciences and Forestry, 16(6), 368. DOI: https://doi.org/10.3832/ifor4305-016
- Seidl R, Thom D, Seibold S, Maroschek M, Rammer W (2025). *Climate change threatens old-growth forests in the Northern Alps*. Environmental Research Letters, 20(9), 094057. DOI: 10.1088/1748-9326/adf861
- Sen PK (1968). *Estimates of the regression coefficient based on Kendall's tau*. Journal of the American statistical association, 63(324), 1379-1389.
- Sen PK (1968). *Estimates of the regression coefficient based on Kendall's tau*. Journal of the American statistical association, 63(324), 1379-1389. DOI: https://doi.org/10.1080/01621459.1968.10480934
- Shestakova TA, Mackey B, Hugh S, Dean J, Kukavskaya EA, Laflamme J, Rogers BM (2022). *Mapping forest stability within major biomes using canopy indices derived from MODIS time series*. Remote Sensing, 14(15), 3813. DOI: https://doi.org/10.3390/rs14153813
- Shi F, Zhou B, Zhou H, Zhang H, Li H, Li R, Gao X (2022). *Spatial autocorrelation analysis of land use and ecosystem service value in the Huangshui River basin at the grid scale*. *Plants*, *11*(17), 2294. DOI: https://doi.org/10.3390/plants11172294
- Shimada M, Itoh T, Motooka T, Watanabe M, Shiraishi T, Thapa R, Lucas R (2014). New global forest/non-forest maps from ALOS PALSAR data (2007–2010). Remote Sensing of environment, 155, 13-31. DOI: https://doi.org/10.1016/j.rse.2014.04.014
- Solano F, Mansi C, Baliva M, Canestrelli D, Chiarucci A, Manicone R, Piovesan G (2025). *Mediterranean strictly protected forests are cooler*. Agricultural and Forest Meteorology, 375, 110858. DOI: https://doi.org/10.1016/j.agrformet.2025.110858
- Spracklen BD, Spracklen DV (2019). *Identifying European old-growth forests using remote sensing: A study in the Ukrainian Carpathians*. Forests, 10(2), 127. DOI: https://doi.org/10.3390/f10020127
- Tian X, de Bruin S, Simoes R, Isik MS, Minarik R, Ho YF, Hengl T (2025). *Spatiotemporal prediction of soil organic carbon density in Europe (2000–2022) using earth observation and machine learning*. PeerJ, 13, e19605. DOI: 10.7717/peerj.19605
- Todaro L, Andreu L, D'Alessandro CM, Gutiérrez E, Cherubini P, Saracino A (2007). *Response of Pinus leucodermis to climate and anthropogenic activity in the National Park of*

Pollino (Basilicata, Southern Italy). Biological conservation, 137(4), 507-519. DOI: https://doi.org/10.1016/j.biocon.2007.03.010

- U.S. Geological Survey (2021). Landsat Collection 2 Level-2 Science Products: U.S. Geological Survey Fact Sheet 2021–3055, 2 p., DOI: https://doi.org/10.3133/fs20213055
- Verbesselt J, Umlauf N, Hirota M, Holmgren M, Van Nes EH, Herold M, Scheffer M (2016). *Remotely sensed resilience of tropical forests*. Nature Climate Change, 6(11), 1028-1031. DOI: https://doi.org/10.1038/nclimate3108
- Versace S, Garfi V, Dalponte M, Febbraro Mirko D, Frizzera L, Gianelle D, Tognetti R (2021). *Species interactions in pure and mixed-species stands of silver fir and European beech in Mediterranean mountains*. iForest-Biogeosciences and Forestry, 14(1), 1. DOI: https://doi.org/10.3832/ifor3476-013
- Wang G, Peng W, Zhang L, Zhang J, Xiang J (2023). *Vegetation EVI changes and response to natural factors and human activities based on geographically and temporally weighted regression*. Global Ecology and Conservation, 45, e02531. DOI: https://doi.org/10.1016/j.gecco.2023.e02531
- Yin G, Mariethoz G, Sun Y, McCabe MF (2017). *A comparison of gap-filling approaches for Landsat-7 satellite data*. International Journal of Remote Sensing, 38(23), 6653-6679. DOI: https://doi.org/10.1080/01431161.2017.1363432
- Yue S, Wang C (2004). *The Mann-Kendall test modified by effective sample size to detect trend in serially correlated hydrological series*. Water resources management, 18(3), 201-218. DOI: https://doi.org/10.1023/B:WARM.0000043140.61082.60
- Zeng Y, Hao D, Park T, Zhu P, Huete A, Myneni R, Chen M (2023). *Structural complexity biases vegetation greenness measures*. Nature Ecology & Evolution, 7(11), 1790-1798. DOI: https://doi.org/10.1038/s41559-023-02187-6
- Zhang J, Xiao J, Tong X, Meng P, Li J, Yu P (2022). *NIRv and SIF better estimate phenology than NDVI and EVI: Effects of spring and autumn phenology on ecosystem production of planted forests*. Agricultural and Forest Meteorology, 315, 108819. DOI: https://doi.org/10.1016/j.agrformet.2022.108819
- Zhang Q, Zheng Z, Wu Z, Cao Z, Luo R (2022). *Using Multi-Source Geospatial Information to Reduce the Saturation Problem of DMSP/OLS Nighttime Light Data*. Remote Sensing, 14(14), 3264. DOI: https://doi.org/10.3390/rs14143264

- Zhang X (2015). *Reconstruction of a complete global time series of daily vegetation index trajectory from long-term AVHRR data*. Remote Sensing of Environment, 156, 457-472. DOI: https://doi.org/10.1016/j.rse.2014.10.012
- Zhu Z, Woodcock CE (2014). *Continuous change detection and classification of land cover using all available Landsat data*. Remote sensing of Environment, 144, 152-171. DOI: https://doi.org/10.1016/j.rse.2014.01.011
- Zribi M, Dridi G, Amri R, Lili-Chabaane Z (2016). *Analysis of the effects of drought on vegetation cover in a Mediterranean region through the use of SPOT-VGT and TERRA-MODIS long time series*. Remote Sensing, 8(12), 992. DOI: https://doi.org/10.3390/rs8120992

Appendices – Chapter 3

Appendix S1. Supplementary Tables

Table S3.1. Block-level spatial autocorrelation (Moran's I) of EVI Sen's slope for mixed and pure beech forests.

Forest type	Forest class	No. of blocks	K (n.neighbours)	Moran's I	Expected I	*p*-value
Mixed forests	Managed	127	4	0.803	−0.00794	< 0.001
	OGF	199	4	0.751	−0.00505	< 0.001
	Managed	127	8	0.773	−0.00794	< 0.001
	OGF	199	8	0.744	−0.00505	< 0.001
	Managed	127	12	0.709	−0.00794	< 0.001
	OGF	199	12	0.725	−0.00505	< 0.001
Beech forest	Managed	380	4	0.632	−0.00264	< 0.001
	OGF	533	4	0.640	−0.00188	< 0.001
	Managed	380	8	0.560	−0.00264	< 0.001
	OGF	533	8	0.569	−0.00188	< 0.001
	Managed	380	12	0.520	−0.00264	< 0.001
	OGF	533	12	0.509	−0.00188	< 0.001

Appendix S2. Supplementary Figures

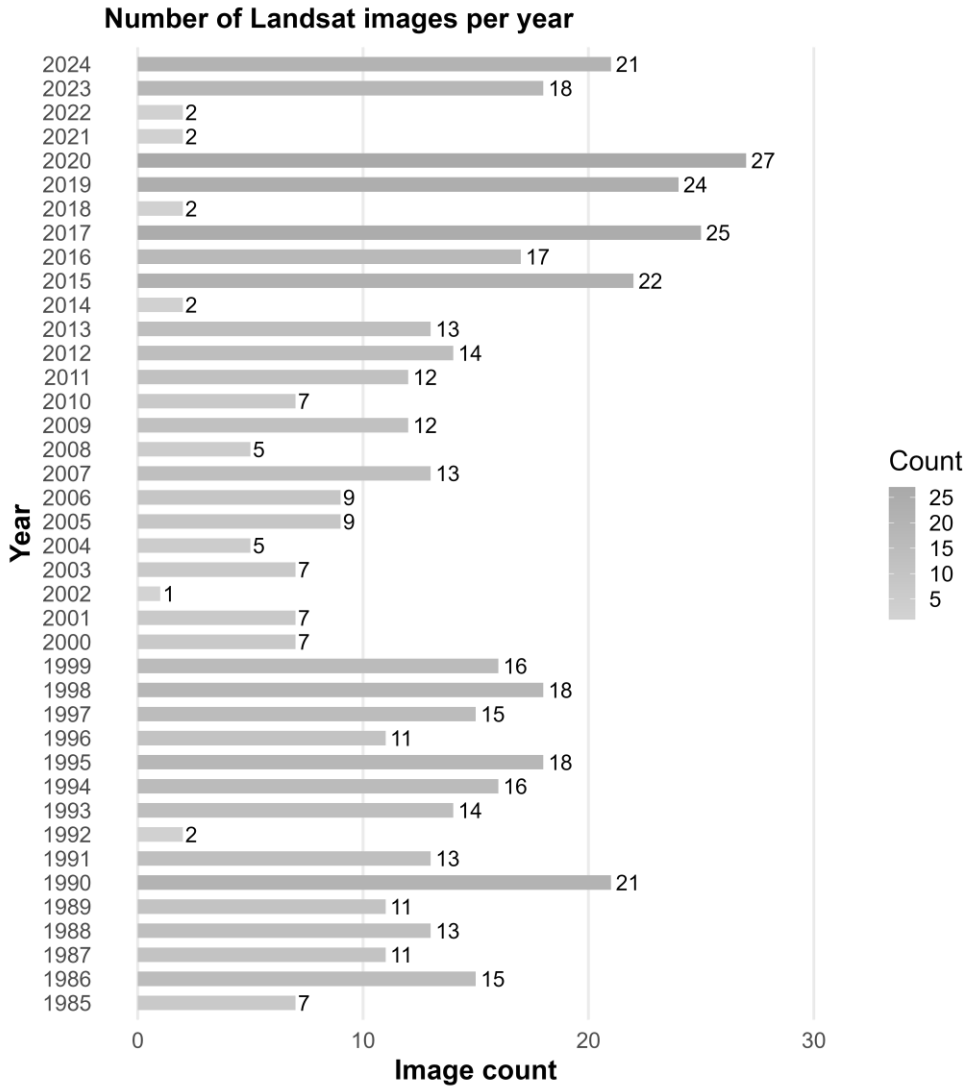

Figure S3.1. Temporal distribution of Landsat observations used for the analysis. Horizontal bars represent the number of cloud-free scenes available for each year after filtering by growing season (April–October) and cloud cover (<20%). The vertical reference lines indicate key thresholds in annual data availability. Variability among years reflects differences in sensor availability, mission continuity, and data gaps.

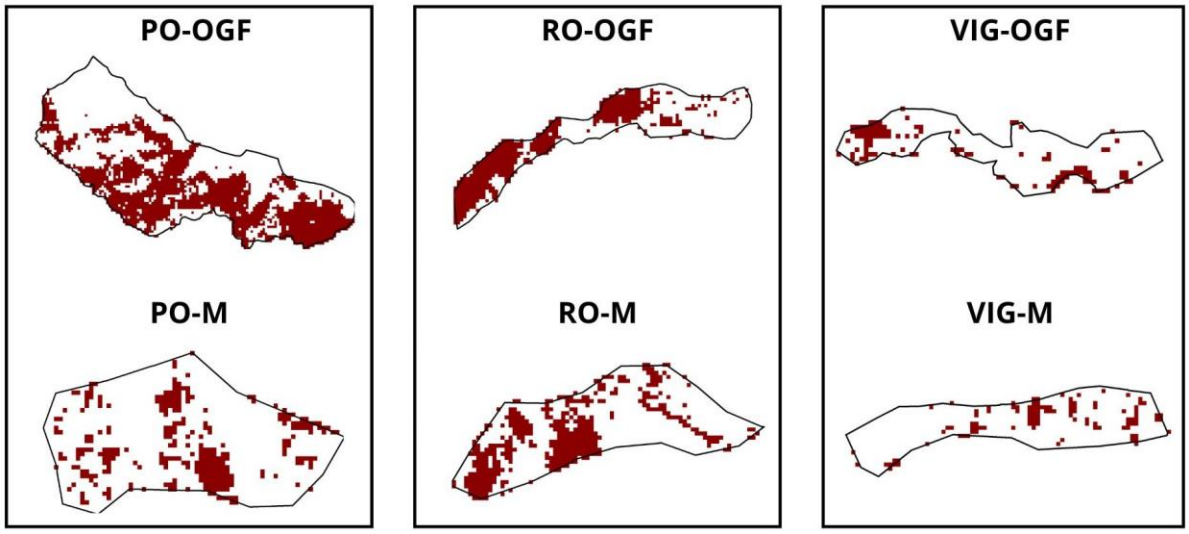

Figure S3.2. Spatial distribution of statistically significant monotonic EVI trends ($p < 0.05$) within pure beech forest stands. In the upper row are shown OGFs: PO, RO, and VIG; while, in the lower row, their corresponding NOGF reference sites: PO-M, RO-M, and VIG-M. Coloured pixels represent areas with a significant long-term trend.

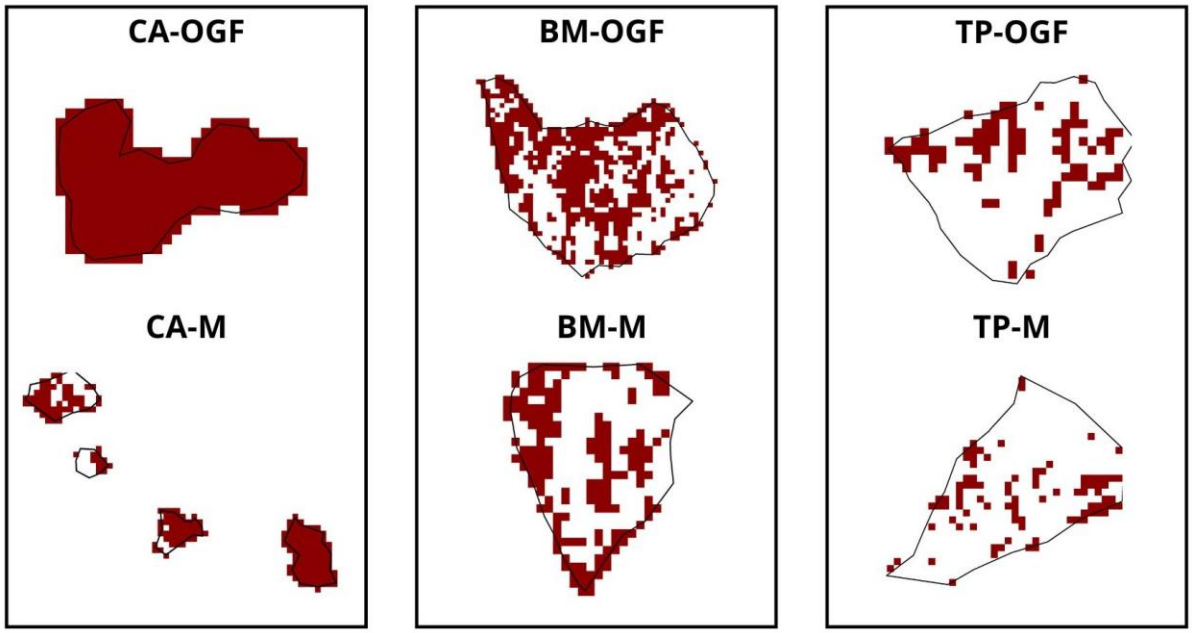

Figura 3.3. Spatial distribution of statistically significant monotonic EVI trends ($p < 0.05$) within mixed forest sites. The upper row comprises OGF sites, such as CA, BM, and TP. By contrast, their paired NOGF reference areas are in the lower row: CA-M, BM-M, TP-M. Coloured pixels denote areas where a monotonic long-term trend was identified.

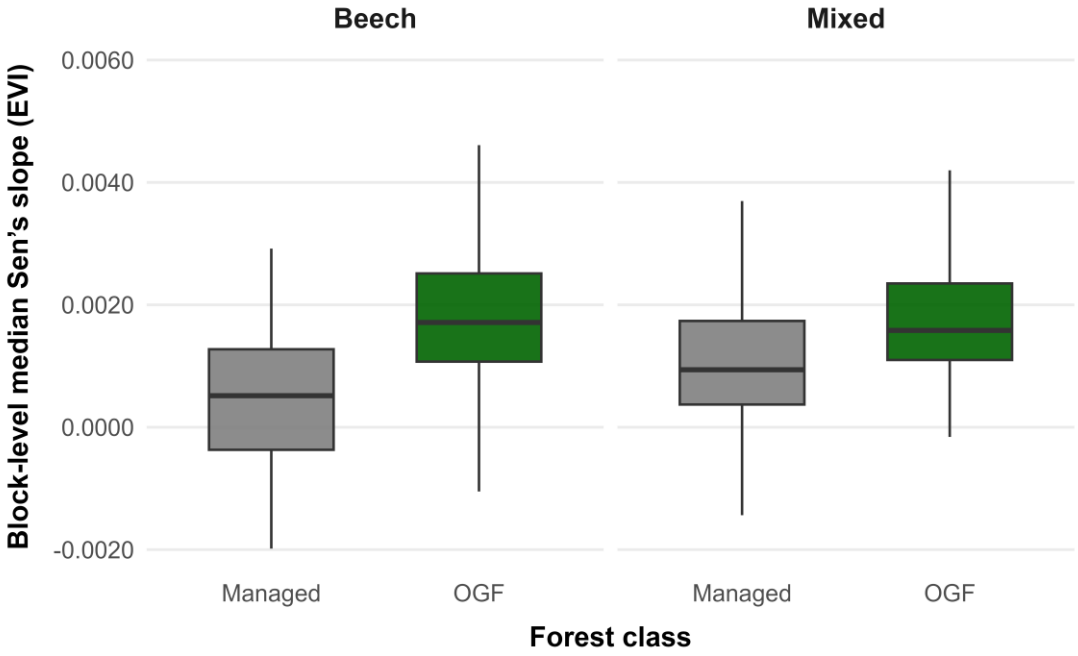

Figure S3.4. Boxplots of block-level median EVI Theil–Sen slopes for managed and old-growth sites, stratified by forest type (pure beech and mixed forests).

Global discussion

From structural indicators to functional continuity

This thesis effectively showed that the old-growth forests (OGFs) located within Pollino National Park are not simply a 'collection of old trees', but rather complex systems characterised by multifaceted dimensions related to their 'old-growthness' degree. Chapter 1 presented findings from the Structural Heterogeneity Index (SHI), which provided an ecological baseline revealing how structural heterogeneity contributes to vascular plant species richness, even when topographic factors are included. Although topography established a physical context, the unconstrained inertia of 81.21% identified by our models suggested that the essential nature of Mediterranean OGFs was defined by fine-scale biotic processes and historical factors. Furthermore, this substantial variability further emphasised that OGFs evolve through long-term ecological processes, including stochastic gap dynamics and natural senescence, which cannot be fully captured by abiotic variables alone.

Exploring structural heterogeneity within designed old-growth boundaries

As depicted in Chapter 2, moving from plot-level data to site-scale mapping effectively proved how remote sensing technologies have evolved from merely descriptive tools to highly effective predictive ones. By using Random Forest classifiers, our research established LiDAR-derived metrics as the most significant predictors for identifying structural heterogeneity.

In addition, the considerable spatial autocorrelation observed in our analyses should not be considered as a statistical constraint, but instead as a signature of forest coherence and integrity. Spatiotemporal dependency could be, in fact, a natural consequence of the biophysical similarity and shared ecological processes which govern forest development. By accounting for these dependencies through spatial thinning techniques, this approach provided a robust, transferable framework that could be used to identify forest patches presenting high conservation value. Notably, its application could effectively bridge current gaps between scientific research and regional management strategies, particularly in the Mediterranean basin.

Functional stability and the principle of continuity

The 40-year time-series analysis, detailed in Chapter 3, conclusively supported the OGF's functional concept. However, by comparing EVI trajectories, our study progressed beyond conventional static approaches, revealing dynamic ecological patterns within the investigated areas. A key finding from this study revealed that OGFs, particularly in pure beech stands, exhibited higher and more stable greenness trends compared to managed stands.

These stable trends should not be interpreted as a lack of dynamic change, but rather as an effective buffering mechanism that ensures their resilience. As discussed previously, their structural complexity, including features such as deadwood, multi-layered canopies and gap mosaics, confers microclimatic and metabolic stability. By contrast, fragmented and variable trends observed in managed forests highlighted how silvicultural practices, even when aimed at promoting sustainability, can potentially influence long-term forest dynamics and functionality.

Implications for conservation and monitoring efforts

This thesis presents an integrated framework promoting an essential transition towards a new set of conservation priorities. Historically, conventional protection strategies have employed age-based thresholds as a metric, but frequently these fail to accurately reflect the true ecological value of these forests. However, according to this study, we should focus on preserving their structural and functional integrity, emphasising their key role.

In this context, Pollino National Park (Pollino NP) represents a pivotal case study for these methodological advancements. By synthesising the Structural Heterogeneity Index (SHI) to assess forest structure at a fine scale and using predictive random forest models (RF) to evaluate forest heterogeneity within designated old-growth forests (OGFs), as well as employing multi-decadal satellite monitoring, this thesis offered a reliable and scalable approach to future research. Even though the SHI focuses on physical heterogeneity, it plays a pivotal role in biological richness, as demonstrated by a large body of existing literature: increased structural complexity leads to the creation and maintenance of diverse habitats, which support higher biodiversity rates. Consequently, our multifaceted approach is closely aligned with the EU Biodiversity Strategy for 2030, which advocates the strict protection of all remaining primary and old-growth forests across European territories.

Furthermore, OGFs should not be regarded as mere relics of the past or as unchanging natural entities, but rather as crucial functional benchmarks. Indeed, these unique ecosystems provide a vital reference for understanding how forests can effectively mitigate climate change, offering valuable insights to inform future policy decisions. By adopting the proposed monitoring framework, local authorities would be able to shift from a traditional 'reactive protection' approach to a new, proactive, evidence-based conservation strategy, aimed at safeguarding complex structures and their associated ecological processes.

General conclusions

Scientific Contributions

The present thesis further contributes to the scientific knowledge of old-growth forest ecosystems by proposing an integrated, field-to-satellite approach that combines structural indices, multi-source remote sensing, and long-term temporal analysis to characterise old-growthness across three distinct dimensions: structural, spatial, and functional. By combining forest structure data, advanced remote sensing techniques and multi-decadal satellite time series analysis, the study provides a robust quantitative approach to assessing old-growth ecosystems located within areas shaped by past human activity - closing a significant knowledge gap by decoupling natural successional trajectories from human-induced disturbances. Employing this framework in designated OGFs within the Pollino National Park not only yielded methodological insights but also provided ecologically relevant regional findings.

Another significant contribution of this work concerned the application of the Structural Heterogeneity Index (SHI) as a synthetic descriptor to represent forest structural complexity. SHI proved to be an effective tool, capturing differences among old-growth stands in terms of tree size distribution, vertical stratification, and deadwood attributes. Notably, the significant proportion of unexplained structural variability across sites emphasised an important aspect: OGFs are not solely driven by broad abiotic factors, but rather result from the interaction between long-term stand development, disturbance history, and local ecological processes.

The spatial modelling approach developed demonstrates how forest structural heterogeneity could be effectively mapped within designated OGF areas by integrating LiDAR-derived metrics, multispectral vegetation indices, long-term trends, and socio-ecological predictors. Among these, canopy height metrics were particularly informative, thus confirming the pivotal role of vertical structural complexity in defining a potential old-growthness gradient.

Integrating multi-season optical metrics enhanced model performance by capturing phenological variability, which cannot be detected through single-date imagery. Crucially, adding long-term trend metrics enabled us to connect current structural heterogeneity to multi-decadal canopy trajectories, introducing a temporal dimension.

Low Sen's slope values also suggested a sustained canopy stability across all the examined stands, in contrast with the rapid recovery expected after recent disturbance events. This temporal perspective is particularly important in the Mediterranean context, where secondary forests often mimic the height profiles and canopy closure of mature stands, which can potentially lead to misidentification of successional recovery as old-growth status. Adopting multiple-decade temporal analysis, this study overcomes the limitations posed by static structural data to evaluate long-term ecological continuity.

Anthropogenic pressure, defined by the Global Human Modification Index, also emerged as a significant predictor, highlighting how the cumulative impact from past activities may continue to affect forest structure, even within protected areas. Alongside topographic variables, such findings confirm that old-growth attributes are inherently linked to broader socio-ecological and environmental factors.

Spatial dependency and biophysical similarity

The pronounced spatial dependency identified within the investigated areas should not be interpreted as a statistical artefact, but rather as an inherent signature of ecosystem coherence. Adjacent forest patches sharing analogous structural attributes — shaped by common processes including tree senescence, canopy gap dynamics, and natural regeneration — reflect the biophysical continuity that characterises intact old-growth landscapes. This finding lends further support to a broader ecological principle: OGFs should be regarded not as isolated entities, but as spatially interconnected systems, where structural complexity propagates across the landscape, thereby ensuring functional integrity at scales exceeding the individual plot.

Implications for conservation and monitoring efforts

Overall, our findings advocate shifting from static, label-based OGFs' definitions towards a dynamic, evidence-based framework. This approach emphasises structural complexity and long-term functional stability beyond simply focusing on the trees' age. Although age remains a crucial parameter, it does not accurately reflect 'old-growthness'. In fact, two stands with the same age could differ greatly in terms of their conservation value, due to their distinct disturbance histories and ecological trajectories.

Consequently, focusing on forest ecosystem dynamics would enable the accurate identification and protection of areas exhibiting the greatest resilience and biodiversity value – aligning with the objectives outlined in the EU Biodiversity Strategy for 2030 and supporting the implementation of targeted conservation and management strategies. Accordingly, this framework can be summarised as follows: structural complexity, as quantified by the SHI, should not be considered a static descriptor of forest status, but rather a proxy for the ecological processes – such as gap dynamics, deadwood accumulation, and multi-cohort regeneration – which sustain long-term functional stability. As established in Chapter 1, structural heterogeneity exerts a greater influence on floristic diversity compared to topographic factors. Building on this, Chapter 2 showed how this spatial heterogeneity can be mapped at a fine scale using multi-source remote sensing data. Chapter 3 then revealed that structurally complex stands generally exhibit more stable long-term canopy trajectories than managed forests. Collectively, these three insights underscore a pivotal principle: within Mediterranean old-growth ecosystems, increased structural complexity yields enhanced functional resilience.

Potential future research opportunities

Several promising avenues for future research are opened by the framework presented in this thesis. Notably, it provides a robust basis to integrate forest structural heterogeneity and biodiversity patterns explicitly. Establishing a connection between SHI-based structural assessments and multi-taxon biodiversity data, particularly concerning saproxylic organisms, should be one of the main objectives. Such organisms are, in fact, closely linked to specific forest structural attributes, including deadwood volume, decay stage, canopy stratification diversity, and gap dynamics – making them valuable indicators for old-growth conditions. Additionally, combining SHI with flora surveys would enable a more comprehensive understanding of how structural complexity supports plant species assemblages, thereby reinforcing its role as a proxy to assess potential biodiversity.

Future research should move towards mechanistic modelling to quantify how structural complexity supports OGFs' function in acting as thermal refugia under extreme climate events. The integration of ecohydrological variables with resilience metrics, such as recovery rates, will enable us to predict more accurately how these ecosystems will evolve in response to future climate conditions.

Lastly, ongoing technological progress provides clear opportunities to refine and expand our framework. For instance, conducting repeated LiDAR acquisitions could offer a direct method to estimate forest structural change over time.

Furthermore, the use of terrestrial laser scanning could provide additional valuable insights, capturing details which are not currently detected by airborne sensors. At broader spatial scales, combining spaceborne LiDAR missions -such as GEDI - would greatly improve our ability to assess structural heterogeneity at regional or continental scales. In conclusion, this thesis provides a comprehensive characterisation, mapping, and monitoring framework for old-growth forest ecosystems, integrating rigorous scientific principles with operational scalability.

The integration of structural indices, remote sensing technologies and long-term temporal analysis offers a novel perspective from which 'old-growthness' may be assessed — not as a static attribute, but as a dynamic ecological property driven by historical, structural, and functional factors. These insights represent a considerable advancement in the scientific and operational ability to detect, protect, and understand old-growth ecosystems — among the most ecologically valuable and threatened forest systems in the Mediterranean region.